Course
Magnetic Resonance

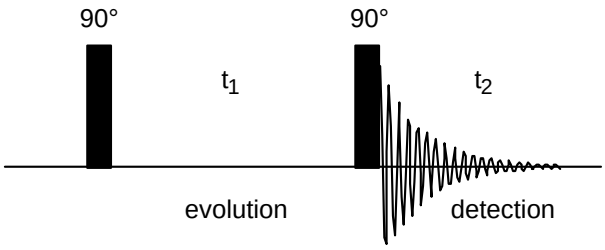

12-SASL

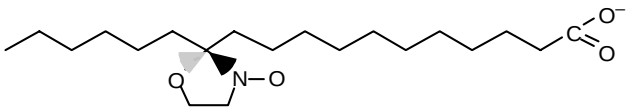

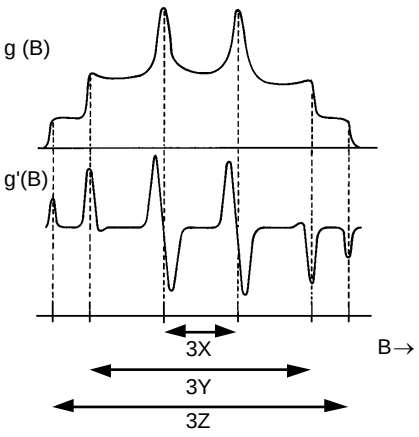

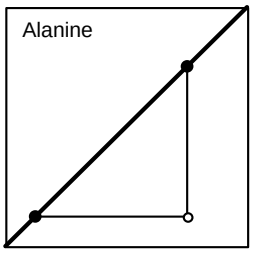

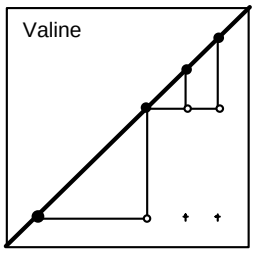

Dr. M.A. Hemminga
Wageningen University
Laboratory of Biophysics
Web site: http://ntmf.mf.wau.nl/hemminga/

Course web site: http://ntmf.mf.wau.nl/coursemr/

Contents

Syllabus Course Magnetic Resonance ..... **i**
Contents ..... **iii**

1 **General information** **1**

1-1 Goals 1
1-2 Examination 1
1-3 Laboratory practicals 2
1-4 Required reading 2
1-5 Introduction to NMR spectroscopy 3
1-6 Introduction to ESR spectroscopy 4

2 **Spin quantum mechanics** **5**

2-1 Spin operators 5
Note 5
Note 5
Note 6
Example 2-1 7
2-2 Step operators 8
Note 8
Note 8
Example 2-2 9
2-3 Operator and matrix representation 9
Note 10
2-4 Selection rules 10
Note 12
2-5 Two-spin systems 12
Note 12
2-6 General solution of the Schrödinger equation 13
Note 13
2-7 Perturbation theory 15
2-8 General procedure to determine a spectrum 16
Step 1 16
Step 2 16
Note 17
Step 3 17
Step 4 17
Note 17
Step 5 17
Step 6 17
Note 17
Step 7 18
Example 2-3 18
Note 20
2-9 Total spin angular momentum 20

Note....21
Note....22
Problems....23
Problem 2-1....23
Problem 2-2....23
Problem 2-3....23
Problem 2-4....23
Problem 2-5....23
Problem 2-6....23
Problem 2-7....23
Problem 2-8....24
Problem 2-9....24
Problem 2-10....24
Problem 2-11....25
Problem 2-12....25
Problem 2-13....25
Problem 2-14....25
Problem 2-15....26
Problem 2-16....26
Answers....27
Answer 2-6....27
Answer 2-14....27

3 **Interactions between spins....31**

3-1 Introduction....31
3-2 The dipole-dipole interaction....31
3-3 Principal axes of a tensor....34
Example 3-1....35
3-4 Fermi-contact interaction....35
3-5 Spin-spin coupling....36
3-6 Spin exchange interaction....36
Example 3-2....37
3-7 General expression of spin-spin interaction....38
Problems....39
Problem 3-1....39
Problem 3-2....39
Problem 3-3....39
Problem 3-4....40
Problem 3-5....40
Problem 3-6....40
Problem 3-7....41
Problem 3-8....41
Answers....43
Answer 3-2....43

4 **Zeeman interaction** **45**
4-1 Interaction of magnetic moments with a magnetic field 45
4-2 Anisotropic g-factor tensor 45

5 **ESR of nitroxide spin labels** **49**
5-1 The spin Hamiltonian 49
5-2 Spin labels in single crystal hosts 50
5-3 Powder spectrum 51
5-4 ESR spectra of mobile spin labels 56
5-5 Isotropic systems 58
5-5.1 Fast molecular motion 58
5-5.2 Slow molecular motion 59
5-5.3 Very slow molecular motion 60
5-5.4 Saturation Transfer (ST) ESR 61
5-6 Anisotropic systems 62
5-6.1 Order parameters 62
5-6.2 Fast molecular motion 64
Problems **69**
Problem 5-1 69
Problem 5-2 69
Problem 5-3 70
Problem 5-4 70
Problem 5-5 71
Problem 5-6 71
Problem 5-7 72

6 **Metalloproteins** **75**
6-1 Introduction 75
6-2 Spin-orbit coupling 75
6-3 Ligand field splitting 76
6-4 Myoglobin 78
6-5 Laccase 79

7 **Triplet ESR** **83**
7-1 Introduction 83
7-2 The spin Hamiltonian 83
7-3 The dipolar spin Hamiltonian 84
7-4 Triplet state in magnetic field 86
Problems **90**
Problem 7-1 90
Problem 7-2 90
Problem 7-3 90

Answers **91**
Answer 7-2 91
Answer 7-3 92

8 **Basic NMR structure analysis** **93**

8-1 Introduction 93
8-2 J modulation in a spin-echo experiment 93
8-3 Two-dimensional NMR 94
8-4 Two-dimensional J spectroscopy 94
8-5 Shift correlation by homonuclear scalar coupling (COSY) 97
8-6 Two-dimensional cross-relaxation and chemical exchange (NOESY) 97
8-7 Conformational analysis using proton NMR spectroscopy 99
Problems **100**
Problem 8-1 100
Problem 8-2 100
Problem 8-3 102
Problem 8-4 102
Answers **103**
Problem 8-1 103
Problem 8-2 103
Problem 8-3 103
Problem 8-4 104

9 **NMR imaging** **105**

9-1 Introduction 105
9-2 Selective excitation 105
9-3 Projection reconstruction 106
9-4 2D NMR imaging 107
Problems **109**
Problem 9-1 109
Problem 9-2 109

10 **Miscellaneous problems** **111**

Introduction 111
Problem 10-1 111
Problem 10-2 112
Problem 10-3 112
Problem 10-4 113
Problem 10-5 114
Problem 10-6 114
Problem 10-7 115
Problem 10-8 115
Problem 10-9 116
Problem 10-10 117

1

General information

1-1 Goals

The course Magnetic Resonance (A500-212) will give the students the opportunity to gain in-depth knowledge about modern applications of NMR en ESR in biological applications. For this purpose, a **physical and quantum mechanical basis** will be given of the phenomenon magnetic resonance. The technique will be illustrated with several application of the technique to **biological systems**. For the course a book will be used (R.K. Harris, Nuclear magnetic resonance spectroscopy, a physicochemical view (Longman Scientific and Technical, 1991), ISBN 0-582-44653-8) in combination with this syllabus. A Web site (http://ntmf.mf.wau.nl/coursemr/) is available for further course material.

The course Magnetic Resonance is a continuation and extension of the elementary spectroscopy course "Blok Spectroscopie" (A500-218).

The following subjects will be treated in the course:

- principles of magnetic resonance
- quantum mechanics of spins
- interactions between spins
- NMR in liquids
- ESR in liquids
- magnetic resonance in the solid state
- relaxation in NMR en ESR
- pulse NMR
- NMR imaging
- applications to biological systems (proteins, nucleic acids, membranes)

1-2 Examination

During the course students are required to submit worked exercises each week. These worked exercises will be marked and replace the "Voortentamen" of previous years.

The course with be finished with a final exam. This is an exam with open problems where all printed course material and notes may be used. The final mark for the course will consist of the average of the final exam and the average mark of the worked exercises. For the final exam the bottom mark is 5.

1-3 Laboratory practicals

The practical part (A500-213) is related to the theoretical part. It gives an illustration of the course material and improves the knowledge about the techniques and applications. **It is strongly advised to follow the practicals**, because the practicals illustrate the various theoretical topics. Furthermore, at the practicals use will be made of advanced research equipment (Bruker 400 MHz DPX NMR spectrometer and Bruker ESP 300 E ESR spectrometer) providing the student a good introduction in practical research.

The following subjects will be treated:

- saturation transfer ESR
- ESR of spin labels in solution and membranes
- NMR study of the binding of metal ions to AMP
- spin echo NMR and flow NMR

1-4 Required reading

The required reading for the final examination is:

- Syllabus Magnetic Resonance
- Web Links treated during the Course
- Course Book "Nuclear Magnetic Resonance Spectroscopy. A physicochemical view" by R.K. Harris, the chapters given in Table 1-1.

Table 1-1. Required reading from the Course Book "Nuclear Magnetic Resonance Spectroscopy. A physicochemical view" by R.K. Harris

Required reading from Course Book	
Chapter 1	all sections
Chapter 2	all sections
Chapter 3	all sections
Chapter 4	sections 4.1 - 4.5, 4.8 - 4.10
Chapter 5	sections 5.1 - 5.4
Chapter 6	sections 6.1 - 6.7
Chapter 7	sections 7.1 - 7.4, 7.6 - 7.8
Chapter 8	none
Appendix 1 - 5	none

1-5 Introduction to NMR spectroscopy

Nuclear Magnetic Resonance (NMR) is a spectroscopic technique based on the magnetic properties of atomic nuclei. The principle of nuclear magnetic resonance was predicted in 1936 by the Dutch physicist Gorter. In 1938, Rabi performed the first resonant experiment on silver atoms using a beam-splitting technique. However, it took up to 1946 before the American physicists Bloch and Purcell actually discovered NMR in the form it is know today. For this work they received the Nobel price for physics in 1952.

Initially, NMR was the domain of physicists, but when in 1950 Proctor and Yu discovered the chemical shift, it became clear that NMR could play an important role in chemistry and other areas of science. As NMR spectroscopy reveals useful information on molecular structure, chemical reaction rates and diffusion processes, it has rapidly progressed to become the most powerful non-destructive analytical tool in chemistry. In biochemistry, NMR spectroscopy has made contributions to elucidating the structure of cellular membranes, nucleic acids, proteins, and viruses.

The importance of NMR further increased by new technological developments on magnetic fields, computers, and methodology. After the presentation of new pioneering ideas of Jeener in 1971, the Swiss scientist Ernst started in 1975 with the development of two-dimensional NMR, that has given a breakthrough in the determination of the three dimensional structure of molecules. For this work, Ernst received the Nobel price for chemistry in 1991.

Another line of applications developed in seventies for medical applications, when in 1973 Damadian showed that NMR might be useful to diagnose cancer. In the same year, Lauterbur produced a two-dimensional proton NMR image of a water sample. For this experiment linear magnetic field gradients were generated that enabled to discriminate between different spatial locations in various objects. First the experiments were carried out on small objects, such as lemons and peppers. Then in rapid succession the technique was applied to live animals and ultimately, humans. The technique is called magnetic resonance imaging (MRI). For biomedical research, the application of NMR to living tissues and organisms enables to study their physiology and metabolism in vivo.

The NMR technique is non-destructive, non-invasive, and applicable to a broad range of systems: liquids, solids, intact materials, and living systems. New generation, user-friendly NMR spectrometers have become available. Numerous pulse sequences have been developed that suit almost every experiment. What may modern scientists expect from these new developments in NMR spectroscopy? Basically, NMR is a molecular technique: it provides detailed information about molecular properties and interactions. In many cases, NMR is the ultimate choice for novel applications in chemistry, biology, medicine, and food science.

1-6 Introduction to ESR spectroscopy

Every molecule that contains magnetic nuclei will produce an NMR spectrum. In general, NMR has almost no limitations. In contrast, most molecules do not give rise to ESR spectra, because the electrons in the molecular orbitals are paired. There is no net spin magnetic moment. ESR can only be detected in molecules that contain an unpaired electron. This is the case for free radicals, but also some metal ions display ESR spectra. Free radicals are very reactive and this requires special techniques to study them.

In biological systems, free radicals are present in the respiration cycle and photosynthesis reactions that can be studied by ESR. Transition ions in proteins (for example, hemoglobin, hemocyanin) are suitable systems for ESR research. Especially spin label ESR has been extremely suitable for biological research. In this approach, stable nitroxide radicals (spin labels) are covalently bound, or alternatively spin-labelled probe molecules are employed.

An important aspect of ESR spectroscopy the use of spin labels to provide information about molecular motions. In ESR spectroscopy three motional windows can be distinguished for the rotational correlation time, τ_c, of the molecular motion. If the motion is very fast ($\tau_c < 3\times10^{-9}$ s), the ESR spectrum consists of three sharp lines that can be analysed in terms of τ_C in a straightforward manner. In the slow motional region ($3\times10^{-9} < \tau_c < 10^{-6}$ s) the ESR spectra are strongly distorted and tend to resemble powder ESR spectra. Analysis of these spectra is possible using empirical theories and computer simulations. In the very slow motional region ($\tau_c > 10^{-6}$ s) the rigid powder spectrum is reached for conventional ESR. However, in this region saturation transfer (ST) ESR results in spectra still sensitive to molecular motions up to a final limit of $\tau_c \approx 10^{-3}$ s. For the analysis of ST-ESR spectra empirical methods have shown to be most useful. This extremely large window for molecular motions (more than 8 decades) makes ESR the best choice to study dynamic properties of biological systems.

2

Spin quantum mechanics

2-1 Spin operators

The components of the spin operator $\hat{\mathbf{I}}$ are $\hat{I}_x, \hat{I}_y, \hat{I}_z$. The spin operators $\hat{\mathbf{I}}^2$ and $\hat{I}_z$ commute:

$$\left[\hat{\mathbf{I}}^2, \hat{I}_z\right] = 0 \tag{2-1}$$

This can be compared to the classical vector model in which the magnetic moment precesses around the magnetic field: in such a situation the time-independent observable values of the magnetic moment are the length and projection at the z axis.

Using the Dirac notation, the eigenfunctions of $\hat{\mathbf{I}}^2$ and $\hat{I}_z$ are $|I,m\rangle$. This gives:

$$\hat{\mathbf{I}}^2|I,m\rangle = I(I+1)|I,m\rangle \tag{2-2}$$

$$\hat{I}_z|I,m\rangle = m|I,m\rangle \tag{2-3}$$

> ***Note***
>
> You should read, for example, Eqn. 2-2 as follows: operator $\hat{\mathbf{I}}^2$ acting on spin function $|I,m\rangle$ returns the value I(I + 1) times the spin function $|I,m\rangle$.

The eigenfunctions $|I,m\rangle$ form an orthonormal set:

$$\langle I,m \| I',m' \rangle = \delta_{II'}\delta_{mm'} \tag{2-4}$$

where the delta functions are 1 for equal indices, and zero for different indices.

> ***Note***
>
> Eqn. 2-2 and 2-3 in fact define the quantum numbers I and m of the eigenfunctions. Eqn. 2-2 defines the "length" of the magnetic moment, and Eqn. 2-3 the "projection" along the z axis.

The components of the spin operator $\hat{\mathbf{I}}$ are related by the following commutation rules that can be transferred to each other by cyclic exchange ($i^2 = -1$):

$$\left[\hat{\mathbf{I}}_x, \hat{\mathbf{I}}_y\right] = i\hat{\mathbf{I}}_z \tag{2-5}$$

$$\left[\hat{\mathbf{I}}_y, \hat{\mathbf{I}}_z\right] = i\hat{\mathbf{I}}_x \tag{2-6}$$

$$\left[\hat{\mathbf{I}}_z, \hat{\mathbf{I}}_x\right] = i\hat{\mathbf{I}}_y \tag{2-7}$$

In the classical model for the magnetic dipole moment, we have the following relation between the magnetic moment $\vec{\boldsymbol{\mu}}$ and the angular momentum $\vec{\mathbf{I}}$:

$$\vec{\boldsymbol{\mu}} = \gamma\vec{\mathbf{I}} \tag{2-8}$$

When we transfer this expression to operators, we will take $\hbar$ explicitly into account:

$$\hat{\boldsymbol{\mu}} = \gamma\hbar\hat{\mathbf{I}} \tag{2-9}$$

> ***Note***
> By using Eqn. 2-9 for the magnetic moment, $\hbar$ is no longer part of the spin operators. *This saves a lot of writing when evaluating the operators for complex spin systems*.

The classical energy of a magnetic moment in an external magnetic field $\vec{\mathbf{B}}$ can be written as:

$$U = -\vec{\boldsymbol{\mu}} \bullet \vec{\mathbf{B}} \tag{2-10}$$

By applying the quantum mechanical rules, we replace U by the Hamilton operator $\hat{H}$ and $\vec{\boldsymbol{\mu}}$ by Eqn. 2-9. The quantum mechanical analogue of Eqn. 2-8 can then be written as:

$$\hat{H} = -\gamma\hbar\hat{\mathbf{I}} \bullet \vec{\mathbf{B}} \tag{2-11}$$

which becomes

$$\hat{H} = -\gamma\hbar B\hat{\mathbf{I}}_z \tag{2-12}$$

when the magnetic field $\vec{\mathbf{B}}$ is in the z direction.

Eqn. 2-11 and 2-12 give the spin Hamiltonian for a spin in an external magnetic field. This interaction is called the Zeeman interaction.

Example 2-1

To solve the spin Hamiltonian for a spin-½-particle, we take the spin functions

$$|\alpha\rangle = \left|\tfrac{1}{2},\tfrac{1}{2}\right\rangle \tag{2-13}$$

and

$$|\beta\rangle = \left|\tfrac{1}{2},-\tfrac{1}{2}\right\rangle \tag{2-14}$$

The energy levels U_1 and U_2 for the case that $\vec{\mathbf{B}}$ is in the z direction are calculated as follows:

$$\hat{H}\left|\tfrac{1}{2},\tfrac{1}{2}\right\rangle = -\gamma\hbar B\hat{I}_z\left|\tfrac{1}{2},\tfrac{1}{2}\right\rangle = -\gamma\hbar B\tfrac{1}{2}\left|\tfrac{1}{2},\tfrac{1}{2}\right\rangle \rightarrow U_1 = -\tfrac{1}{2}\gamma\hbar B \tag{2-15}$$

$$\hat{H}\left|\tfrac{1}{2},-\tfrac{1}{2}\right\rangle = -\gamma\hbar B\hat{I}_z\left|\tfrac{1}{2},-\tfrac{1}{2}\right\rangle = -\gamma\hbar B\left(-\tfrac{1}{2}\right)\left|\tfrac{1}{2},-\tfrac{1}{2}\right\rangle \rightarrow U_2 = \tfrac{1}{2}\gamma\hbar B \tag{2-16}$$

This gives for the energy difference ΔU:

$$\Delta U = U_2 - U_1 = \gamma\hbar B \tag{2-17}$$

This situation corresponds to a spectrum with a single resonance line at frequency (see **Section 2-4 Selection rules**)

$$\omega = \gamma B \tag{2-18}$$

or

$$\nu = (\gamma/2\pi)B \tag{2-19}$$

This frequency is equal to the Larmor precession frequency in the classical model.

2-2 Step operators

The step operators (raising and lowering operators) are defined as:

$$\hat{\mathbf{I}}_+ = \hat{\mathbf{I}}_x + i\hat{\mathbf{I}}_y \tag{2-20}$$

and

$$\hat{\mathbf{I}}_- = \hat{\mathbf{I}}_x - i\hat{\mathbf{I}}_y \tag{2-21}$$

The following useful commutation relationships apply for the step operators:

$$\left[\hat{\mathbf{I}}^2, \hat{\mathbf{I}}_\pm\right] = 0 \tag{2-22}$$

$$\left[\hat{\mathbf{I}}_z, \hat{\mathbf{I}}_\pm\right] = \pm\hat{\mathbf{I}}_\pm \tag{2-23}$$

$$\left[\hat{\mathbf{I}}_+, \hat{\mathbf{I}}_-\right] = 2\hat{\mathbf{I}}_z \tag{2-24}$$

Furthermore it can be shown that:

$$\hat{\mathbf{I}}_x^2 + \hat{\mathbf{I}}_y^2 = \hat{\mathbf{I}}^2 - \hat{\mathbf{I}}_z^2 = \tfrac{1}{2}\left(\hat{\mathbf{I}}_+\hat{\mathbf{I}}_- + \hat{\mathbf{I}}_-\hat{\mathbf{I}}_+\right) \tag{2-25}$$

> ***Note***
> Because the step operators do not commute, the order of application in Eqn. 2-25 is important.

It can be shown that the effect of the step operators on the spin functions $\left|I,m\right\rangle$ is:

$$\hat{\mathbf{I}}_+\left|I,m\right\rangle = \sqrt{I(I+1) - m(m+1)}\left|I,m+1\right\rangle \tag{2-26}$$

$$\hat{\mathbf{I}}_-\left|I,m\right\rangle = \sqrt{I(I+1) - m(m-1)}\left|I,m-1\right\rangle \tag{2-27}$$

> ***Note***
> All quantum mechanical effects of spins can be calculated from the four **key equations**: Eqn. 2-2, 2-3, 2-26, and 2-27. This is illustrated in the following example.

Example 2-2

By using Eqn. 2-26 and 2-27 the effect of the step operators on the spin functions $|\alpha\rangle$ and $|\beta\rangle$ of a spin-½-particle (I=½ and m=½) can be calculated as follows:

$$\hat{\mathbf{I}}_+|\alpha\rangle = 0 \qquad \hat{\mathbf{I}}_+|\beta\rangle = |\alpha\rangle \tag{2-28}$$

$$\hat{\mathbf{I}}_-|\alpha\rangle = |\beta\rangle \qquad \hat{\mathbf{I}}_-|\beta\rangle = 0 \tag{2-29}$$

Furthermore, we have from Eqn. 2-2 and 2-3:

$$\hat{\mathbf{I}}_z|\alpha\rangle = \tfrac{1}{2}|\alpha\rangle \qquad \hat{\mathbf{I}}_z|\beta\rangle = -\tfrac{1}{2}|\beta\rangle \tag{2-30}$$

$$\hat{\mathbf{I}}^2|\alpha\rangle = \tfrac{3}{4}|\alpha\rangle \qquad \hat{\mathbf{I}}^2|\beta\rangle = \tfrac{3}{4}|\beta\rangle \tag{2-31}$$

This effect can be displayed in terms of the so-called Pauli spin matrices:

$\hat{\mathbf{I}}_+$	$\|\alpha\rangle$	$\|\beta\rangle$
$\langle\alpha\|$	0	1
$\langle\beta\|$	0	0

$\hat{\mathbf{I}}_-$	$\|\alpha\rangle$	$\|\beta\rangle$
$\langle\alpha\|$	0	0
$\langle\beta\|$	1	0

$\hat{\mathbf{I}}_z$	$\|\alpha\rangle$	$\|\beta\rangle$
$\langle\alpha\|$	$\frac{1}{2}$	0
$\langle\beta\|$	0	$-\frac{1}{2}$

$\hat{\mathbf{I}}^2$	$\|\alpha\rangle$	$\|\beta\rangle$
$\langle\alpha\|$	$\frac{3}{4}$	0
$\langle\beta\|$	0	$\frac{3}{4}$

The calculation of the spin matrices proceeds as follows:

For example, $\langle\alpha|\hat{\mathbf{I}}_+|\beta\rangle = \langle\alpha\|\alpha\rangle = 1$, and $\langle\beta|\hat{\mathbf{I}}_+|\beta\rangle = \langle\beta\|\alpha\rangle = 0$, since the spin functions $|\alpha\rangle$ and $|\beta\rangle$ form an orthonormal set.

2-3 Operator and matrix representation

The matrices belonging to the operators $\hat{\mathbf{I}}^2$ and $\hat{\mathbf{I}}_z$ are diagonal: these diagonal values are the eigenvalues of the operators.

When we write the orthonormal spin functions $|\alpha\rangle$ and $|\beta\rangle$ as column matrices, we have the following relations:

$$|\alpha\rangle = \begin{pmatrix} 1 \\ 0 \end{pmatrix} \qquad |\beta\rangle = \begin{pmatrix} 0 \\ 1 \end{pmatrix}$$

The complex conjugates are row matrices:

$$\langle\alpha| = \begin{pmatrix} 1 & 0 \end{pmatrix} \qquad \langle\beta| = \begin{pmatrix} 0 & 1 \end{pmatrix}$$

This allows us to write:

$$\hat{\mathbf{I}}_+|\beta\rangle = \begin{pmatrix} 0 & 1 \\ 0 & 0 \end{pmatrix}\begin{pmatrix} 0 \\ 1 \end{pmatrix} = \begin{pmatrix} 1 \\ 0 \end{pmatrix} = |\alpha\rangle$$

and

$$\langle\beta|\hat{\mathbf{I}}_+|\beta\rangle = \begin{pmatrix}0 & 1\end{pmatrix}\begin{pmatrix}0 & 1\\ 0 & 0\end{pmatrix}\begin{pmatrix}0\\ 1\end{pmatrix} = \begin{pmatrix}0 & 1\end{pmatrix}\begin{pmatrix}1\\ 0\end{pmatrix} = 0\,.$$

> ***Note***
> When the operator is a Hamiltonian, the corresponding matrix is called a Hamiltonian matrix. A Hamiltonian matrix is always hermitic (or, symmetric in the case that no complex matrix elements are involved), but not always diagonal. **The procedure that diagonalises a Hamiltonian matrix results in the eigenvalues and eigenfunctions.** This is generally done by using the mathematical tools of matrices and linear algebra. The eigenvalues of a hermitic operator are always real and represent physical observable vales.

2-4 Selection rules

The spin Hamiltonian of a magnetic moment in an external magnetic field $\vec{\mathbf{B}}$ in the z direction is given by

$$\hat{H} = -\gamma\hbar B\hat{\mathbf{I}}_z \tag{2-12}$$

The energy levels follow from the solution of the time-independent Schrödinger equation

$$\hat{H}\psi = U\psi \tag{2-32}$$

From the foregoing, we know that the spin functions $|I,m\rangle$ are the eigenfunctions of $\hat{\mathbf{I}}_z$ and thus of $\hat{H}$:

$$\hat{H}|I,m\rangle = -\gamma\hbar B\hat{\mathbf{I}}_z|I,m\rangle = -\gamma\hbar B\times m|I,m\rangle \tag{2-33}$$

The energy levels are now given by

$$U_m = -\gamma\hbar Bm \tag{2-34}$$

These energy levels are schematically depicted in Fig. 2-1.

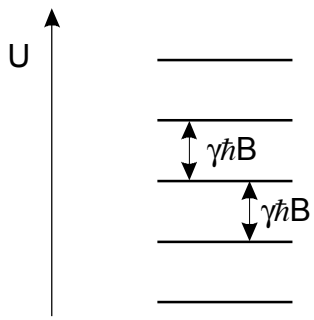

Fig. 2-1.
Schematic illustration of the energy levels of a spin in a magnetic field. Transitions can take place between successive energy levels. Only two transitions are shown.

From the classical vector model of magnetic resonance it is known that the radiofrequency field $\vec{\mathbf{B}}_1$ must be perpendicular to the external field $\vec{\mathbf{B}}$ to give rise to transitions between the quantum states. In the spectrometer this radiofrequency field is $2B_1 \cos\omega t$. If the radiofrequency field is applied along the x direction, a small time-dependent term is added to the spin Hamiltonian:

$$\hat{H}_1(t) = -2\gamma\hbar B_1 \cos\omega t \hat{\mathbf{I}}_x \tag{2-35}$$

This small time-dependent Hamiltonian does not disturb the position of the energy levels, but induces transitions between the states. The resulting transition probability for a transition from $|I,m\rangle$ to $|I,m'\rangle$ is given by:

$$P_{mm'} = \gamma^2 B_1^2 \left|\langle I,m|\hat{\mathbf{I}}_x|I,m'\rangle\right|^2 g(\nu) \tag{2-36}$$

where $g(\nu)$ is the lineshape function.

Because we can write

$$\hat{\mathbf{I}}_x = \tfrac{1}{2}\left(\hat{\mathbf{I}}_+ + \hat{\mathbf{I}}_-\right) \tag{2-37}$$

the matrix elements $\langle I,m|\hat{\mathbf{I}}_x|I,m'\rangle$ of Eqn. 2-36 become

$$\tfrac{1}{2}\langle I,m|\left(\hat{\mathbf{I}}_+ + \hat{\mathbf{I}}_-\right)|I,m'\rangle = \tfrac{1}{2}\left(\langle I,m|\hat{\mathbf{I}}_+|I,m'\rangle + \langle I,m|\hat{\mathbf{I}}_-|I,m'\rangle\right) \tag{2-38}$$

As the step operators raise and lower m by one unit, the selection rule is

$$\Delta m = \pm 1 \tag{2-39}$$

From Eqn. 2-34 this results in a energy difference

$$\Delta U = \gamma\hbar B \tag{2-40}$$

This situation corresponds to a spectrum with a single resonance line with lineshape $g(\nu)$ centred at a frequency given by

$$\nu = (\gamma/2\pi)B \tag{2-41}$$

Note

Quantum mechanics learns us also that the radiofrequency field $\vec{\mathbf{B}}_1$ must be perpendicular to the external field $\vec{\mathbf{B}}$. If the radiofrequency field is applied along the y direction, the calculation follows the same lines as described above. However, if $\vec{\mathbf{B}}_1$ is along the z direction, the matrix elements of Eqn. 2-36 become

$$\langle I,m|\hat{I}_z|I,m'\rangle = m'\delta_{mm'}$$

which are always zero, unless m = m'. In this case, no transitions take place, but the energy levels are modulated by the radiofrequency field.

2-5 Two-spin systems

For simplicity we will consider only two spin-½-particles (I=½ and m=½). For each spin particle the spin functions are $|\alpha\rangle$ and $|\beta\rangle$. In accordance with normal quantum mechanical considerations the overall spin states may be designated by the products of the functions of the individual spin particles. This gives four new spin functions given by

$$\begin{aligned}\phi_1 &= \alpha_1\alpha_2 = \alpha\alpha \\ \phi_2 &= \alpha_1\beta_2 = \alpha\beta \\ \phi_3 &= \beta_1\alpha_2 = \beta\alpha \\ \phi_4 &= \beta_1\beta_2 = \beta\beta\end{aligned} \qquad (2\text{-}42)$$

In a more general way, the product spin functions can be written as $|m_1m_2\rangle$.

Note

It is customary to omit the indices of the individual spins in the product spin function. However, remember that an operator for spin particle 1 only acts on its own spin functions $|\alpha_1\rangle$ and $|\beta_1\rangle$.

The spin Hamiltonian of this two-spin system in an external magnetic field $\vec{\mathbf{B}}$ in the z direction is given by

$$\hat{H} = -\gamma_1\hbar B\hat{I}_{1z} - \gamma_2\hbar B\hat{I}_{2z} \qquad (2\text{-}43)$$

where the indices relate to the different spin particles.

It can easily be seen that the product spin functions $|m_1m_2\rangle$ are the eigenfunctions of the spin Hamiltonian:

$$\begin{aligned}&\hat{H}\left|m_1m_2\right\rangle \\ &=\left(-\gamma_1\hbar B\hat{\mathbf{I}}_{1z}-\gamma_2\hbar B\hat{\mathbf{I}}_{2z}\right)\left|m_1m_2\right\rangle \\ &=-\gamma_1\hbar B\hat{\mathbf{I}}_{1z}\left|m_1m_2\right\rangle-\gamma_2\hbar B\hat{\mathbf{I}}_{2z}\left|m_1m_2\right\rangle \\ &=-\gamma_1\hbar Bm_1\left|m_1m_2\right\rangle-\gamma_2\hbar Bm_2\left|m_1m_2\right\rangle \\ &=\left(-\gamma_1m_1-\gamma_2m_2\right)\hbar B\left|m_1m_2\right\rangle\end{aligned} \tag{2-44}$$

The energy levels are thus given by

$$U(m_1,m_2)=\left(-\gamma_1m_1-\gamma_2m_2\right)\hbar B \tag{2-45}$$

The possible transitions follow from the transition probability:

$$\Delta m_1=\pm1,\Delta m_2=0;\text{spin 1 flips} \tag{2-46}$$

$$\Delta m_2=\pm1,\Delta m_1=0;\text{spin 2 flips} \tag{2-47}$$

2-6 General solution of the Schrödinger equation

The time-independent Schrödinger equation

$$\hat{H}\psi=U\psi \tag{2-48}$$

assumes that the spin functions ψ are eigenfunctions of the spin Hamiltonian $\hat{H}$. In cases that we solely deal with z-spin operators, the spin functions $\left|I,m\right\rangle$ or the product spin functions are solutions of the Schrödinger equation. However, in general this is not true. Here we will develop a general mathematical method by which we can find the eigenvalues and eigenfunctions of the spin Hamiltonian $\hat{H}$.

We assume that we have a complete, orthonormal set of spin functions ϕ_n that are used as basis functions in our further approach. The eigenfunction ψ of the spin Hamiltonian $\hat{H}$ can then be written as a linear combination of these basis functions:

$$\psi=\sum_{n=1}^{N}a_n\phi_n \tag{2-49}$$

where n sums over all basis functions. The strategy of this approach is to use a set of basis spin functions of which the properties are well known (for example the spin functions $\left|I,m\right\rangle$), and determine the coefficients a_n using the tools of linear algebra.

> ***Note***
> For example for a spin system of two spin-½-particles there are four basis functions as given by Eqn. 2-42.

From the Schrödinger equation, Eqn. 2-48, it follows that

$$\hat{H}\psi = \sum_n a_n \hat{H}\phi_n = U\sum_n a_n \phi_n \tag{2-50}$$

Multiplying left with ϕ_m^* and integrating over the entire space gives

$$\sum_n a_n \int \phi_m^* \hat{H} \phi_n d\tau = U\sum_n a_n \int \phi_m^* \phi_n d\tau \tag{2-51}$$

or, in the Dirac notation

$$\sum_n a_n \langle m|\hat{H}|n\rangle = U\sum_n a_n \langle m\|n\rangle \tag{2-52}$$

The left-hand part of the equation contains the matrix elements of the Hamiltonian matrix H_{mn}, whereas the right-hand part contains a delta function, because the basis set is orthonormal:

$$\sum_n a_n H_{mn} = U\sum_n a_n \delta_{mn} \tag{2-53}$$

This equation can be rewritten as follows:

$$\sum_n a_n (H_{mn} - U\delta_{mn}) = 0 \tag{2-54}$$

This system of linear equations can be solved by setting the secular determinant to zero:

$$|H_{mn} - U\delta_{mn}| = 0 \tag{2-55}$$

The solution of the determinant gives the eigenvalues U (N in total). Substitution of these eigenvalues into the secular equations

$$\begin{pmatrix} H_{11}-U & H_{12} & \cdots \\ H_{21} & H_{22}-U & \cdots \\ \cdots & \cdots & \cdots \end{pmatrix} \begin{pmatrix} a_1 \\ a_2 \\ \vdots \end{pmatrix} = 0 \tag{2-56}$$

finally gives the coefficients a_n and the eigenfunctions ψ (also N in total).

The spin Hamiltonian $\hat{H}$ is hermitic, so that for the matrix elements

$$H_{mn} = H_{nm}^* \tag{2-57}$$

This equation tells us that we only need to determine the diagonal and upper (or lower) triangle of the Hamiltonian matrix. This saves a lot of time in calculating the total matrix.

2-7 Perturbation theory

Calculating and solving the secular determinant takes a lot of work. However, in many cases it is possible to make approximations that considerable reduce the work. This approach is based on perturbation theory. Perturbation theory can be applied if the system is described by the following Hamilton operator:

$$\hat{H} = \hat{H}^0 + \hat{H}^1 \tag{2-58}$$

where for $\hat{H}^0$ the exact eigenvalues and eigenfunctions are known and $\hat{H}^1$ is a small stationary perturbation of the system.

For the non-perturbed system the Schrödinger equation is:

$$\hat{H}^0 \phi_n = U_n^0 \phi_n \tag{2-59}$$

with eigenfunctions ϕ_n and eigenvalues U_n^0. For this reason the Hamiltonian matrix H_{mn}^0 is diagonal. At the same time the functions ϕ_n form a complete, orthonormal set. Now we are able to solve the Schrödinger equation for the total Hamiltonian, Eqn. 2-58, following the method that is described before. This gives the secular determinant

$$\left|H_{mn} - U\delta_{mn}\right| = \left|H_{mn}^1 + \left(H_{nn}^0 - U\right)\delta_{mn}\right| = 0 \tag{2-60}$$

Because we can write

$$H_{nn}^0 = U_n^0 \tag{2-61}$$

the secular determinant can be written as follows

$$\begin{vmatrix} U_n^0 + H_{nn}^1 - U & H_{nm}^1 & \cdots \\ H_{mn}^1 & U_m^0 + H_{mm}^1 - U & \cdots \\ \cdots & \cdots & \cdots \end{vmatrix} = 0 \tag{2-62}$$

The operator $\hat{H}^1$ represents a small perturbation. This means that the matrix elements H_{mn}^1 are small as compared to the diagonal elements of the operator $\hat{H}^0$, which are U_n^0. In a first-order approximation of the evaluation of the secular determinant, we can neglect the non-diagonal elements of the determinant, so that the first-order solutions of the secular determinant are the diagonal elements:

$$U_n = U_n^0 + H_{nn}^1 \tag{2-63}$$

In general the calculation of H_{nn}^1 is rather simple, giving rise to a straightforward calculation of the energy levels.

In the case that the energy levels U_n^0 are degenerated, Eqn. 2-63 can not be applied. It is then necessary to exactly solve the sub-determinant in which the degenerated energy levels appear.

Therefore the general rule for using a first-order approximation of the secular determinant with elements H_{mn} is:

$$\text{If } |H_{mm} - H_{nn}| >> |H_{mn}| \tag{2-64}$$

the non-diagonal elements H_{mn} can be neglected.

(In Eqn. 2-64 |...| means the absolute value.)

2-8 General procedure to determine a spectrum

Based on our discussion above, we can now develop a general procedure to determine the magnetic resonance spectrum of a spin system.

Step 1

Determine the spin Hamiltonian of the spin system. Take into account all magnetic interactions: interactions of the spins with an external magnetic field (Zeeman interaction), as well as the interactions between the spins (see **Chapter 3**). If necessary, use approximations to reduce the spin Hamiltonian. For example, certain operators, such as $\hat{\mathbf{I}}_x$, give rise to non-diagonal elements in the Hamiltonian matrix and can often be neglected in non-degenerated systems if their contributions are small as compared to the diagonal elements, i.e. in the presence of a strong Zeeman interaction (see **Section 2-7 Perturbation theory**).

Step 2

Select a suitable basis set of spin functions. In the presence of a strong external magnetic field the spin functions $|I,m\rangle$ or their products are generally a good choice. Also it is often useful to make a basis set of spin functions based on a linear combination of spin functions, given by symmetry. For example, the following combinations of the spin functions are symmetric and anti-symmetric for exchange of the spins:

$$\begin{aligned} \varphi_1 &= T_1 = \alpha\alpha \\ \varphi_2 &= T_0 = \tfrac{1}{2}\sqrt{2}(\alpha\beta + \beta\alpha) \\ \varphi_3 &= T_{-1} = \beta\beta \end{aligned} \tag{2-65}$$

are symmetric for exchange of the spin indices, and

$$\varphi_4 = S = \tfrac{1}{2}\sqrt{2}(\alpha\beta - \beta\alpha) \tag{2-66}$$

is anti-symmetric.

This grouping of the spin functions directly gives the so-called triplet ($T_{1,0,-1}$, Eqn. 2-65) and singlet (S , Eqn. 2-66) spin functions. This situation only applies if the spins are identical (magnetic equivalence).

> ***Note***
> The triplet spin functions $T_{1,0,-1}$ behave identical to the three spin functions $|I,m\rangle$ with I = 1, m = 1, 0 , and -1. The singlet spin function S is identical to $|0,0\rangle$. In fact, this is equivalent to a "spin-less" particle with no magnetic properties.

The triplet functions are quantised along the z axis. We can make new linear combinations of these functions that are independent of direction. These functions are useful in situations in the absence of an external magnetic field, and are called zero-field functions:

$$\begin{aligned} T_x &= \tfrac{1}{2}\sqrt{2}(\beta\beta - \alpha\alpha) = \tfrac{1}{2}\sqrt{2}(T_{-1} - T_1) \\ T_y &= \tfrac{1}{2}i\sqrt{2}(\beta\beta + \alpha\alpha) = \tfrac{1}{2}i\sqrt{2}(T_{-1} + T_1) \\ T_z &= \tfrac{1}{2}\sqrt{2}(\alpha\beta + \beta\alpha) = \varphi_2 = T_0 \end{aligned} \qquad (2\text{-}67)$$

Step 3

Determine the Hamiltonian matrix H_{mn} using the basis set of spin functions.

Step 4

Solve the secular determinant, which gives the energy levels U_1, U_2, ...:

$$\begin{vmatrix} H_{11} - U & H_{12} & \dots \\ H_{21} & H_{22} - U & \dots \\ \dots & \dots & \dots \end{vmatrix} = 0 \qquad (2\text{-}68)$$

> ***Note***
> If the Hamiltonian matrix contains several non-diagonal elements that are zero, try to factorise the matrix into sub-matrices.

Step 5

Determine the coefficients of the eigenfunctions by solving the secular equations.

Step 6

Determine the transitions probabilities using the eigenfunctions with Eqn. 2-36.

> ***Note***
> When the Hamiltonian matrix is not diagonal, the basis spin functions will mix. If the basis spin functions are z quantised, so-called *second order transitions*

will appear. In other words, transitions that are forbidden with the basis spin functions are now allowed.

Step 7

Draw the magnetic resonance spectrum.

Example 2-3

The following example illustrates steps 1 to 7 for a spin-½-particle in an external magnetic field $\vec{\mathbf{B}}$ that is directed along the x axis.

Step 1: Spin Hamiltonian.
In analogy with Eqn. 2-12 the spin Hamiltonian is:

$$\hat{H} = -\gamma\hbar B\hat{I}_x \tag{2-69}$$

Step 2: Basis spin functions.
A good choice are the spin functions $|\alpha\rangle$ and $|\beta\rangle$. These functions form a complete orthonormal set for this 2-dimensional spin space of a spin-½-particle. The functions are not the eigenfunctions of the spin Hamiltonian, however we can easily calculate the effect of operator $\hat{I}_x$ on these functions.

Step 3: Hamiltonian matrix H_{mn}.

$$\begin{array}{ccc} \hat{H} & |\alpha\rangle & |\beta\rangle \\ \langle\alpha| & 0 & -\frac{1}{2}\gamma\hbar B \\ \langle\beta| & -\frac{1}{2}\gamma\hbar B & 0 \end{array} \tag{2-70}$$

Step 4: Secular determinant.

$$\begin{vmatrix} -U & -\frac{1}{2}\gamma\hbar B \\ -\frac{1}{2}\gamma\hbar B & -U \end{vmatrix} = 0 \tag{2-71}$$

Solving this determinant gives:

$$U^2 - \frac{1}{4}\gamma^2\hbar^2B^2 = 0 \rightarrow U_{1,2} = \pm\frac{1}{2}\gamma\hbar B \tag{2-72}$$

Step 5: Eigenfunctions.
The secular equations are:

$$\begin{pmatrix} -U & -\frac{1}{2}\gamma\hbar B \\ -\frac{1}{2}\gamma\hbar B & -U \end{pmatrix}\begin{pmatrix} a_1 \\ a_2 \end{pmatrix} = 0 \tag{2-73}$$

Substituting $U_1 = \frac{1}{2}\gamma\hbar B$ gives $a_1 = -a_2$. Taking into account the normalisation the first eigenfunction is:

$$\psi_1 = \tfrac{1}{2}\sqrt{2}\left(|\alpha\rangle - |\beta\rangle\right) \tag{2-74}$$

Substituting $U_2 = -\frac{1}{2}\gamma\hbar B$ gives $a_1 = a_2$. Taking into account the normalisation the second eigenfunction is:

$$\psi_2 = \tfrac{1}{2}\sqrt{2}\left(|\alpha\rangle + |\beta\rangle\right) \tag{2-75}$$

Step 6: Transition probabilities.
Quantum mechanics has learned us that the radiofrequency field $\vec{\mathbf{B}}_1$ must be perpendicular to the external field $\vec{\mathbf{B}}$. For convenience, we take $\vec{\mathbf{B}}_1$ along the z direction. The transition probability $P_{mm'}$ for the transition between the two energy levels now contains the matrix element:

$$\langle 1|\hat{\mathbf{I}}_z|2\rangle \tag{2-76}$$

It can easily be verified that this is term is non-zero, so that the transition is allowed:

$$\begin{aligned}
&\left\langle \tfrac{1}{2}\sqrt{2}\left(|\alpha\rangle - |\beta\rangle\right)\middle|\hat{\mathbf{I}}_z\middle|\tfrac{1}{2}\sqrt{2}\left(|\alpha\rangle + |\beta\rangle\right)\right\rangle \\
&= \tfrac{1}{2}\left\langle\left(\langle\alpha| - \langle\beta|\right)|\hat{\mathbf{I}}_z|\left(|\alpha\rangle + |\beta\rangle\right)\right\rangle \\
&= \tfrac{1}{2}\left\langle\left(\langle\alpha| - \langle\beta|\right)\left\|\left(\tfrac{1}{2}|\alpha\rangle + \left(-\tfrac{1}{2}\right)\beta\right\rangle\right\rangle\right\rangle \\
&= \tfrac{1}{4}\left\langle\left(\langle\alpha| - \langle\beta|\right)\left\|\left(|\alpha\rangle - |\beta\rangle\right)\right\rangle\right\rangle \\
&= \tfrac{1}{4}\left(\langle\alpha\|\alpha\rangle - \langle\alpha\|\beta\rangle - \langle\beta\|\alpha\rangle + \langle\beta\|\beta\rangle\right) \\
&= \tfrac{1}{4}(1+0+0+1) \\
&= \tfrac{1}{2}
\end{aligned} \tag{2-77}$$

Step 7: The spectrum.
The magnetic resonance spectrum consists of a single line, given by the resonance condition (see step 4):

$$\Delta U = \gamma\hbar B \tag{2-78}$$

and

$$\nu = (\gamma/2\pi)B \tag{2-79}$$

This is pretty obvious result and the question is whether we could have predicted it beforehand. The answer is, yes, of course! The selection of the axes system in which we place the magnetic moment is completely free. We could equally well

have selected the external magnetic field $\vec{\mathbf{B}}$ along the z axis, and this result has been discussed (see **section 2-1 Spin operators**). In fact only the size of the magnetic field is important.

good use of symmetry bad use of symmetry

Fig. 2-2.
Good and bad use of symmetry in defining an axes system for the spin Hamiltonian.

We can further understand this by considering symmetry relations. As is shown in Fig. 2-2, a magnetic dipole moment $\vec{\boldsymbol{\mu}}$ has a cylinder symmetry with the symmetry axis passing through the poles. Also a magnetic field has a cylinder symmetry with an axis given by the direction of the field. The optimal situation for a physical analysis of such a system is to let those symmetry axes coincide, *i.e.* by selecting $\vec{\mathbf{B}}$ along the z axis. Indeed the calculations are then simple. However, by selecting $\vec{\mathbf{B}}$ along the x axis, we do not take into account the symmetry relations and are confronted with a lot of work, finally leading to the same answer.

> ***Note***
> The moral from this story is that a good choice of an axes system for describing the spin Hamiltonian can save a lot of work. If we are dealing with strong Zeeman interactions, in most cases it is sensible to place $\vec{\mathbf{B}}$ along the z axis. This generally applies for NMR and ESR in solutions. However, if we have to deal with solid state situations, often the z axis is determined by the principal axes system of the interaction tensors (see for example **Chapter 4**.

2-9 Total spin angular momentum

By making use of the description of the total spin angular momentum a large spin system with several identical spins can be analysed in a general way. In the following, we will illustrate this principle for a system of two identical spin-½-particles.

The operator $\hat{\mathbf{F}}$ for the total spin angular momentum is given by

$$\hat{\mathbf{F}} = \hat{\mathbf{I}}_1 + \hat{\mathbf{I}}_2 \tag{2-80}$$

The z component of $\hat{\mathbf{F}}$ is given by

$$\hat{\mathbf{F}}_z = \hat{\mathbf{I}}_{1z} + \hat{\mathbf{I}}_{2z} \tag{2-81}$$

Based on the commutation relationships of the individual operators, it can be shown that $\hat{\mathbf{F}}^2$ and $\hat{\mathbf{F}}_z$ commute:

$$\left[\hat{\mathbf{F}}^2, \hat{\mathbf{F}}_z\right] = 0 \tag{2-82}$$

> ***Note***
> This is a tedious, but straightforward calculation. Useful to test your knowledge of commutation rules. Remember that the operators for particle 1 and 2 commute.

This result means that there is a complete set of functions which are simultaneously eigenfunctions of both operators (see **Section 2-1 Spin operators**).

The properties of these eigenfunctions can be deduced as follows.
In general the total magnetic quantum number F_T can have the following values:

$$\left| I_1 - I_2 \right| \leq F_T \leq I_1 + I_2 \tag{2-83}$$

Since we deal with spin-½-particles, $I_1 = I_2 = ½$, we have only two possible values for F_T:

$$F_T = \frac{1}{2} + \frac{1}{2} = 1 \tag{2-84}$$

$$F_T = \frac{1}{2} - \frac{1}{2} = 0 \tag{2-85}$$

The eigenfunctions belonging to $F_T = 1$ can be identified as the triplet spin functions, and $F_T = 0$ gives the singlet spin function.

Now the spin system is placed in an external magnetic field $\mathbf{B}_0$. The two spin-½-particles are identical: $\gamma_1 = \gamma_2 = \gamma$, and the spin Hamiltonian is given by

$$\hat{H} = -\gamma\hbar B\left(\hat{\mathbf{I}}_{1z} + \hat{\mathbf{I}}_{2z}\right) = -\gamma\hbar B\hat{\mathbf{F}}_z \tag{2-86}$$

Clearly in this case of identical spins the Zeeman interaction is determined by the total spin operator.

Because the spin Hamiltonian only contains the operator $\hat{\mathbf{F}}_z$, it is immediately clear that the triplet and singlet spin functions are eigenfunctions of the spin Hamiltonian.

We have two different situations, belonging to the two values of F_T:

Situation 1: $F_T = 0$
The eigenfunction is the singlet $|0,0\rangle$ and the corresponding energy level is 0:

$$S = |0,0\rangle; \qquad U_S = 0 \tag{2-87}$$

Situation 2: $F_T = 1$
The eigenfunctions and corresponding energy levels are:

$$T_{m_T} = |1, m_T\rangle; \qquad U_T(m_T) = -\gamma\hbar B m_T \tag{2-88}$$

where the quantum number m_T is 1, 0, and -1 (these are the eigenvalues of $\hat{\mathbf{F}}_z$).

The resulting energy levels and eigenfunctions are schematically illustrated in Fig. 2-3.

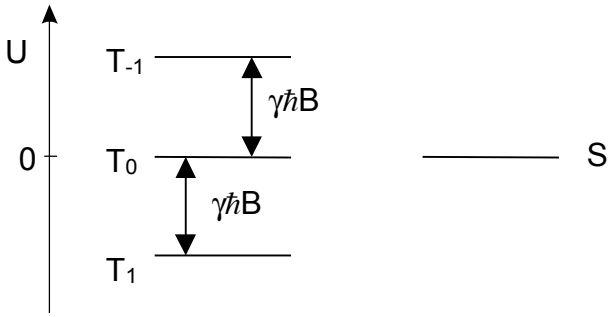

Figure 2-3. Energy levels and allowed transitions in a two-spin system with identical spins.

For a transition $|r\rangle \rightarrow |s\rangle$ the relative intensity is given by (see Eqn. 2-36)

$$\left|\langle s|\hat{\mathbf{F}}_x|r\rangle\right|^2 \tag{2-89}$$

where

$$\hat{\mathbf{F}}_x = \hat{\mathbf{I}}_{1x} + \hat{\mathbf{I}}_{2x} \tag{2-90}$$

Based on the properties of the triplet and singlet spin functions, it can easily be shown that the transition between the singlet and triplet spin states is forbidden, because the values for F_T are different. Within the triplet levels the selection rule gives

$$\Delta m_T = \pm 1 \tag{2-91}$$

The allowed transitions are shown in Fig. 2-3. In this figure it can be seen that the singlet state is isolated from the triplet states. In fact, it has no spin and does not play a role in the magnetic resonance experiment.

> ***Note***
> This calculation illustrates that in the case that two or more spin particles are identical (magnetic equivalent), it is convenient to work within the concept of total spin operators.

Problems

Problem 2-1

Calculate the matrix representation of the operators $\hat{\mathbf{I}}_x$ and $\hat{\mathbf{I}}_y$ of a spin-½-particle (I=½ and m=½). The matrices are hermitic. Show that this is the case and explain this result.

Problem 2-2

Using the expressions for the step operators, show that:

$$\hat{\mathbf{I}}_x\alpha = \tfrac{1}{2}|\beta\rangle \qquad \hat{\mathbf{I}}_x|\beta\rangle = \tfrac{1}{2}|\alpha\rangle$$

$$\hat{\mathbf{I}}_y|\alpha\rangle = \tfrac{1}{2}\mathrm{i}|\beta\rangle \qquad \hat{\mathbf{I}}_y|\beta\rangle = -\tfrac{1}{2}\mathrm{i}|\alpha\rangle$$

Problem 2-3

The step operators are not hermitic. Explain why this is the case.

Problem 2-4

Consider a spin-½-particle in an external magnetic field $\vec{\mathbf{B}}$ that is directed along the y axis. Calculate the energy levels and eigenfunctions.

Problem 2-5

Show that the singlet and triplet spin functions $|\alpha\alpha\rangle$, $\frac{1}{2}\sqrt{2}\left(|\alpha\beta\rangle \pm |\beta\alpha\rangle\right)$, and $|\beta\beta\rangle$ form a complete set of orthonormal functions.

Problem 2-6

Determine the Pauli spin matrices for a spin particle with a spin quantum number I = 1.

Problem 2-7

Consider a spin system of two spin-½-particles.

a. Determine the Hamiltonian matrix using the product spin functions $|\alpha\alpha\rangle$, $|\alpha\beta\rangle$, $|\beta\alpha\rangle$, and $|\beta\beta\rangle$.

b. What are the energy levels?

c. Calculate the transition probabilities.

Problem 2-8

Take the triplet functions T_1, T_0 and T_{-1} of two spin-½-particles. Write this in matrix notation:

$$T_1 = \begin{pmatrix} 1 \\ 0 \\ 0 \end{pmatrix} \qquad T_0 = \begin{pmatrix} 0 \\ 1 \\ 0 \end{pmatrix} \qquad T_{-1} = \begin{pmatrix} 0 \\ 0 \\ 1 \end{pmatrix}$$

a. Calculate the matrix representation of $\hat{\mathbf{F}}_x, \hat{\mathbf{F}}_y$, and $\hat{\mathbf{F}}_z$, using the concept of the total spin operator $\hat{\mathbf{F}} = \hat{\mathbf{I}}_1 + \hat{\mathbf{I}}_2$.

b. Show by matrix multiplication that $\left[\hat{\mathbf{F}}_x, \hat{\mathbf{F}}_y\right] = i\hat{\mathbf{F}}_z$.

Problem 2-9

Using the commutation relationships of components of the spin operator $\hat{\mathbf{I}}$ show that:

a. $\left[\hat{\mathbf{I}}^2, \hat{\mathbf{I}}_\pm\right] = 0$

b. $\left[\hat{\mathbf{I}}_z, \hat{\mathbf{I}}_\pm\right] = \pm\hat{\mathbf{I}}_\pm$

c. $\left[\hat{\mathbf{I}}_+, \hat{\mathbf{I}}_-\right] = 2\hat{\mathbf{I}}_z$

d. $\hat{\mathbf{I}}_x^2 + \hat{\mathbf{I}}_y^2 = \hat{\mathbf{I}}^2 - \hat{\mathbf{I}}_z^2 = \frac{1}{2}\left(\hat{\mathbf{I}}_+\hat{\mathbf{I}}_- + \hat{\mathbf{I}}_-\hat{\mathbf{I}}_+\right)$

e. $\hat{\mathbf{I}}_z\hat{\mathbf{I}}_\pm = \hat{\mathbf{I}}_\pm\left(\hat{\mathbf{I}}_z \pm 1\right)$

f. $\hat{\mathbf{I}}^2 = \hat{\mathbf{I}}_+\hat{\mathbf{I}}_- + \hat{\mathbf{I}}_z^2 - \hat{\mathbf{I}}_z$

Problem 2-10

Given the spin functions

$$\psi_1 = c_1\left|\alpha\beta\right\rangle - c_2\left|\beta\alpha\right\rangle$$

and

$$\psi_2 = c_2\left|\alpha\beta\right\rangle + c_1\left|\beta\alpha\right\rangle$$

with

$$c_1^2 + c_2^2 = 1$$

Show that ψ_1 and ψ_2 are orthonormal.

Problem 2-11

Given the so-called flip-flop Hamiltonian of a two-spin system

$$\hat{H} = \hat{\mathbf{I}}_{1+}\hat{\mathbf{I}}_{2-} + \hat{\mathbf{I}}_{1-}\hat{\mathbf{I}}_{2+}$$

and the spin functions

$$\tfrac{1}{2}\sqrt{2}\left(|\alpha\beta\rangle \pm |\beta\alpha\rangle\right)$$

Calculate the Hamiltonian matrix and determine the corresponding eigenvalues of the flip-flop Hamiltonian.

Problem 2-12

Given the spin functions

$$T_x = \tfrac{1}{2}\sqrt{2}(\beta\beta - \alpha\alpha)$$
$$T_y = \tfrac{1}{2}i\sqrt{2}(\beta\beta + \alpha\alpha)$$

Show that T_x and T_y are orthonormal.

Problem 2-13

Given the Hamiltonian $\hat{H} = \hat{\mathbf{I}}_x$ for a spin-1-particle.
a. Determine the Hamiltonian matrix, starting from the in the z quantised spin functions.

b. Calculate the energy levels.

Problem 2-14

Assume a system of two identical spin-½-particles and a spin Hamiltonian given by

$$\hat{H} = \hat{\mathbf{F}}^2$$

where $\hat{\mathbf{F}}$ is the operator for the total spin angular momentum given by

$$\hat{\mathbf{F}} = \hat{\mathbf{I}}_1 + \hat{\mathbf{I}}_2$$

Take the product spin functions as basis functions for the further calculations:

$$|\alpha\alpha\rangle, |\alpha\beta\rangle, |\beta\alpha\rangle, |\beta\beta\rangle$$

a. Determine the Hamiltonian matrix. Because the basis functions are no eigenfunctions of $\hat{\mathbf{F}}^2$, the matrix is not diagonal.

b. Calculate the eigenvalues and eigenfunctions by solving the secular determinant. Is it allowed to use perturbation theory?.

c. Show that the eigenfunctions found are also eigenfunctions of operator $\hat{\mathbf{F}}_z$. What are the eigenvalues of $\hat{\mathbf{F}}_z$?

d. The results found are not surprising. Give arguments how you could have predicted these results beforehand?

Problem 2-15

Assume a system of two identical spin-½-particles and a spin Hamiltonian given by

$$\hat{H} = \hat{\mathbf{F}}^2$$

a. Show that the zero-field functions T_x, T_y, and T_z are eigenfunctions of the spin Hamiltonian.

b. Calculate the corresponding energy levels.

Problem 2-16

The following problem illustrates the perturbation theory on a 2x2 matrix. Even for such a small matrix, the algebra can become quite laborious.

Given the Hamiltonian matrix

$$\begin{pmatrix} U_1^0 + H_{11}^1 & H_{12}^1 \\ H_{21}^1 & U_2^0 + H_{22}^1 \end{pmatrix}$$

a. Calculate the exact energy levels U_n (n = 1, 2) by solving the secular determinant.
b. Show that in the first order approximation the non-diagonal elements can be neglected and that the energy levels are given by:

$$U_n = U_n^0 + H_{nn}^1$$

provided

$$H_{12}^1 << U_n^0, \text{and } U_1^0 \neq U_2^0$$

c. Can we use this solution when $U_1^0 = U_2^0$? Explain. Calculate the correct energy levels in this case.

Answers

Answer 2-6

$$\hat{\mathbf{I}}_x = \frac{1}{2}\sqrt{2}\begin{pmatrix} 0 & 1 & 0 \\ 1 & 0 & 1 \\ 0 & 1 & 0 \end{pmatrix}$$

$$\hat{\mathbf{I}}_y = \frac{1}{2}\sqrt{2}\begin{pmatrix} 0 & -i & 0 \\ i & 0 & -i \\ 0 & i & 0 \end{pmatrix}$$

$$\hat{\mathbf{I}}_z = \begin{pmatrix} 1 & 0 & 0 \\ 0 & 0 & 0 \\ 0 & 0 & -1 \end{pmatrix}$$

Answer 2-14

The spin Hamiltonian is

$$\hat{H} = \hat{\mathbf{F}}^2$$

which must be applied to the product spin functions:

$$|\alpha\alpha\rangle, |\alpha\beta\rangle, |\beta\alpha\rangle, |\beta\beta\rangle$$

The problem here is that the spin Hamiltonian is written in terms of the total spin angular momentum $\hat{\mathbf{F}} = \hat{\mathbf{I}}_1 + \hat{\mathbf{I}}_2$, whereas the spin functions are related to the individual operators $\hat{\mathbf{I}}_1$ and $\hat{\mathbf{I}}_2$. This means that we must substitute the individual spin operators in the spin Hamiltonian to be able to calculate the Hamiltonian matrix

$$\hat{H} = \left(\hat{\mathbf{I}}_1 + \hat{\mathbf{I}}_2\right)^2 = \hat{\mathbf{I}}_1^2 + \hat{\mathbf{I}}_2^2 + 2\hat{\mathbf{I}}_1 \bullet \hat{\mathbf{I}}_2$$

The scalar product of the operators can be expanded to give

$$\hat{H} = \hat{\mathbf{I}}_1^2 + \hat{\mathbf{I}}_2^2 + 2\hat{I}_{1z}\hat{I}_{2z} + \hat{I}_{1+}\hat{I}_{2-} + \hat{I}_{1-}\hat{I}_{2+}$$

We know the effect of all these individual spin operators on the spin functions and are now able to produce the Hamiltonian matrix:

$\hat{H}$	$\alpha\alpha$	$\alpha\beta$	$\beta\alpha$	$\beta\beta$
$\alpha\alpha$				

$\alpha\beta$				
$\beta\alpha$				
$\beta\beta$				

Let's first have a general look at the spin Hamiltonian in relation to the spin functions. It can easily be verified that the operator

$$\hat{I}_1^2 + \hat{I}_2^2 + 2\hat{I}_{1z}\hat{I}_{2z}$$

produces diagonal elements, but the operator

$$\hat{I}_{1+}\hat{I}_{2-} + \hat{I}_{1-}\hat{I}_{2+}$$

does not act on the diagonal. Closer inspection of this flip-flop term reveals that it only couples $\alpha\beta$ and $\beta\alpha$.

We then have the following general structure of the spin Hamiltonian, which nicely factorises into three main blocks:

$\hat{H}$	$\alpha\alpha$	$\alpha\beta$	$\beta\alpha$	$\beta\beta$
$\alpha\alpha$	X	0	0	0
$\alpha\beta$	0	X	X	0
$\beta\alpha$	0	X	X	0
$\beta\beta$	0	0	0	X

We can directly see that $\alpha\alpha$ and $\beta\beta$ are eigenfunctions, but $\alpha\beta$ and $\beta\alpha$ will mix through the effect of the flip-flop term.

After these general considerations, we must now calculate the matrix elements that are indicated by an "X". Remember that the matrix is hermitic, so that we only need to calculate one of the non-diagonal elements. For example the matrix element connecting $\beta\alpha$ and $\alpha\beta$ is calculated as follows:

$$\begin{aligned}
&\langle\beta\alpha|\hat{I}_{1+}\hat{I}_{2-} + \hat{I}_{1-}\hat{I}_{2+}|\alpha\beta\rangle \\
&= \langle\beta_1\alpha_2|\hat{I}_{1+}\hat{I}_{2-}|\alpha_1\beta_2\rangle + \langle\beta_1\alpha_2|\hat{I}_{1-}\hat{I}_{2+}|\alpha_1\beta_2\rangle \\
&= 0 + \langle\beta_1\alpha_2\|\beta_1\alpha_2\rangle \\
&= 0 + 1 \\
&= 1
\end{aligned}$$

For clarity, we have introduced the indices 1 and 2 to illustrate that the operators of spin 1 and 2 only act on their own spin functions.

The diagonal matrix element for spin function $\alpha\alpha$ is:

$$\frac{3}{4} + \frac{3}{4} + 2\times\frac{1}{2}\times\frac{1}{2}$$

The other diagonal elements are calculated in a similar way, leading to:

$\hat{H}$	$\alpha\alpha$	$\alpha\beta$	$\beta\alpha$	$\beta\beta$
$\alpha\alpha$	2	0	0	0
$\alpha\beta$	0	1	1	0
$\beta\alpha$	0	1	1	0
$\beta\beta$	0	0	0	2

We can directly observe that the eigenvalues belonging to the eigenfunctions $\psi_1 = \alpha\alpha$ and $\psi_4 = \beta\beta$ are 2. For the other two eigenvalues we need to solve the middle 2x2 block of the matrix. Of course, it is not allowed to use perturbation theory, since the non-diagonal matrix elements are of the same size as the diagonal elements.

The secular determinant of the 2x2 block is

$$\begin{vmatrix} 1-U & 1 \\ 1 & 1-U \end{vmatrix} = 0$$

Solving this determinant gives:

$$(1-U)^2 - 1 = U^2 - 2U = 0 \rightarrow U_{2,3} = 0, 2$$

The eigenfunctions follow from the secular equations:

$$\begin{pmatrix} 1-U & 1 \\ 1 & 1-U \end{pmatrix} \begin{pmatrix} a_1 \\ a_2 \end{pmatrix} = 0$$

Substituting $U_2 = 0$ gives $a_1 = -a_2$. Taking into account normalisation the corresponding eigenfunction is:

$$\psi_2 = \tfrac{1}{2}\sqrt{2}(\alpha\beta - \beta\alpha)$$

Substituting $U_3 = 2$ gives $a_1 = a_2$. Taking into account normalisation the corresponding eigenfunction is:

$$\psi_3 = \tfrac{1}{2}\sqrt{2}(\alpha\beta + \beta\alpha)$$

The final result is that the singlet and triplet functions are eigenfunctions of $\hat{\mathbf{F}}^2$, with eigenvalues 0 and 2, respectively. This result is in agreement with the findings of the total spin angular momentum (see **Section 2-9 Total spin angular momentum**), where was shown that the singlet and triplet functions are obtained for $F_T = 0$ and 1. The corresponding eigenvalues belonging to these values of F_T, which are given by $F_T(F_T + 1)$, are 0 and 2.

It is left to the reader to show that the eigenfunctions found are also eigenfunctions of operator $\hat{\mathbf{F}}_z$.

3

Interactions between spins

3-1 Introduction

In this section we will describe the general forms of interactions that can take place between magnetic moments. These interactions can be sub-divided into **isotropic** spin-spin interactions that show up in fluids: the nuclear-nuclear interaction is called the spin-spin coupling or J-coupling; the nuclear-electron interaction is called the Fermi-contact interaction; the electron-electron interaction is often referred to as the spin-exchange interaction. The magnetic resonance (NMR and ESR) spectra in solution are determined by one or more of these spin-spin interactions and the isotropic Zeeman interaction.

The **anisotropic** interactions are angular dependent and occur in the solid state. A very important interaction in solids is the dipole-dipole interaction. Dipole-dipole interactions can take place between all types of spin particles: nuclei and electrons. The anisotropic Zeeman interaction and dipolar interactions determine the magnetic resonance spectra in solids.

3-2 The dipole-dipole interaction

The classical expression for the energy U of dipole-dipole coupling between two magnetic point dipoles $\vec{\boldsymbol{\mu}}_1$ and $\vec{\boldsymbol{\mu}}_2$ separated at a distance $\vec{\mathbf{r}}$ is given by the following expression (see also R.K. Harris, Nuclear Magnetic Resonance Spectroscopy. A physicochemical view, chapter 4.1)

$$U = \frac{\mu_0}{4\pi}\left\{\frac{\vec{\boldsymbol{\mu}}_1 \bullet \vec{\boldsymbol{\mu}}_2}{r^3} - 3\frac{(\vec{\boldsymbol{\mu}}_1 \bullet \vec{\mathbf{r}})(\vec{\boldsymbol{\mu}}_2 \bullet \vec{\mathbf{r}})}{r^5}\right\}$$

The appropriate quantum mechanical expression is obtained by using $\hat{\boldsymbol{\mu}} = \gamma\hbar\hat{\mathbf{I}}$ and replacing the energy by the spin Hamiltonian:

$$\hat{H} = \frac{\mu_0}{4\pi}\gamma_1\gamma_2\hbar^2\left\{\frac{\hat{\mathbf{I}}_1 \bullet \hat{\mathbf{I}}_2}{r^3} - 3\frac{(\hat{\mathbf{I}}_1 \bullet \vec{\mathbf{r}})(\hat{\mathbf{I}}_2 \bullet \vec{\mathbf{r}})}{r^5}\right\} \qquad (3\text{-}1)$$

where γ_1 and γ_2 are the gyromagnetic ratios of the two magnetic particles (see Fig. 3-1).

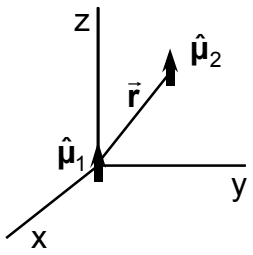

Figure 3-1.
Two magnetic point dipoles $\hat{\mu}_1$ and $\hat{\mu}_2$ separated at a distance $\vec{r}$.

We can write out the vector products in Eqn. 3-1 as follows:

$$\hat{I}_1 \bullet \hat{I}_2 = \hat{I}_{1x}\hat{I}_{2x} + \hat{I}_{1y}\hat{I}_{2y} + \hat{I}_{1z}\hat{I}_{2z} \tag{3-2}$$

$$\hat{I}_1 \bullet \vec{r} = \hat{I}_{1x}x + \hat{I}_{1y}y + \hat{I}_{1z}z$$

$$\hat{I}_2 \bullet \vec{r} = \hat{I}_{2x}x + \hat{I}_{2y}y + \hat{I}_{2z}z$$

where x, y, an z are the components of $\vec{r}$.

The spin Hamiltonian, Eqn. 3-1, can now be rewritten as

$$\hat{H} = \frac{\mu_0}{4\pi}\frac{\gamma_1\gamma_2\hbar^2}{r^5}\left\{\begin{array}{l}\hat{I}_{1x}\hat{I}_{2x}\left(r^2-3x^2\right)+\hat{I}_{1y}\hat{I}_{2y}\left(r^2-3y^2\right)+\hat{I}_{1z}\hat{I}_{2z}\left(r^2-3z^2\right)\\ -\left(\hat{I}_{1x}\hat{I}_{2y}+\hat{I}_{1y}\hat{I}_{2x}\right)3xy-\left(\hat{I}_{1y}\hat{I}_{2z}+\hat{I}_{1z}\hat{I}_{2y}\right)3yz-\left(\hat{I}_{1z}\hat{I}_{2x}+\hat{I}_{1x}\hat{I}_{2z}\right)3zx\end{array}\right\} \tag{3-3}$$

This equation can be transferred into a simple matrix equation

$$\hat{H} = \hat{I}_1 \bullet \mathbf{D} \bullet \hat{I}_2 \tag{3-4}$$

in which $\hat{I}_1$ is a row vector, $\hat{I}_2$ a column vector, and **D** a matrix with elements D_{ij} (i, j = x, y, z)

$$\hat{H} = \begin{pmatrix}\hat{I}_{1x} & \hat{I}_{1y} & \hat{I}_{1z}\end{pmatrix}\begin{pmatrix}D_{xx} & D_{xy} & D_{xz}\\ D_{yx} & D_{yy} & D_{yz}\\ D_{zx} & D_{zy} & D_{zz}\end{pmatrix}\begin{pmatrix}\hat{I}_{2x}\\ \hat{I}_{2y}\\ \hat{I}_{2z}\end{pmatrix} \tag{3-5}$$

The matrix **D**, which is called the dipolar coupling tensor, is given by

$$\mathbf{D} = \frac{\mu_0}{4\pi}\frac{\gamma_1\gamma_2\hbar^2}{r^5}\begin{pmatrix}r^2-3x^2 & -3xy & -3xz\\ -3xy & r^2-3y^2 & -3yz\\ -3xz & -3yz & r^2-3z^2\end{pmatrix} \tag{3-6}$$

Note that the tensor **D** is symmetric. In addition, from Eqn. 6 it follows that the trace of **D** is zero, i.e.

$$\mathrm{Tr}(\mathbf{D}) = \sum_i D_{ii} = \left(r^2 - 3x^2\right) + \left(r^2 - 3y^2\right) + \left(r^2 - 3z^2\right) = 0 \qquad (3\text{-}7)$$

because from Fig. 1 it follows: $x^2 + y^2 + z^2 = r^2$.

From matrix theory it can be found that the trace of a matrix is invariant for a rotation in space. Thus the trace of **D** is zero at all orientations of the magnetic point dipoles in space.

Let us assume that the vector $\vec{\mathbf{r}}$ is fixed in a molecule that makes random rotational fluctuations in space (rotational diffusion). If the motion is isotropic, all positions of $\vec{\mathbf{r}}$ in space have an equal probability. The average value of the dipolar coupling tensor $\overline{\mathbf{D}}$ can then be found by calculating the average values of the elements $\overline{D_{ij}}$ if the motion is fast.

Because

$$\overline{x}^2 = \overline{y}^2 = \overline{z}^2 = \frac{1}{3} r^2$$

it follows from Eqn. 3-6 that

$$\overline{D}_{xx} = \overline{D}_{yy} = \overline{D}_{zz} = 0 .$$

Furthermore

$$\overline{xy} = \overline{x} \,.\, \overline{y} = 0 ,$$

so that

$$\overline{D}_{xy} = 0 ,$$

since $\overline{x} = \overline{y} = 0$ and x and y are not correlated. The same applies for the other non-diagonal tensor elements. In conclusion, we find that the average tensor $\overline{\mathbf{D}}$ vanishes for fast isotropic rotational diffusion. This is the reason that in fluids the dipolar interaction does not contribute to the stationary spin Hamiltonian that determines the positions of the lines in the magnetic resonance spectra. However, the time-dependent fluctuations of the elements $D_{ij}(t)$ generated by the motion contribute to relaxation processes (T_1 and T_2 relaxation).

The dipolar tensor represents a so-called **through-space** interaction, because this is a direct interaction. This is in contrast with, for example, the spin-spin coupling between nuclei, which is mediated through the bonds. Such an interaction is called a **through-bond** interaction.

3-3 Principal axes of a tensor

The dipolar coupling tensor **D** is a matrix with nine components given by Eqn. 3-6. This generates a complex dipolar spin Hamiltonian. Therefore it is useful to reduce it to a more simple form. This is done by using a diagonal representation of the tensor **D**. From matrix theory it is known that, apart from a few exceptions, every matrix can be diagonalized (this is equivalent to the determination of the eigenvalues of a matrix). In fact, such a diagonalization is a rotation of the matrix in space until the non-diagonal elements vanish. The axes system in which the matrix is diagonal is called the principal axes system. Working in the principal axes systems saves a lot of calculations in evaluating spin Hamiltonians and is generally a good strategy.

In the principal axes system {X, Y, Z}, the dipolar coupling matrix **D** is

$$\mathbf{D} = \begin{pmatrix} D_{XX} & 0 & 0 \\ 0 & D_{YY} & 0 \\ 0 & 0 & D_{ZZ} \end{pmatrix}$$

where D_{XX}, D_{YY}, and D_{ZZ} are the principal values of tensor **D**. In this case Eqn. 3-4 reduces to

$$\hat{H} = D_{XX}\hat{I}_{1x}\hat{I}_{2x} + D_{YY}\hat{I}_{1y}\hat{I}_{2y} + D_{ZZ}\hat{I}_{1z}\hat{I}_{2z} \qquad (3\text{-}8)$$

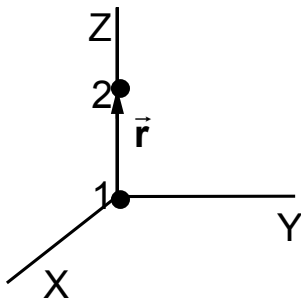

Figure 3-2.
Principal axes system {X, Y, Z} of two nuclei 1 and 2 separated at a distance r. The Z axis is the axial symmetry axis of the system.

Example 3-1

The principal axes coincide with the symmetry axes of a spin system. This is illustrated in an example of two nuclei at a distance r (see Fig. 3-2). It can easily be verified that one of the principal axes must be chosen through the two nuclei, which is the axial symmetry axis of the system. Taking this as the Z axis, and noting that $\vec{\mathbf{r}} = (0 \quad 0 \quad r)$, we obtain the following principal values for the dipolar coupling tensor **D**

$$D_{XX} = \frac{\mu_0}{4\pi}\frac{\gamma_1\gamma_2\hbar^2}{r^5}\left(r^2 - 3X^2\right) = \frac{\mu_0}{4\pi}\frac{\gamma_1\gamma_2\hbar^2}{r^3} \tag{3-9a}$$

$$D_{YY} = \frac{\mu_0}{4\pi}\frac{\gamma_1\gamma_2\hbar^2}{r^5}\left(r^2 - 3Y^2\right) = \frac{\mu_0}{4\pi}\frac{\gamma_1\gamma_2\hbar^2}{r^3} \tag{3-9b}$$

$$D_{ZZ} = \frac{\mu_0}{4\pi}\frac{\gamma_1\gamma_2\hbar^2}{r^5}\left(r^2 - 3Z^2\right) = -2\frac{\mu_0}{4\pi}\frac{\gamma_1\gamma_2\hbar^2}{r^3} \tag{3-9c}$$

Clearly, the tensor **D** is axially symmetric since $D_{XX} = D_{YY}$. In matrix form, **D** can thus be written as

$$\mathbf{D} = \frac{\mu_0}{4\pi}\frac{\gamma_1\gamma_2\hbar^2}{r^3}\begin{pmatrix} 1 & 0 & 0 \\ 0 & 1 & 0 \\ 0 & 0 & -2 \end{pmatrix} \tag{3-10}$$

In the case of a dipolar interaction of a nucleus with an electron in an orbit, or for two electrons in an orbit, the interaction should be averaged over the spatial distribution of the electrons. If Ψ is the electronic wave function, the principal axes are now determined by the symmetry axis of the wave function (or: electron density), and we obtain the following averaged principal values $\langle D_{ii} \rangle$

$$\langle D_{ii} \rangle = \int \Psi^* D_{ii} \Psi d\tau \tag{3-11}$$

3-4 Fermi-contact interaction

A magnetic nucleus and an electron may have a magnetic interaction by virtue of their contact: this magnetic interaction is the Fermi-contact interaction. In the derivation of the spin Hamiltonian of the dipole-dipole interaction, we assumed point magnetic dipoles. This is true at a distance far from the dipoles, but close to the nucleus, the point-source nature is invalid and the magnetic field is characteristic of a circular loop of non-vanishing diameter. Far from the nucleus, the electron experiences a pure dipole magnetic moment, but if it penetrates the nucleus it enters quite a different region, where the field flows in only one direction. The magnetic interaction between this non-dipolar field and the magnetic moment of the electron is the contact interaction. Only s-electrons can show a Fermi-contact interaction, since they have a density at the nucleus. Since s-electrons are

spherically symmetrical it also follows that the interaction has no directional characteristics, and indeed it is found to be isotropic.

For the 1s-orbital in the hydrogen atom the contact interaction is equivalent to a magnetic field of 50.8 mT acting on the electron. The Fermi-contact interaction play an important role in ESR spectra, because the extra local field appears in the spectrum as a hyperfine structure. The contact interaction, being isotropic, does not vanish in fluid media. It also plays an important role in NMR because it is a contribution to one of the mechanisms of spin-spin coupling.

The Hamiltonian for Fermi-contact interaction is given by

$$\hat{H} = A\hat{\mathbf{S}} \bullet \hat{\mathbf{I}} \tag{3-12}$$

where A is the hyperfine constant, which is proportional to the probability to find the electron at the nucleus: $\left|\Psi_s(0)\right|^2$. $\hat{\mathbf{S}}$ is the spin operator for the electron.

Note that in Eqn. 3-12, the hyperfine constant A is in energy units, but generally the hyperfine constant is expressed in Tesla (T) as determined from the splittings in the experimental ESR spectra. Clearly, the hyperfine constant A is independent of the external magnetic field.

3-5 Spin-spin coupling

The interaction between nuclei that in NMR spectra give rise to the fine structure is called spin-spin coupling. Its magnitude is generally denoted J and quoted in Hz. The origin of the interaction comes from the Fermi-contact interaction, but the effect is transmitted from one nucleus to the other via the electrons in the bonds. The spin-spin coupling is isotropic, because the Fermi-contact interaction is isotropic. Because the interactions take place via the bonds, this type of interaction is referred to as a "through bond" interaction.
The Hamiltonian for spin-spin coupling is given by

$$\hat{H} = hJ\hat{\mathbf{I}}_1 \bullet \hat{\mathbf{I}}_2 \tag{3-13}$$

where J is the coupling constant, or J-coupling, expressed in Hz. Because in the mechanism of the Fermi-contact interaction and spin-spin coupling an external magnetic field plays no role, the contribution of the spin-spin coupling is independent of a magnetic field.

3-6 Spin exchange interaction

A spin exchange interaction takes place between two electrons that have overlapping orbitals. The exchange contribution J_{12} arises from the Pauli principle and the behaviour of wave functions when electrons are exchanged. The resulting spin Hamiltonian is given by

$$\hat{H} = -2J_{12}\hat{\mathbf{S}}_1 \bullet \hat{\mathbf{S}}_2 \tag{3-14}$$

Spin exchange interactions take place in concentrated solutions of free radicals, where collisions occur so that an overlap of orbitals takes place. Also in paramagnetic solids strong exchange interactions are found and the exchange interaction can be visualised as electron spins that are hopping fast over paramagnetic centres. This effect can be so strong that it averages out the dipolar interaction (that would give very broad ESR spectra) between the spins. This process is called exchange narrowing.

Example 3-2

Consider two electron spins with a strong exchange. From the theory of chemical bonds it is known that such an exchange interaction leads to a singlet and triplet state of the spins with a separation $2J_{12}$, where J_{12} is the exchange integral

$$J_{12} = \frac{1}{4\pi\varepsilon_0} \iint \phi_a^*(1)\phi_b^*(2)\frac{e^2}{r_{12}}\phi_b(1)\phi_a(2)d\tau_1 d\tau_2$$

The term e^2/r_{12} represents the exchange interaction; ϕ_a and ϕ_b are the orbital wave functions; the electrons are denoted by the numbers 1 and 2.

This result also follows from Eqn. 3-14, as will be shown below. For this purpose, rewrite Eqn. 3-14 as follows:

$$\hat{H} = J_{12}\left(\hat{\mathbf{S}}_1^2 + \hat{\mathbf{S}}_2^2 - \hat{\mathbf{S}}^2\right) \tag{3-15}$$

where the total spin operator $\hat{\mathbf{S}}$ is given by the sum of the individual operators

$$\hat{\mathbf{S}} = \hat{\mathbf{S}}_1 + \hat{\mathbf{S}}_2 . \tag{3-16}$$

The eigenfunctions of $\hat{\mathbf{S}}^2$ are the triplet and singlet functions $\left|S,m_s\right\rangle$ with eigenvalues S(S+1), with S= 0, or 1. The effect of the operators $\hat{\mathbf{S}}_1^2$ and $\hat{\mathbf{S}}_2^2$ on triplet and singlet functions is always (**Explain this!**)

$$\tfrac{1}{2}\left(\tfrac{1}{2}+1\right) = \tfrac{3}{4}$$

With this result, Eqn. 3-15 becomes

$$\hat{H} = J_{12}\left(\tfrac{3}{2} - \hat{\mathbf{S}}^2\right) \tag{3-17}$$

which has the following eigenvalues

$$U = J_{12}\left\{\tfrac{3}{2} - S(S+1)\right\} \tag{3-18}$$

For the singlet S = 0, so that $U_S = \frac{3}{2}J_{12}$. For the triplet S = 1, which gives $U_T = -\frac{1}{2}J_{12}$ (see the energy levels in Fig. 3-3). The energy difference $\Delta U = U_S - U_T = 2J_{12}$, which is identical to the exchange energy from orbital theory.

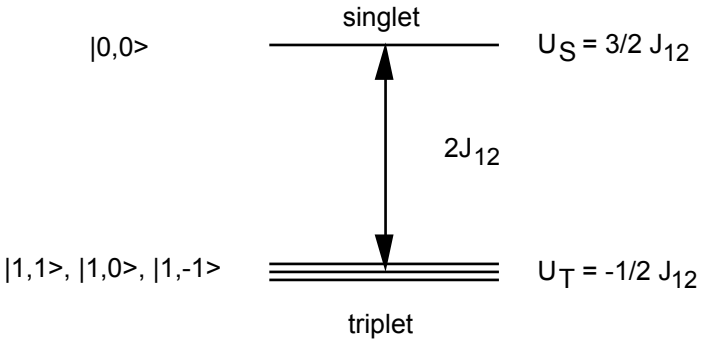

Figure 3-3.
Energy levels of a two electron spin system with an exchange interaction. For the singlet the spin function is |0,0>. The triplet has the spin functions |1,1>, |1,0>, and |1,-1>.

3-7 General expression of spin-spin interaction

By combining the anisotropic and isotropic interactions in a single expression for the Hamiltonian, we obtain the following equation:

$$\hat{H} = \hat{\mathbf{J}}_1 \bullet \mathbf{T} \bullet \hat{\mathbf{J}}_2 \tag{3-19}$$

Here the tensor **T** represents the interaction, $\hat{\mathbf{J}}_1$ and $\hat{\mathbf{J}}_2$ describe the general operators for nuclei or electrons. The tensor **T** can be separated into an isotropic part A, and an anisotropic dipolar part D_{ij}

$$T_{ij} = A\delta_{ij} + D_{ij} \tag{3-20}$$

By making use of Eqn. 3-7, it can be seen that the isotropic part A is related to the trace of tensor **T**:

$$\frac{1}{3}\mathrm{Tr}(\mathbf{T}) = \frac{1}{3}\sum_i T_{ii} = A \tag{3-21}$$

Problems

Problem 3-1

Consider the spin Hamiltonian for spin exchange

$$\hat{H} = -2J_{12}\hat{\mathbf{S}}_1 \bullet \hat{\mathbf{S}}_2$$

a. Show that this equation can be written as

$$\hat{H} = -2J_{12}\left[\hat{\mathbf{S}}_{1z}\hat{\mathbf{S}}_{2z} + \tfrac{1}{2}\left(\hat{\mathbf{S}}_{1+}\hat{\mathbf{S}}_{2-} + \hat{\mathbf{S}}_{1-}\hat{\mathbf{S}}_{2+}\right)\right]$$

b. Determine the Hamiltonian matrix, starting from the singlet and triplet spin functions $|\alpha\alpha\rangle$, $\frac{1}{2}\sqrt{2}\left(|\alpha\beta\rangle \pm |\beta\alpha\rangle\right)$, and $|\beta\beta\rangle$.

c. Determine the energy levels. Compare your answer with the calculations in Example 3-2. What conclusions can you draw?

Problem 3-2

Consider the spin Hamiltonian for two identical spin-½-particles (for example: protons) with spin-spin coupling

$$\hat{H} = -\gamma\hbar B\left(\hat{\mathbf{I}}_{1z} + \hat{\mathbf{I}}_{2z}\right) + hJ\hat{\mathbf{I}}_1 \bullet \hat{\mathbf{I}}_2$$

a. Write this equation in terms of the total spin operator concept.

b. Show that the singlet $S = |0,0\rangle$ and triplet $T_{m_T} = |1,m_T\rangle$ spin functions are eigenfunctions of this spin Hamiltonian

c. Determine the energy levels. Compare your answer with the calculations in Problem 2-14 and Section 2-9. What conclusions can you draw?

d. What are the selection rules? What is the role of the singlet state in the transitions?

Problem 3-3

Consider the dipolar interaction of an electron in an electron orbital with a nucleus.

a. Show that for the electron in a spherical orbital:

$$\langle D_{ii}\rangle = \int \psi^* D_{ii}\psi d\tau = 0 \text{ for } i = x,y,z$$

b. Calculate $\langle D_{ii}\rangle$ for the electron in a $2p_z$ orbital.

Hint: What are the favourable principal axes of tensor **D**?. What can you derive from the symmetry of the systems?

Given: The expressions for the electron orbitals are as follows:

$$\psi_{1s} = f_1(r) \text{ and } \psi_{2p_z} = f_2(r)\cos\theta$$

where $f_1(r)$ en $f_2(r)$ are functions of the distance r and θ is the polar angle. Note that the shape of these functions is not relevant. Can you explain why?

Problem 3-4

Show that the spin Hamiltonian for dipolar interaction of two identical protons can be written as:

$$h^{-1}\hat{H} = \tfrac{1}{2}R\left(1-3\cos^2\theta\right)\left(3\hat{\mathbf{I}}_{1z}\hat{I}_{2z} - \hat{\mathbf{I}}_1 \bullet \hat{\mathbf{I}}_2\right)$$

Problem 3-5

An electron spin interacts with a nucleus (I = ½) according to the following spin Hamiltonian:

$$\hat{H} = A\hat{\mathbf{S}}_x\hat{\mathbf{I}}_z$$

There is no magnetic field present.

a. Show that the eigenfunctions of this spin Hamiltonian are given by

$$\tfrac{1}{2}\sqrt{2}\left(\alpha_e\alpha_N \pm \beta_e\alpha_N\right) \text{ and } \tfrac{1}{2}\sqrt{2}\left(\alpha_e\beta_N \pm \beta_e\beta_N\right)$$

where the index e indicates the electron, and N the nucleus.

b. Give the energy levels.

c. Calculate the transition probabilities for a small rf field in the x or z direction. Furthermore, indicate which transitions are NMR or ESR transitions.

Problem 3-6

Two protons are placed in an external magnetic field $\vec{\mathbf{B}}$ that is directed along the z axis. The protons are placed on the y axis at a distance a from the origin (see Fig. 3-4).

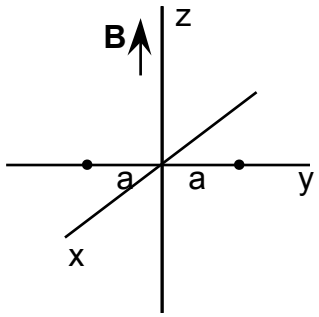

Fig. 3-4.

Two protons on the y axis placed in an external magnetic field $\vec{\mathbf{B}}$ directed along the z axis. The distance of the protons to the origin is a.

a. Assume that a = ∞. In this case the protons do not experience any interaction. Give the spin Hamiltonian, determine the energy levels of the spin system, determine the allowed transitions and draw the NMR spectrum.

b. The protons approach each other, thereby experiencing an increasing dipolar interaction. Assume that the dipolar interactions are small as compared to the Zeeman interaction. For this case, give the spin Hamiltonian, determine the energy levels of the spin system, determine the allowed transitions and draw the NMR spectrum.

c. Sketch the energy levels and spectral changes as a function of parameter a. Where is the breakdown of the perturbation theory?

Problem 3-7

A carbon nucleus (^{13}C) and a proton (^{1}H) approach each other from infinity, thereby experiencing an increasing dipolar interaction. Both nuclei are placed in an external magnetic field $\vec{\mathbf{B}}$ that is directed along the z axis. The axis connecting both nuclei is directed along the x axis. The distance between the nuclei is r.

a. Assume that the distance between the two nuclei is so large that they do not experience a dipolar interaction. Give the spin Hamiltonian, determine the energy levels of the spin system, determine the allowed transitions and draw the NMR spectrum.

b. The nuclei approach each other, such that the dipolar interactions are small as compared to the Zeeman interaction. For this case, give the spin Hamiltonian, determine the energy levels and allowed transitions, and draw the NMR spectrum.

c. Do you expect an NMR spectrum for the case that the dipolar interactions are much stronger than the Zeeman interaction? Give a motivation.

Problem 3-8

Consider two electrons with different g factors experience an exchange interaction in a molecule. The exchange term is given by:

$$\hat{H}_{ex} = J\hat{\mathbf{S}}_1 \bullet \hat{\mathbf{S}}_2$$

a. Give the total spin Hamiltonian of the spin system in the presence of a strong external magnetic field.

b. In the case that the two g factors are equal, show that the exchange term of the spin Hamiltonian commutates with the Zeeman interaction.

c. Will the exchange term also commutate with the Zeeman interaction if the g factors are different? Motivate your answer.

d. Assume that the g factors are equal and consider the situation that the magnetic field B is varied. Calculate and plot the energy levels of the spin system as a function of B, starting from B = 0. Discuss this plot in relation to the ratio B/J.

Answers

Answer 3-2

a. In terms of the spin operator $\hat{\mathbf{F}}$ for the total spin angular momentum the spin Hamiltonian can be written as follows:

$$\hat{H} = -\gamma\hbar B\hat{\mathbf{F}}_z + hJ\frac{1}{2}\left(\hat{\mathbf{F}}^2 - \hat{\mathbf{I}}_1^2 - \hat{\mathbf{I}}_2^2\right)$$

The problem here is that we still are left with the operators $\hat{\mathbf{I}}_1^2$ and $\hat{\mathbf{I}}_2^2$. However, no matter what spin function we have, the effect of these operators is always related to the "length" of the separate spins, which means that we can substitute both operators by their eigenvalue ½(½ + 1). This gives:

$$\hat{H} = -\gamma\hbar B\hat{\mathbf{F}}_z + \frac{1}{2}hJ\left(\hat{\mathbf{F}}^2 - \frac{3}{2}\right)$$

b. Both the singlet $S = |0,0\rangle$ and triplet $T_{m_T} = |1,m_T\rangle$ spin functions are eigenfunctions of this spin Hamiltonian.

For the singlet we have:

$$\hat{H}S = -\gamma\hbar B\hat{\mathbf{F}}_z S + \frac{1}{2}hJ\left(\hat{\mathbf{F}}^2 - \frac{3}{2}\right)S = -\frac{3}{4}hJS$$

giving the energy level:

$$U_S = -\frac{3}{4}hJ$$

For the triplet the result is:

$$\begin{aligned}\hat{H}T_{m_T} &= -\gamma\hbar B\hat{\mathbf{F}}_z T_{m_T} + \frac{1}{2}hJ\left(\hat{\mathbf{F}}^2 - \frac{3}{2}\right)T_{m_T}\\ &= -\gamma\hbar Bm_T T_{m_T} + \frac{1}{2}hJ\left(2 - \frac{3}{2}\right)T_{m_T}\\ &= \left(-\gamma\hbar Bm_T + \frac{1}{4}hJ\right)T_{m_T}\end{aligned}$$

giving the energy levels:

$$U_T(m_T) = -\gamma\hbar Bm_T + \frac{1}{4}hJ$$

c. The energy levels follow from the calculation given above. Note that the coupling constant J appears in the position of the energy levels of the singlet and triplet, but not in the splitting of the triplet.

d. The selection rules are based on the transition probability $|r\rangle \rightarrow |s\rangle$ given by (see Eqn. 2-36):

$$\left|\langle s|\hat{\mathbf{F}}_x|r\rangle\right|^2$$

where

$$\hat{\mathbf{F}}_x = \hat{\mathbf{I}}_{1x} + \hat{\mathbf{I}}_{2x}$$

Since the operator $\hat{\mathbf{F}}_x$ only couples states with $\Delta m_T = \pm 1$ with the same total magnetic quantum number F_T, it can be seen that the transition between singlet and triplet is forbidden, and only two transitions are allowed:

$$T_{-1} \leftrightarrow T_0$$
$$T_0 \leftrightarrow T_1$$

This results for both transitions in the same energy difference

$$\Delta U = \gamma \hbar B$$

This situation corresponds to a spectrum with a single resonance line with lineshape $g(\nu)$ centred at a frequency given by

$$\nu = (\gamma/2\pi)B$$

> ***Note***
> From this calculation, we can conclude that two identical spins show only one resonance line. This is the basis for the rule in NMR spectroscopy that magnetically identical protons do not split each other. There is always an effect of the J-coupling on the spin states, but because the transition between singlet and triplet is not allowed, this J-coupling is not observed. In fact, the singlet is a spin-less state, and does not play a role in the calculation of the spectra.

4

Zeeman interaction

4-1 Interaction of magnetic moments with a magnetic field

In solid materials we have to deal with their anisotropic properties, which are generally described by tensors. For magnetic resonance the dipolar interaction has already been described by the dipolar coupling tensor **D** (see **Section 3-2 The dipole-dipole interaction**).

In analogy with the general expression Eqn. 3-19 of the spin-spin interactions, we can write a general expression for the anisotropic interaction of a magnetic moment with a magnetic field $\vec{\mathbf{B}}$. This so-called Zeeman interaction is expressed by a g-factor tensor **g** for ESR and a chemical shielding tensor $\boldsymbol{\sigma}$ for NMR spectroscopy. The resulting spin Hamiltonians are then as follows

ESR:

$$\hat{H} = \mu_B \vec{\mathbf{B}} \bullet \mathbf{g} \bullet \hat{\mathbf{S}} \tag{4-1}$$

NMR:

$$\hat{H} = -\gamma\hbar \vec{\mathbf{B}} \bullet (\mathbf{1} - \boldsymbol{\sigma}) \bullet \hat{\mathbf{I}} \tag{4-2}$$

In Eqn. 4-2, **1** is a tensor with diagonal values 1 and zero non-diagonal elements. In solution, with molecules tumbling rapidly and isotropically, averaging of the g-factor and shielding tensors occurs and the isotropic quantities observed are given by Eqn. 3-21.

4-2 Anisotropic g-factor tensor

In the following we will work out the Zeeman interaction of an unpaired electron in a molecule in the presence of a magnetic field. We chose a principal axes system {x, y, z} in which the g-factor tensor **g** is diagonal. From Eqn. 4-1 we obtain

$$\hat{H} = \mu_B \left(g_{xx} B_x \hat{\mathbf{S}}_x + g_{yy} B_y \hat{\mathbf{S}}_y + g_{zz} B_z \hat{\mathbf{S}}_z \right) \tag{4-3}$$

where g_{xx}, g_{yy}, and g_{zz} are the principal values of tensor **g**. By using the Pauli matrices of the electron, the Hamiltonian matrix can be found

$$\hat{H} = \tfrac{1}{2}\mu_B \begin{pmatrix} g_{zz}B_z & g_{xx}B_x - ig_{yy}B_y \\ g_{xx}B_x + ig_{yy}B_y & -g_{zz}B_z \end{pmatrix} \tag{4-4}$$

The solution of the secular determinant

$$\begin{vmatrix} \tfrac{1}{2}\mu_B g_{zz}B_z - U & \tfrac{1}{2}\mu_B\left(g_{xx}B_x - ig_{yy}B_y\right) \\ \tfrac{1}{2}\mu_B\left(g_{xx}B_x + ig_{yy}B_y\right) & -\tfrac{1}{2}\mu_B g_{zz}B_z - U \end{vmatrix} = 0 \tag{4-4}$$

gives the following energy levels

$$U = \pm\tfrac{1}{2}\mu_B\sqrt{g_{xx}^2B_x^2 + g_{yy}^2B_y^2 + g_{zz}^2B_z^2} \tag{4-5}$$

For the magnetic field $\vec{\mathbf{B}}$ expressed in polar coordinates:

$$\begin{aligned} B_x &= B\sin\theta\cos\phi \\ B_y &= B\sin\theta\sin\phi \\ B_z &= B\cos\theta \end{aligned} \tag{4-6}$$

with

$$B = \left|\vec{\mathbf{B}}\right| \tag{4-6}$$

Eqn. 4-5 becomes

$$U = \pm\tfrac{1}{2}\mu_B B\sqrt{g_{xx}^2\sin^2\theta\cos^2\phi + g_{yy}^2\sin^2\theta\sin^2\phi + g_{zz}^2\cos^2\theta} \tag{4-7}$$

From Eqn. 4-5 or 4-7, it can be seen that the ESR spectrum consists of a **single resonance line** that moves when the orientation of the magnetic field $\vec{\mathbf{B}}$ is changed with respect to the principal axes system of tensor **g**. This looks as if the apparent g-factor has an orientational dependence.

When the magnetic field $\vec{\mathbf{B}}$ is along the x axis, the resonance condition is

$$B = \frac{h\nu}{\mu_B g_{xx}} \tag{4-8}$$

Similar relations can be obtained for $\vec{\mathbf{B}}$ along the y and z axis. If the **g** tensor is axially symmetric and the symmetry axis is chosen along the z axis, i.e.

$$g_{xx} = g_{yy} = g_\perp \text{ and } g_{zz} = g_{//}$$

Eqn. 4-7 becomes

$$U = \pm\tfrac{1}{2}\mu_B B\sqrt{g_\perp^2 \sin^2\theta + g_{//}^2 \cos^2\theta} \tag{4-9}$$

Because of the axial symmetry around the z-axis, there is no ϕ dependence in Eqn. 4-9.

The situation described above applies for a single crystal system in which the orientation of the magnetic field can be varied with respect to the principal axes system. In a polycrystalline system (a powder), all orientations of $\vec{\mathbf{B}}$ with respect to the principal axes system exist. This results in a distribution of ESR lines over a broad range of resonance fields, a so-called **powder ESR spectrum**. The calculation of powder spectra is described in the following sections.

> ***Note***
> When we deal with solid systems, the axes system for the spin Hamiltonian is taken in accordance with the principal axes system of the dipolar interaction tensors. The magnetic field $\vec{\mathbf{B}}$ is then oriented at an arbitrary position in this axes system. Although this gives a more complicated Zeeman term in the spin Hamiltonian, as show above, the dipolar interaction reduces from nine terms to three diagonal terms in the principal axes representation.

5

ESR of nitroxide spin labels

5-1 The spin Hamiltonian

The spin Hamiltonian of a nitroxide radical, expressed in energy units, is given by

$$\hat{H} = \mu_B \vec{\mathbf{B}} \bullet \mathbf{g} \bullet \hat{\mathbf{S}} + \hat{\mathbf{I}} \bullet \mathbf{A} \bullet \hat{\mathbf{S}} \qquad (5\text{-}1)$$

The first term describes the Zeeman-interaction. This interaction is anisotropic as indicated by the g-factor tensor **g**. The second term give the hyperfine interaction of the unpaired electron with the ^{14}N nucleus (nuclear spin I = 1). This interaction is also anisotropic and given by a hyperfine tensor **A**. Various nitroxide spin labels used in biological applications are shown in Scheme 5-1.

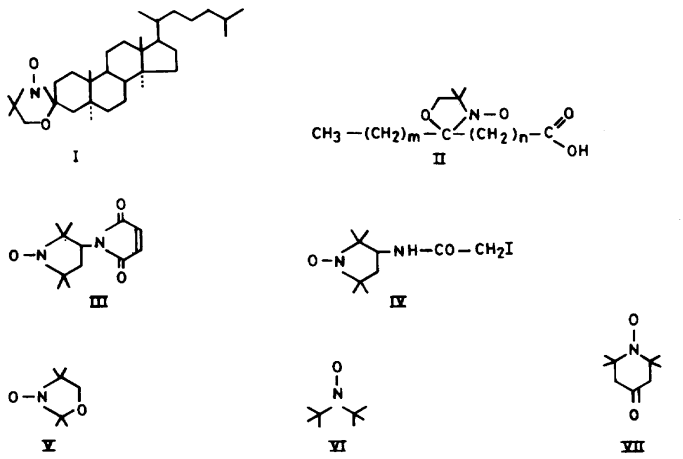

Scheme 5-1.
Various nitroxide spin labels for membrane and protein studies. The cholestane spin label **I** and fatty acid spin labels **II**(m, n) are used to monitor lipid systems. The maleimide spin label **III** and iodoacetamide spin label **IV** can be covalently attached to proteins. Spin labels **V** (2-doxyl propane), **VI** (di-t-butyl nitroxide), and **VII** (tempone) have been used to determine the magnetic properties of the spin labels in single crystal hosts.

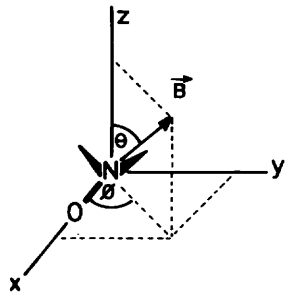

Figure 5-1.
The nitroxide principal axes system {x, y, z}. The orientation of the magnetic field $\vec{\mathbf{B}}$ is given by the polar angles θ and ϕ.

In the spin Hamiltonian in Eqn. 5-1 a number of approximations have been made: (1) the nuclear Zeeman interaction is neglected; (2) the hyperfine interaction with protons and ^{13}C nuclei is neglected; (3) the interaction between spin labels is neglected. For dilute systems under normal conditions all these approximations are valid.

It is convenient to define a Cartesian molecule-fixed axes system {x, y, z} for nitroxides as depicted in Fig. 5-1. The x-axis coincides with the N-O bond and the z axis is along the $2p\pi$ orbital, which is occupied by the unpaired electron. Because of the symmetry of the $2p\pi$ orbital, the {x, y, z} axes system coincides with the principal axes of the **g** and **A** tensors. Thus **g** and **A** are diagonal in this axes system. The diagonal elements (or principal values) are indicated by g_{xx}, A_{xx}, etc. These values are listed in Table 5-1.

Table 5-1. Principal values of the **g** and **A** tensor components of nitroxide spin labels.

Component	Value
g_{xx}	2.009
g_{yy}	2.006
g_{zz}	2.002
A_{xx}	0.6 mT
A_{yy}	0.6 mT
A_{zz}	3.2 mT

5-2 Spin labels in single crystal hosts

To illustrate the anisotropic behaviour of the **g** and **A** tensors, we apply the magnetic field $\vec{\mathbf{B}}$ along the z axis of the spin label in a single crystal host, and calculate the ESR spectrum. The spin Hamiltonian Eqn. 5-1 then becomes

$$\hat{H} = \mu_B g_{zz} B \hat{\mathbf{S}}_z + A_{zz} \hat{\mathbf{I}}_z \hat{\mathbf{S}}_z \tag{5-2}$$

This spin Hamiltonian is readily solved, yielding the energy levels

$$U(m_s, m_I) = \mu_B g_{zz} B m_s + A_{zz} m_I m_s \tag{5-3}$$

The electron spin quantum number m_s takes the values +½ and -½, whereas m_I can take the values 1, 0, and -1.

From Eqn. 5-3, it can be seen that the ESR spectrum consists of three resonance lines with equal height and separation given by

$$\Delta U = h\nu_0 = \mu_B g_{zz} B + A_{zz} m_I \tag{5-4}$$

A similar analysis can be made for the magnetic field $\vec{\mathbf{B}}$ oriented along the x- and y-axes. This is illustrated in Fig. 5-2. From this figure, it can be seen that because the components of the **g** and **A** tensors are different, the ESR spectra depend strongly on the orientation of $\vec{\mathbf{B}}$. This makes nitroxide spin labels very suitable and powerful probes to study the structure and dynamics of spin-labelled (bio)systems (*i.e.* proteins and membranes).

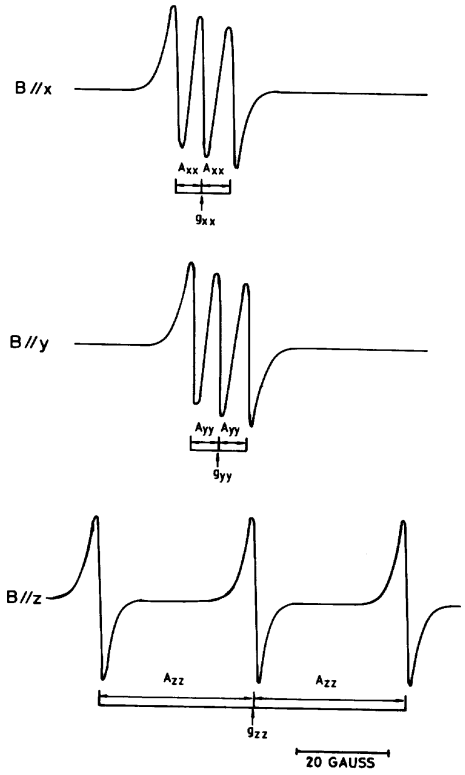

Figure 5-2.
Theoretical ESR spectra of a nitroxide molecule with the magnetic field $\vec{\mathbf{B}}$ directed along the principal axes x, y, and z at a microwave frequency of 9.5 GHz.

5-3 Powder spectrum

For a quantitative description of the ESR spectra with a general orientation of $\vec{\mathbf{B}}$, a first-order solution of Eqn. 5-1 yields

$$\Delta U = h\nu_0 = \mu_B g(\theta,\phi) B + A(\theta,\phi) m_I \tag{5-5}$$

where

$$g(\theta,\phi) = g_{xx}\sin^2\theta\cos^2\phi + g_{yy}\sin^2\theta\sin^2\phi + g_{zz}\cos^2\theta \tag{5-6}$$

and

$$A(\theta,\phi) = \sqrt{A_{xx}\sin^2\theta\cos^2\phi + A_{yy}\sin^2\theta\sin^2\phi + A_{zz}\cos^2\theta} \tag{5-7}$$

Fig. 5-2 shows the ESR spectra that are obtained for nitroxide spin labels embedded in single crystal hosts. For samples that are not oriented single crystals, but consist of a random isotropic distribution of molecules, a so-called **powder spectrum** is obtained, which is a super-position of spectra of all orientations of $\vec{\mathbf{B}}$ with respect to the molecule-fixed principal axes system {x, y, z}.

Because of the complexity of Eqn. 5-6 and 5-7 this is carried out using computer programs. However, for a simple case of a radical (S = ½) with only an axially symmetric **g** tensor (*i.e.* $g_{xx} = g_{yy} = g_\perp$ and $g_{zz} = g_{//}$) and no hyperfine interaction, an analytical expression of the powder spectrum can be obtained.

From Eqn. 5-5 it follows then that

$$h\nu_0 = \mu_B\left(g_\perp\sin^2\theta + g_{//}\cos^2\theta\right)B \tag{5-8}$$

and the angular dependent resonance value $B(\theta)$ is

$$B(\theta) = \frac{h\nu_0}{\mu_B\left(g_\perp\sin^2\theta + g_{//}\cos^2\theta\right)} \tag{5-9}$$

The powder line shape L(B) is given by the proportionality

$$L(B) \propto \left(\frac{dB(\theta)}{d\theta}\right)^{-1}\sin\theta \tag{5-10}$$

which results in

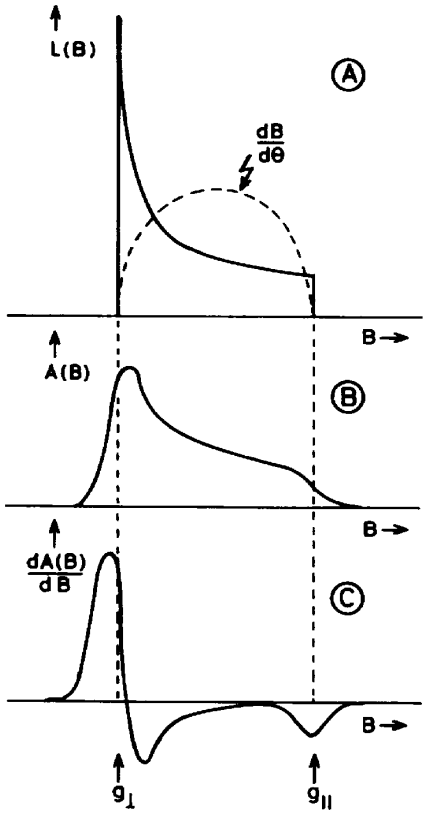

Figure 5-3.
Theoretical line shapes for a random distribution of simple radicals (S = ½) with an axially symmetric **g** tensor and no hyperfine interaction. (A) Non-broadened powder line shape function L(B) as given by Eqn. 5-11. The broken line is the function $dB(\theta)/d\theta$ (see Eqn. 5-25); (B) Broadened absorption spectrum A(B) calculated from Eqn. 5-12; (C) ESR powder spectrum dA(B)/dB. The principal values of the **g** tensor are $g_{//}$ and $g_{\perp}$.

$$L(B) \propto \frac{1}{\{B(\theta)\}^2 (g_{//} - g_{\perp}) \cos\theta} \tag{5-11}$$

This function is depicted in Fig. 5-3A. In real situations line broadening mechanisms (*e.g.* unresolved proton hyperfine splittings) broaden the line shape function. If f(B) denotes the line broadening function, the broadened absorption line shape A(B) is given by the convolution integral

$$A(B) = \int f(B') L(B - B')\, dB' \tag{5-12}$$

This results in the absorption powder spectrum in Fig. 5-3B. The ESR spectrum is the first derivative of this spectrum (Fig. 5-3C). Note that $g_{//}$ can be obtained from the right extreme in Fig. 5-3C. The point at which the left peak crosses the base line yields an approximate value for $g_{\perp}$.

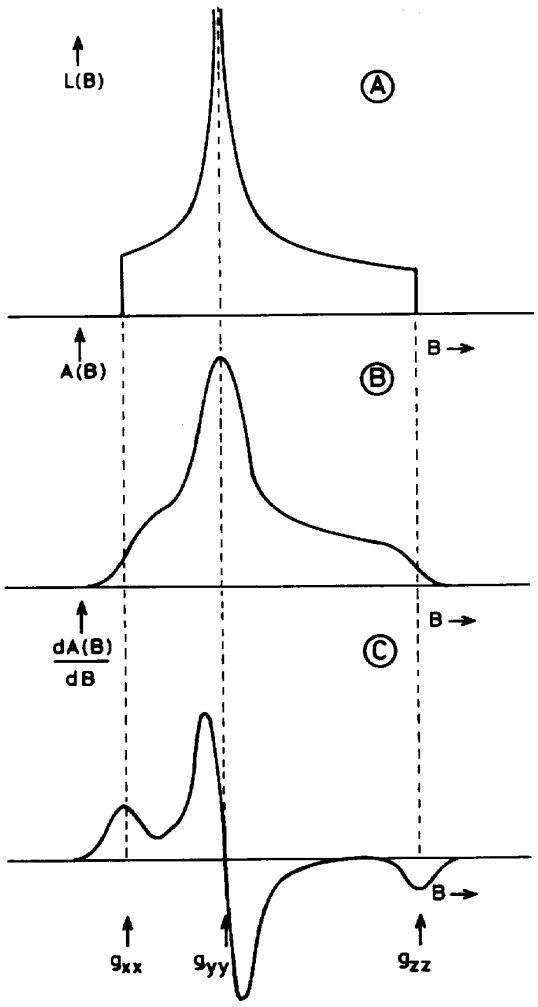

Figure 5-4.
Schematic line shapes for a random distribution of simple radicals (S = ½) with **g** tensor components $g_{xx} < g_{yy} < g_{zz}$ and no hyperfine interaction. (A) Non-broadened absorption powder spectrum; (B) Broadened absorption spectrum; (C) ESR powder spectrum dA(B)/dB.

Without going into complex mathematics, we present in Fig. 5-4 the schematic line shape of a powder sample of a radical with $g_{xx} < g_{yy} < g_{zz}$ by joining two line shapes, as in Fig. 5-3A back to back. Note again that such a powder spectrum allows the determination of the components of the tensor **g**. Fig. 5-4 actually represents the $m_I = 0$ part of the ESR spectrum for a nitroxide radical. We may also apply the same principle to the $m_I = \pm 1$ parts, as is illustrated in Fig. 5-5. This demonstrates that the powder spectrum of a nitroxide radical is a sum of three shapes as given in Fig. 5-4. Although this simple principle does not quantitatively predict ESR powder line shapes, the main features can be well understood qualitatively.

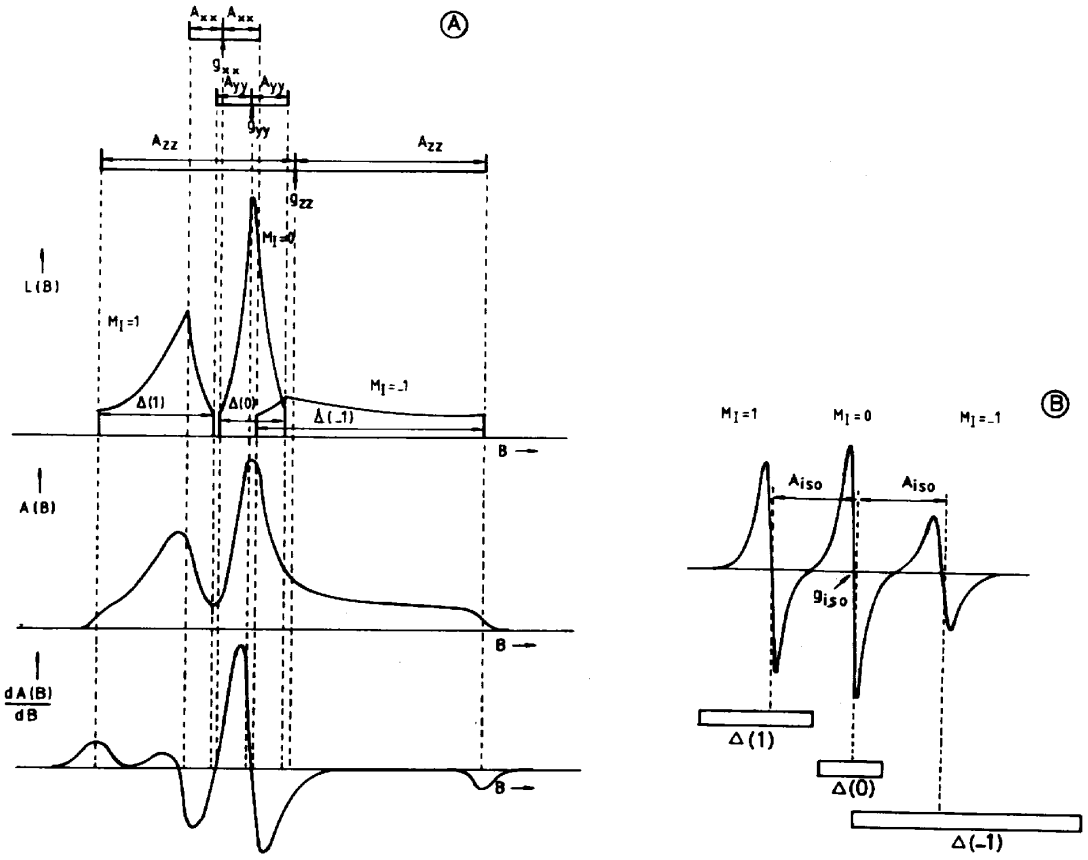

Figure 5-5.
Schematic line shapes of randomly oriented (A) and rapidly reorienting (B) nitroxide radicals at 9.5 GHz. For the calculation the **g** and **A** tensor components from Table 5-1 have been used. $\Delta(m_I)$ indicates the spectral anisotropies for m_I = 1, 0, and -1. The isotopic values of the **g** and **A** tensors are g_{iso} and A_{iso}.

In principle, the powder spectrum in Fig. 5-5A contains the same information as the single crystal spectrum in Fig. 5-2. The central peaks, however, of the nitroxide powder spectrum in the X-band (9.5 GHz) overlap and information about A_{xx}, A_{yy}, g_{xx}, and g_{yy} is lost. Only A_{zz} can be measured directly from the outer extreme in the powder spectrum, and g_{zz} follows from halving this distance. Powder spectra in the Q-band (35 GHz) show a four-fold increase in resolution in the centre and allow a better determination of the x and y components. This is illustrated in Fig. 5-6.

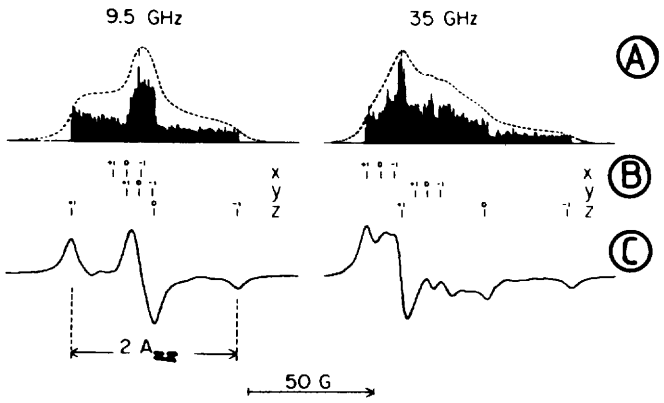

Figure 5-6.
Calculated powder line shapes at microwave frequencies of 9.5 and 35 GHz.

5-4 ESR spectra of mobile spin labels

Let us see what happens when nitroxide molecules are allowed to tumble rapidly in an isotropic way as is the case for a liquid. The spin Hamiltonian in Eqn. 5-1 becomes time-dependent, but it is possible to separate the Hamiltonian into two part, a stationary part $\hat{H}_0$ and a time-dependent part $\hat{H}_1(t)$:

$$\hat{H} = \hat{H}_0 + \hat{H}_1(t) \tag{5-13}$$

where

$$\hat{H}_0 = \mu_B g_{iso} \vec{\mathbf{B}} \bullet \hat{\mathbf{S}} + A_{iso} \hat{\mathbf{I}} \bullet \hat{\mathbf{S}} \tag{5-14}$$

and

$$\hat{H}_1(t) = \mu_B \vec{\mathbf{B}} \bullet [\mathbf{g}(t) - g_{iso}] \bullet \hat{\mathbf{S}} + \hat{\mathbf{I}} \bullet [\mathbf{A}(t) - A_{iso}] \bullet \hat{\mathbf{S}} \tag{5-15}$$

Eqn. 5-15 contains the anisotropic parts of the **g** and **A** tensors. The isotropic values of the tensors **g** and **A**, g_{iso} and A_{iso}, are given by

$$g_{iso} = \tfrac{1}{3}(g_{xx} + g_{yy} + g_{zz}) \tag{5-16}$$

and

$$A_{iso} = \tfrac{1}{3}(A_{xx} + A_{yy} + A_{zz}) \tag{5-17}$$

When the molecular motion with a rotational correlation time τ_c is fast enough, so that

$$\left| \hat{H}_1(t) \right| \tau_c \leq 1$$

$\hat{H}_1(t)$ can be considered as a time-dependent perturbation. Such a perturbation acts similar to the coherent microwave radiation field that induces transitions between the electron spin states. The main difference is that the motion of the nitroxide molecule is random, and that therefore $\hat{H}_1(t)$ not only induces transitions between the electron spin states, but also induces transitions between the nuclear spin states and modulates the energy levels. $\hat{H}_1(t)$ is therefore responsible for relaxation effects and line broadening.

The line positions are easily calculated from Eqn. 5-14, analogous to Eqn. 5-2, yielding a three line ESR spectrum with splitting A_{iso} and centre determined by g_{iso}. The liquid ESR spectrum in the case of rapid isotropic motion is shown in Fig. 5-5B.

Qualitatively the effect of molecular motion can be visualised as an averaging of the spectral anisotropies, indicated in Fig. 5-5. This averaging is easily done when the spectral anisotropy is small, resulting in a narrow line. This is the case for the m_I = 0 line. In contrast, when the spectral anisotropy is large, the resulting resonance line is broad, as is the case for the m_I = -1 line.

Assuming a two-state jump model, the peak-to-peak line widths $\Delta\nu_{pp}$ (in Hz) are approximately given by

$$\Delta\nu_{pp}(m_I) = \left\{\Delta(m_I)\right\}^2 \tau_c \qquad (5\text{-}18)$$

where $\Delta(m_I)$ is the spectral anisotropy expressed in frequency units. From Fig. 5-5 the break-down of this time-dependent perturbation approach may be estimated:

$$\Delta(-1)\tau_c \leq 1 \quad \text{or} \quad \tau_c \leq 10^{-8}\ \text{s}. \qquad (5\text{-}19)$$

If the motion is very fast, i.e. $\tau_c < 10^{-11}$ s, the spectrum will consist of three sharp lines of equal height. As the motion becomes progressively slower, there is a differential broadening of the line in the spectrum, given by Eqn. 5-18, while the line positions remain constant. This is the so-called the fast motional region (see Fig. 5-7). For values of $\tau_c > 3\times10^{-9}$ s a distortion of the line positions and line shape is observed. This region is called the slow motional region. In the very slow motional region ($\tau_c > 10^{-7}$ - 10^{-6} s) the rigid powder spectrum is reached for conventional ESR. In this region, however, saturation-transfer (ST) ESR results in spectra still sensitive for molecular motion, the final limit of τ_c being approx. 10^{-3} s. This is because ST-ESR is sensitive for the transfer of spin saturation within the spin-lattice relaxation time T_1. The various ranges of molecular motion and the resulting isotropic ESR and ST-ESR spectra are shown in Fig. 5-8. By using the integral of the ST-ESR spectrum, the limit of motion can be further pushed to a τ_c of about 10^2 s.

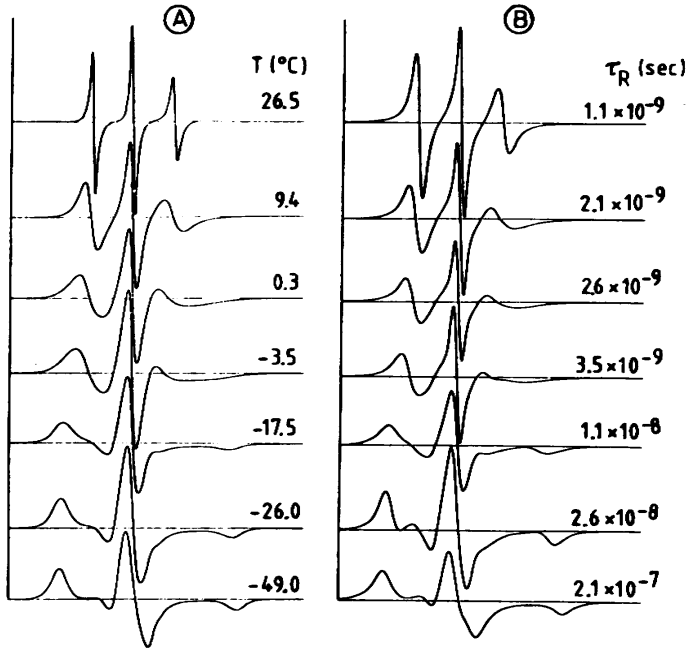

Figure 5-7.
Experimental (A) and computer simulated (B) ESR spectra.

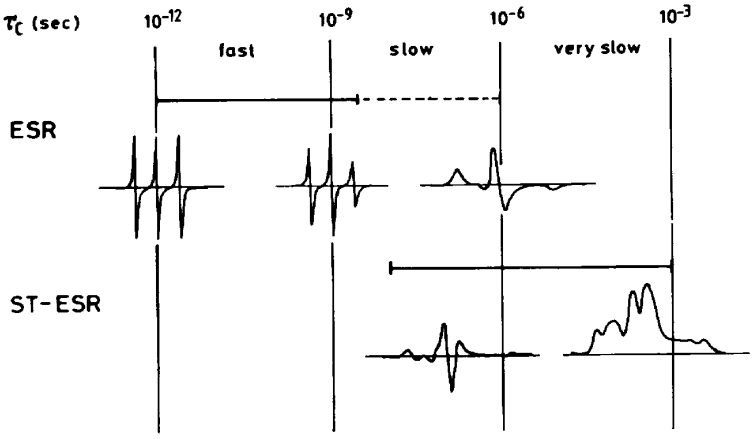

Figure 5-8.
Survey of the various motional regions and characteristic ESR and ST-ESR spectra for isotropic motion. The isotropic rotational correlation time is τ_c.

5-5 Isotropic systems

5-5.1 Fast molecular motion

For fast isotopic motion it can be calculated that the ESR lines have a Lorentzian shape and peak-to-peak line widths $\Delta B(m_I)$ (in T) are given by

$$\Delta B(m_I) = A + Bm_I + Cm_I^2 \qquad (5\text{-}20)$$

For a Lorentzian line shape, the peak-to-peak height h varies with the inverse square of the width ΔB, so that the parameters B and C from Eqn. 5-20 can be expressed in terms of the ratios of the line heights h_{m_I}:

$$B = \tfrac{1}{2}\Delta B(0)\left(\sqrt{\frac{h_0}{h_{+1}}} - \sqrt{\frac{h_0}{h_{-1}}}\right) \tag{5-21}$$

$$C = \tfrac{1}{2}\Delta B(0)\left(\sqrt{\frac{h_0}{h_{+1}}} + \sqrt{\frac{h_0}{h_{-1}}} - 2\right) \tag{5-22}$$

(Note that the m_I = 1 line is the **low-field** line in the ESR spectrum).

In X-band ESR spectra, for τ_c in the range from 5×10^{-11} to 10^{-9} s, it follows from relaxation theory that

$$\tau_c = -1.22\times10^{-9}B \tag{5-23}$$

$$\tau_c = 1.19\times10^{-9}C \tag{5-24}$$

Eqn. 5-23 and 5-24 allow two independent determinations of the rotational correlation time for isotropic motion from the experimental ESR spectra. Differences between the values of τ_c calculated from Eqn. 5-23 and 5-24 can arise from anisotropy of motion, effects of molecular ordering, or motion in the slow regime ($\tau_c > 3\times10^{-9}$ s), rather than in the fast motional region.

5-5.2 Slow molecular motion

For nitroxide spin labels in the slow motional region ($\tau_c > 3\times10^{-9}$ s), $\hat{H}_1(t)$ in Eqn. 5-13 does not fluctuate rapidly enough and the relaxation theory, based on a perturbation approach, is no longer valid. In this case no direct theoretical expression can be found for τ_c. In fact it is necessary to simulate the ESR spectra, since both the positions and the line widths depend on τ_c. Fig. 5-9 illustrates the slow motional absorption line shapes of a simple radical (S = ½) with only an axially symmetric **g** tensor (*i.e.* $g_{xx} = g_{yy} = g_\perp$ and $g_{zz} = g_{//}$) and no hyperfine interaction. In the fast motional region $\Delta\times\tau_c$, where Δ is the spectral anisotropy in Fig. 5-9 expressed in frequency units), a sharp line is obtained (the motional narrowing region).

On increasing $\Delta\times\tau_c$ the line starts to broaden up to $\Delta\times\tau_c \cong 1$. For values of $\Delta\times\tau_c > 1$ the line shifts down field and becomes increasingly asymmetric and eventually approaches the rigid powder spectrum, given by Eqn. 5-11 and 5-12. Some calculated ESR spectra of a nitroxide spin label are shown in Fig. 5-7. By comparing experimental and calculated ESR spectra, τ_c can be well determined, especially in the region where the shape of the spectrum is sensitive to τ_c.

5-5.3 Very slow molecular motion

For rotational correlation times $\tau_c > 10^{-7} - 10^{-6}$ s, conventional ESR spectroscopy yields the rigid-powder line shape that is insensitive to the rate of molecular motion. It is, however, possible to obtain line shapes which are sensitive to τ_c in this region by carrying out ESR under saturation conditions. This non-linear ESR technique is called saturation transfer (ST) ESR spectroscopy.

The effects of saturation and very slow molecular motion on the line shape can be qualitatively explained in the following "thought" experiment. Let us consider the rigid powder line shape of randomly oriented nitroxide spin labels (see Fig. 5-5A). Each point in the line shape represents a number of spin labels with a specific orientation in the powder. Suppose we set a magnetic field at a value B_0 and apply a strong resonant pule of microwave radiation to the sample. Then a hole will be burned in the line shape at field position B_0. This arises from those spin labels that have an orientation (θ,ϕ) satisfying the resonance condition Eqn. 5-5. The width of the hole is determined by the line shape function f(B) of Eqn. 5-12. This is illustrated in Fig. 5-9, where the microwave radiation is assumed to be strong enough for complete saturation. After switching-off the microwave radiation, the hole will exponentially fill up at a rate T_1^{-1}, and the powder spectrum will return to its original shape.

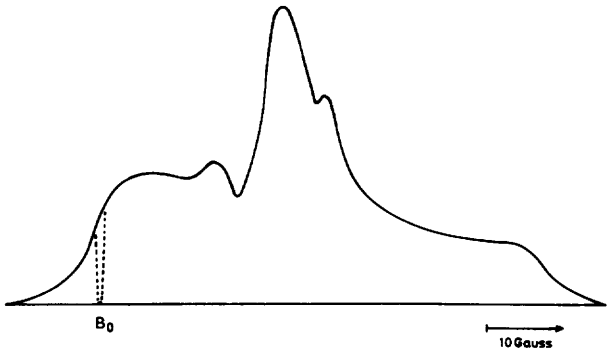

Figure 5-9.
Schematic drawing of the absorption line shape of randomly oriented nitroxide spin labels. The broken line indicates a hole that is burned in the line shape at B_0 by strong resonant microwave radiation.

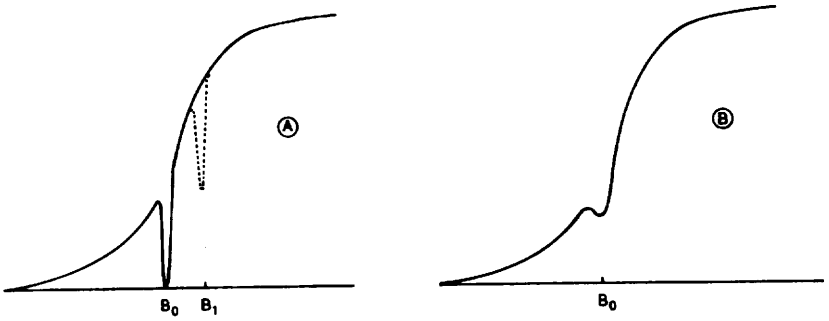

Figure 5-10.
Schematic drawing of the effect of rotational motion on hole burning. (A) A hole is burned in the absorption line shape at B_0 with a strong pulse of resonant

microwave radiation. The hole shifts to B_1 when all nitroxide spin labels make a similar coherent very slow rotational motion. (B) Random rotational diffusion broadens the hole at B_0 after a pulse of resonant microwave radiation, because holes of individual nitroxide spin labels shift randomly around B_0.

Suppose now that, after the pulse of microwave radiation, the spin labels make a coherent rotational motion with a rate fast as compared to T_1. The hole will then move in the line shape to a field value b_1, belonging to the new orientation of the spin labels. In the case of a random rotational diffusion with a rotational correlation time $\tau_c < T_1$, the hole at B_0 will broaden and eventually fill up as the spectral diffusion of holes (*i.e.* transfer of saturation) proceeds. The shorter τ_c, the faster the hole at B_0 fills up. This is very similar to the effect of T_1 on the hole-burning process, except that a broadening of the hole also appears. The effect of motion on the holes is illustrated in Fig. 5-10.

5-5.4 Saturation Transfer (ST) ESR

In ST-ESR field modulation (modulation frequency ω_m) in combination with phase-sensitive detection, is used to observe the signal under continuous microwave radiation, similar as in conventional ESR. Under saturation conditions at high microwave power, holes are then continuously burned in the line shape. These hole fill up again during the modulation cycles. This means that especially strong effects on the line shape are observed if

$$\omega_1^{-1} \cong T_1 \cong \tau_c$$

Since T_1 is approx. 10^{-5} - 10^{-6} s, ST-ESR spectroscopy is sensitive to values of τ_c around 10^{-5} - 10^{-6} s for modulation frequencies around 100 kHz.

Experimentally it has been found that ST-ESR spectra detected in quadrature (90° out-of-phase) at the second harmonic ($2\omega_m$) are most suitable.
The rate of spectral diffusion $dB(\theta)/d\theta$ can be directly calculated from the resonance equation for the simple radical (S = ½) with only an axially symmetric **g** tensor (*i.e.* $g_{xx} = g_{yy} = g_\perp$ and $g_{zz} = g_{//}$) and no hyperfine interaction.

From Eqn. 5-9 we obtain

$$\frac{dB(\theta)}{d\theta} = \left(\frac{h\nu_0}{\mu_B}\right) \frac{\left(g_{//} - g_\perp\right)\sin 2\theta}{\left(g_\perp \sin^2\theta + g_{//}\cos^2\theta\right)^2} \qquad (5\text{-}25)$$

This function, which is indicated by the broken line in Fig. 5-3, is zero at the extreme "turning" points determined by $g_{//}$ and $g_\perp$ and has a maximum at a filed value determined approximately by

$$\tfrac{1}{2}\left(g_{//} + g_\perp\right)$$

Therefore saturation transfer leaves the turning points unaffected and has a maximal effect between the turning points. The same argument holds for the different m_I parts of the nitroxide powder line shape (see Fig. 5-5). The sensitivity of ST-ESR spectra to very slow isotropic motion is illustrated in Fig. 5-8.

5-6 Anisotropic systems

5-6.1 Order parameters

In lipid systems and biological membranes a molecular ordering exists and the motion is strongly anisotropic. These effects greatly change the spectroscopic properties of nitroxide spin labels in these systems as compared to the spectra obtained in isotropic systems. In anisotropic systems the mean orientation of spin labels is conveniently described using the so-called order parameters.
Consider the lipid bilayer depicted in Fig. 5-11. The x, y, and z axes are the molecule-fixed principal axes of the **g** and **A** tensors. The order parameters relate the mean orientation of these axes to a space-fixed reference axis, which is taken as the normal (director, or optical axis) perpendicular to the bilayer. Note that the lipid bilayer has an axial symmetry around the director.

If the angles between the x, y, and z axes and the director are denoted by $\theta_1, \theta_2,$ and θ_3, the order parameters S_i are defined by

$$S_i = \frac{1}{2}\left\langle 3\cos^2\theta_i - 1 \right\rangle \quad i = 1,2,3 \;\; (= x, y, z) \tag{5-26}$$

The brackets $\langle \cdots \rangle$ indicate the ensemble average. Due to the orthogonality properties of the cosines, it follows that

$$\sum_i S_i = 0 \tag{5-27}$$

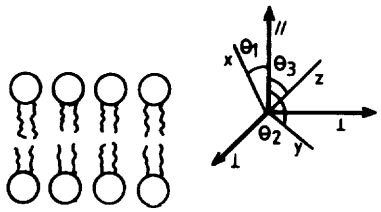

Figure 5-11.
Schematic representation of a lipid bilayer with a nitroxide spin label, the orientation of which is indicated by the molecule-fixed axes principal axes x, y, and z of the **g** and **A** tensors. The symmetry axes of the bilayer a indicated by // and $\perp$. The $//-$axis is called the director. The angles $\theta_1, \theta_2,$ and θ_3 indicate the orientation of the spin label with respect to the director.

For molecules with an axially symmetric shape, one order parameter S is sufficient to describe the mean orientation. If we take the molecular z axis as the symmetry axis, it then follows that

$$S_3 = S \qquad (5\text{-}28)$$
$$S_1 = S_2 = -\frac{1}{2}S$$

In the case of perfect ordering θ = 0°, so that S = 1; all molecules are then oriented with their z- axes along the director. For an isotropic distribution of the molecules, S = 0. In the case the molecules are perfected oriented with their z axes perpendicular to the director, θ = 90° and S = -½.

Thus far we have not explicitly involved the rates of motion of the spin label. In fact order parameters are independent of the rate of motion, making the general assumption that the ensemble average in Eqn. 5-26 equals the time average (the ergodic principle).

Depending on the rate of molecular motions, however, the molecular distribution enters in different ways into the analysis of the ESR spectra of spin labels and membrane systems. If the anisotropic motions are fast the ESR spectrum reflects the time-averaged position of the spin label and the ESR spectra are determined by the time average of Eqn. 5-26. If the spin labels are immobilised a static space distribution determines the ESR spectrum, the overall line shape being determined by the geometry of the sample and the internal distribution of the molecules.

5-6.2 Fast molecular motion

In the case of fast anisotropic motion ($\tau_c < 3\times10^{-9}$ s), the stationary part $\hat{H}_0$ of Eqn. 5-13 becomes

$$\hat{H}_0 = \mu_B \vec{\mathbf{B}} \bullet \overline{\mathbf{g}} \bullet \hat{\mathbf{S}} + \hat{\mathbf{I}} \bullet \overline{\mathbf{A}} \bullet \hat{\mathbf{S}} \tag{5-29}$$

The time-averaged tensors $\overline{\mathbf{g}}$ and $\overline{\mathbf{A}}$ (indicated by the bar) are still anisotropic, because the anisotropic motion only partially averages the time-dependent tensors **g**(t) and **A**(t).

From the symmetry of the lipid bilayer system it follows that the tensors $\overline{\mathbf{g}}$ and $\overline{\mathbf{A}}$ are axially symmetric, with time-averaged components $g_{//}$ and $A_{//}$ parallel to the director, and $g_\perp$ and $A_\perp$ perpendicular to the director. The order parameters directly relate the time-averaged tensor components and the molecule-fixed tensor components as given below:

$$\begin{aligned} g_\perp &= g_{iso} - \tfrac{1}{3}\sum_i S_i g_{ii} \qquad A_\perp = A_{iso} - \tfrac{1}{3}\sum_i S_i A_{ii} \\ g_{//} &= g_{iso} + \tfrac{2}{3}\sum_i S_i g_{ii} \qquad A_{//} = A_{iso} + \tfrac{2}{3}\sum_i S_i A_{ii} \end{aligned} \tag{5-30}$$

Note that from Eqn. 5-30 it directly follows that

$$g_{iso} = \tfrac{1}{3}\left(2g_\perp + g_{//}\right) \qquad A_{iso} = \tfrac{1}{3}\left(2A_\perp + A_{//}\right) \tag{5-31}$$

From Eqn. 5-30 an expression can be obtained for the order parameters:

$$S_3 = \frac{A_{//} - A_\perp}{A_{zz} - A_{xx}} \tag{5-32}$$

$$S_1 = \frac{\left(g_{//} - g_\perp\right) + S_3\left(g_{yy} - g_{zz}\right)}{g_{xx} - g_{yy}} \tag{5-33}$$

where we have used the experimental fact that $A_{xx} \approx A_{yy}$. S_2 follows from Eqn. 5-27.

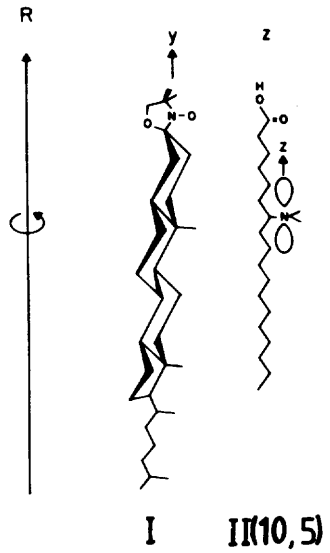

Figure 5-12.
Orientation of the principal axes of the **g** and **A** tensors with respect to the long molecular axes R of the cholestane spin label **I** and the fatty acid spin label **II**(10, 5).

The principal values of the **g** and **A** tensors given in Table 5-1 cannot be used directly in Eqn. 5-32 and 5-33. They have to be corrected for the polarity of the medium in which the spin label is located. This is done by multiplying g_{xx}, g_{yy}, and g_{zz} from Table 5-1 by

$$\frac{2g_{\perp} + g_{//}}{g_{xx} + g_{yy} + g_{zz}} \tag{5-34}$$

The components $g_{//}$ and $g_{\perp}$ are determined by the experiment. The principal values of the **A** tensor are corrected in the same way.

For the two most common types of lipid-like spin labels, the cholestane spin label **I** and the fatty acid spin labels **II**(m, n), one usually employs a definition of an order parameter S_{mol} for the long axes of these spin labels and assumes that the spin labels have an axial symmetric shape. For the fatty acid spin labels **II**(m, n) the principal z axis of the **g** and **A** tensors is almost parallel to the long molecular axis (see Fig. 5-12) so that

$$S_{mol} \cong S_3 \quad \text{(fatty acid spin labels } \mathbf{II}(m, n)) \tag{5-35}$$

For the cholestane spin label **I** the principal z axis is approximately perpendicular to the long molecular axis (see Fig. 5-12) and S_{mol} is given by

$$S_{mol} \cong -2S_3 \quad \text{(cholestane spin label } \mathbf{I}) \tag{5-36}$$

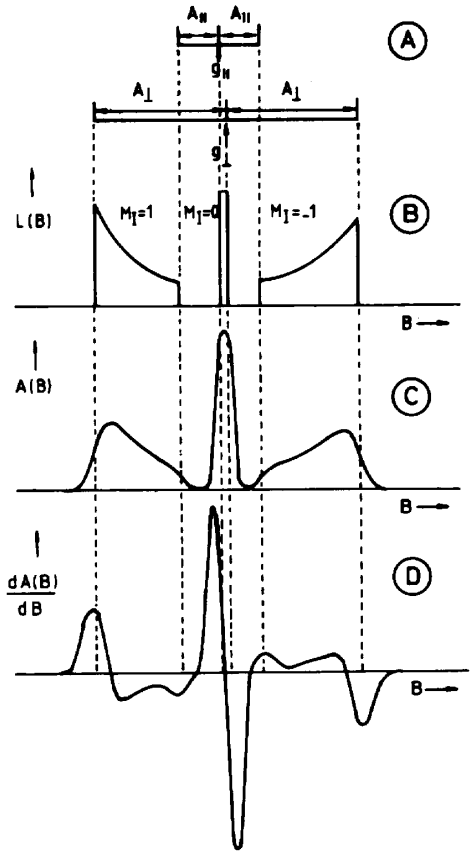

Figure 5-13.
(A) Theoretical line positions of perfectly oriented (S_{mol} = 1) cholestane spin labels **I** in planar oriented multibilayer samples at θ = 0° and 90°. The spin label performs a fast anisotropic motion about its long molecular axis. The components $A_{//}, A_{\perp}, g_{//}$, and $g_{\perp}$ are time-averaged tensor components. The microwave frequency is 9.5 GHz. (B) Schematic non-broadened powder absorption spectrum L(B) of the cholestane spin label **I** from (A) in an unoriented lipid dispersion. (C) Broadened absorption spectrum A(B). (D) Schematic ESR powder spectrum (dA(B)/dB).

It is interesting to consider the effect of averaging of the **g** and **A** tensors in the ideal case of perfectly oriented cholestane spin label **I** and the fatty acid spin labels **II**(m, n) in a bilayer (S_{mol} = 1). The only motion that can then take place is a rotational motion of the spin labels about their long molecular axis. Such a system may be considered as a two-dimensional liquid.

For example, in the case of the cholestane spin label **I** the component of the **A** tensor along the molecular axis (that is parallel to the director) remains the same: $A_{//} = A_{yy}$ = 0.6 mT (see Table 5-1). Perpendicular to the director a two-dimensional average of A_{xx} and A_{zz} is obtained, yielding

$$A_{\perp} = \frac{1}{2}(A_{xx} + A_{zz}) \cong 19.5\,\text{mT}$$

The resulting ESR spectra are schematically illustrated in Fig. 5-13. The time-averaged tensor components $A_{//}, A_{\perp}, g_{//}$, and $g_{\perp}$ directly follow from the splitting and centres of the spectra at orientations samples θ = 0 and 90°.

This situation actually arises in planar oriented multibilayer samples, in which the directors of all micro-regions are parallel. In random samples (lipid dispersions, liposomes, vesicles, or biomembranes), the directors are completely isotropically distributed. powder-like spectra arise that are a superposition of all ESR spectra. By analogy with the powder spectrum of randomly oriented nitroxide spin labels (Fig. 5-9), the resulting powder spectrum can be found schematically. This is shown in Fig. 5-13.

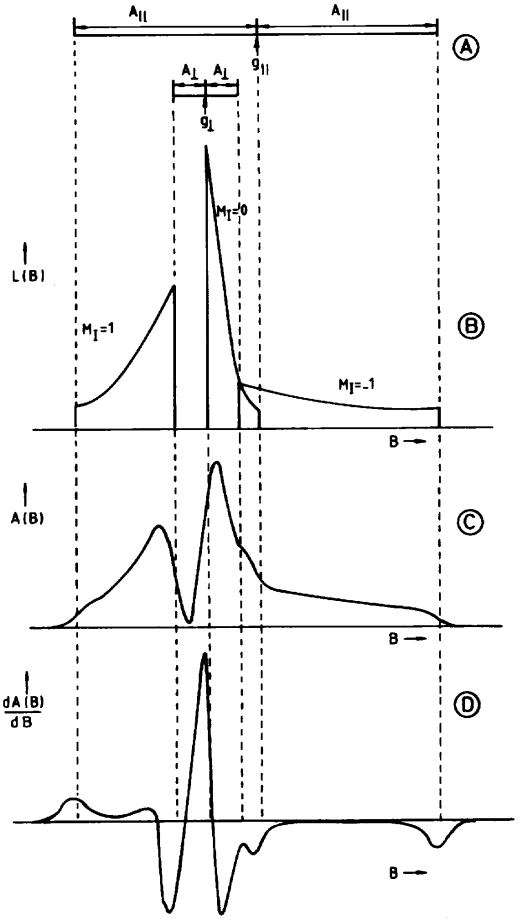

Figure 5-14.
(A) Theoretical line positions of perfectly oriented (S_{mol} = 1) fatty acid spin labels **II**(m, n) in planar oriented multibilayer samples at θ = 0 and 90°. The spin label performs a fast anisotropic motion about its long molecular axis. The components $A_{//}, A_{\perp}, g_{//}$, and $g_{\perp}$ are time-averaged tensor components. The microwave frequency is 9.5 GHz. (B) Schematic non-broadened powder absorption spectrum L(B) of the fatty acid spin labels **II**(m, n) from (A) in an unoriented lipid dispersion. (C) Broadened absorption spectrum A(B). (D) Schematic ESR powder spectrum (dA(B)/dB).

The effect of averaging the **g** and **A** tensors for perfectly oriented (S_{mol} = 1) fatty acid spin labels **II**(m, n) in oriented and unoriented samples is shown schematically in Fig. 5-14, were we have used the same principle as in Fig. 5-13. In this case the outer extreme are determined by $A_{//}$, whereas $A_{\perp}$ gives the inner extreme.

When the molecular order decreases (S_{mol} < 0.8) the relatively strong inner extreme become easily observed, yielding a value for $A_{\perp}$, so that S_{mol} can be obtained experimentally. For lower values of S_{mol} the spectra will tend to isotropic three-line ESR spectra (S_{mol} = 0).The inner and outer extreme move to the isotropic positions. This effect is illustrated in Fig. 5-15.

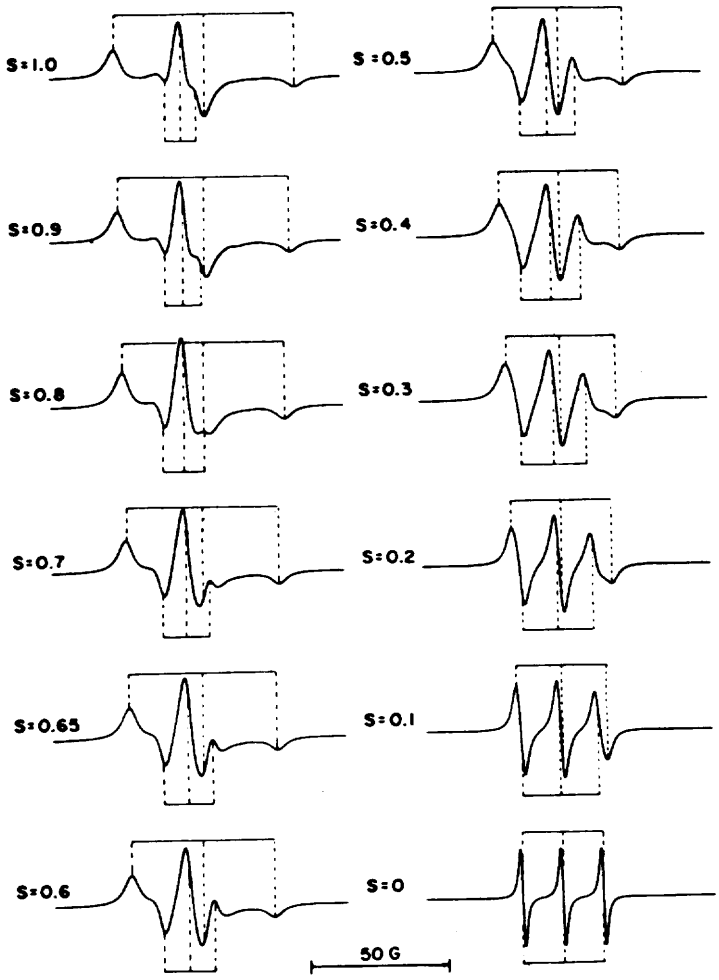

Figure 5-15.
Simulated ESR line shapes for randomly oriented samples of fatty acid spin labels **II**(m, n) as a function of the order parameter S_{mol}. The dashed lines indicate the exact positions of the three ESR lines defined by $A_{//}$ and $g_{//}$ (large splittings) and $A_{\perp}$ and $g_{\perp}$ (small splittings) (see Fig. 5-14).

Problems

Problem 5-1

The ESR spectrum of the copper (Cu^{2+})-containing protein conalbumin is given in Fig. 5-16.

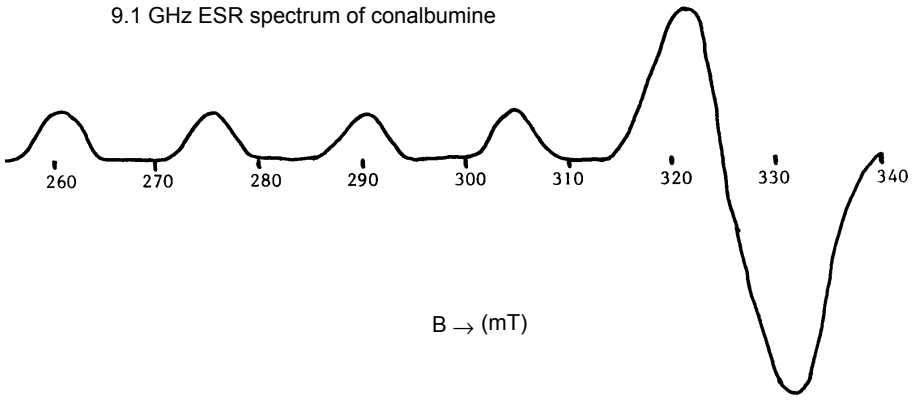

Fig. 5-16.
ESR spectrum of the protein conalbumin.

a. Give a qualitative explanation for the spectra line shape. Make a clear picture to underline your arguments.

b. Calculate the components of the **g** and **A** tensors from the spectrum. Assume that both tensors are axially symmetric.

Problem 5-2

Phosphorus (^{31}P) NMR is a suitable technique to study the polymorphism of phospholipid-water systems. In Fig. 5-17 a number of phases is shown in which phospholipid-water systems can appear.

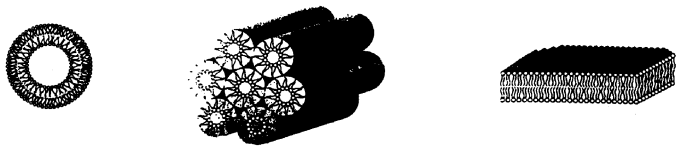

Fig. 5-17.
Phospholipid-water polymorphism.

The experimental ^{31}P NMR spectra are shown in Fig. 5-18, however, in an incorrect order.

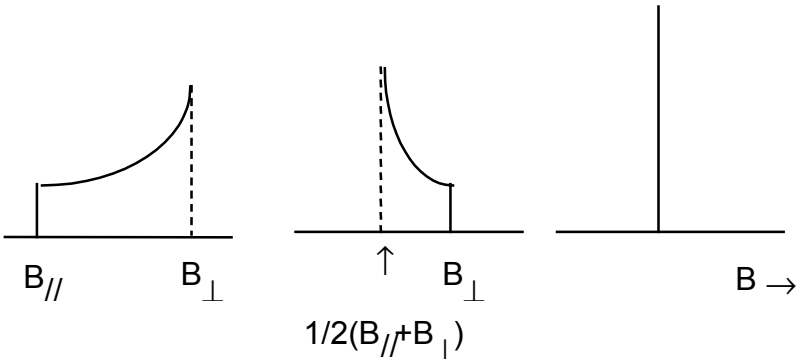

Fig. 5-18.
^{31}P NMR spectra of phospholipid-water systems.

Which spectrum corresponds to which phase? Give a discussion and provide arguments.

Problem 5-3

An unpaired electron occupies a $2p_z$ orbital of a nitrogen atom. The system is placed in a strong magnetic field $\vec{\mathbf{B}}$.

a. Discuss the properties of the **g** and **A** tensors of the system.
(**Hint**: Are the tensors symmetric or asymmetric?)

b. Give the complete spin Hamiltoniaan for this system.
Which approximations can be made in the calculation of the ESR spectra?
Provide arguments!

c. Schematically draw the ESR spectra for the case that $\vec{\mathbf{B}}$ is along the x, y, or z axis of the system.

d. Schematically draw the powder ESR spectrum.

Problem 5-4

The molecule $^{35}ClO_2$ is a stable free radical. From single crystal ESR experiments the following components of the **g** and **A** tensors are found:

$g_{xx} = 2.000$, $A_{xx} = 3.0$ mT
$g_{yy} = 2.002$, $A_{xx} = 0.5$ mT
$g_{zz} = 2.006$, $A_{xx} = 2.5$ mT

The ESR spectrometer operates at a frequency of 9.5 GHz and the nuclear spin $I(^{35}Cl) = \frac{3}{2}$.

a. Schematically draw the ESR spectrum of the radical in the liquid phase.

When the ClO_2 molecule is placed in a $KClO_2$ lattice, **two** anisotropic g-values are found along the principal axes 1 and 2:

$g_1 = 2.003$
$g_2 = 2.002$

b. What conclusions can be drawn from this observation?

c. Schematically draw the single crystal ESR spectrum of the radical in the $KClO_2$ lattice for the case that $\vec{\mathbf{B}}$ is along the 1 or 2 axis.

Problem 5-5

Consider a nitroxide radical with an isotropic **g** tensor and an **A** tensor given by the principal values A_{xx} = 0.6 mT, A_{yy} = 0.6 mT en A_{zz} = 3.2 mT.

a. Schematically draw and discuss the ESR spectrum of this radical for the case that $\vec{\mathbf{B}}$ is directed along the x, y, or z axis of the principal axes system.

b. The nitroxide radical reorients very fast about its x-axis. Schematically draw and discuss the ESR spectrum for the case that $\vec{\mathbf{B}}$ is along and perpendicular to the x-as.
(**Hint**: This is a case of a two-dimensional liquid.)

c. Schematically draw and discuss the ESR spectrum of nitroxide radical from item **b**, for the case that the motion about the x-as is frozen. Take $\vec{\mathbf{B}}$ along the x-axis and perpendicular to the x-axis.
(**Hint**: This is a case of a two-dimensional powder, in which the position of the y and z axes is statistically random.)

Problem 5-6

Consider the fatty acid spin label 12-SASL (see Fig. 5-19) in a lipid-water bilayer system in the liquid crystalline state. The nitroxide group of 12-SASL is connected to the acyl chain with a spirobond, such that the NO direction is perpendicular to the long axis. of the acyl chain. The 12-SASL molecule may be considered as a cylinder-like molecule. Assume that the lipid molecules are perfectly oriented in the bilayer.

12-SASL

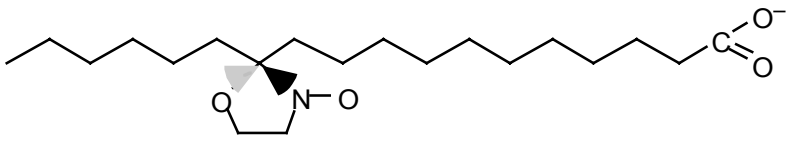

Fig. 5-19.
Chemical structure of the 12-SASL spin label.

The g-factor tensor and hyperfijntensor of 12-SASL in the principal axes system are given by:

$$\mathbf{g} = \begin{pmatrix} 2.009 & 0 & 0 \\ 0 & 2.006 & 0 \\ 0 & 0 & 2.003 \end{pmatrix}$$

$$\mathbf{A} = \begin{pmatrix} 0.6 & 0 & 0 \\ 0 & 0.6 & 0 \\ 0 & 0 & 3.2 \end{pmatrix} \text{ (in mT)}$$

a. Sketch the principal axes of the g-factor tensor and hyperfijntensor in the 12-SASL molecule. Which principal axis is the rotation axis of 12-SASL molecule in the lipid bilayer? Motivate your answer.

b. Calculate the averaged tensors in the case that the 12-SASL molecule rotates very fast about this rotation axis. Motivate your calculation.

c. For which value of the rotational correlation time will this be the case? Estimate the rotational correlation time by applying a two-site jump model.

d. Schematically sketch the ESR spectrum of 12-SASL in the lipid-water bilayer system.

Problem 5-7

Consider the deuterated TEMPONE spin label as shown below.

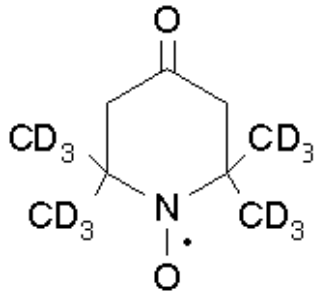

a. Discuss what would be the advantage in ESR spectroscopy of replacing protons by deuterons.

The ESR spectra of this spin label measured at 9 and 94 GHz at various temperatures in a glycerol-water solution are presented on the next page.

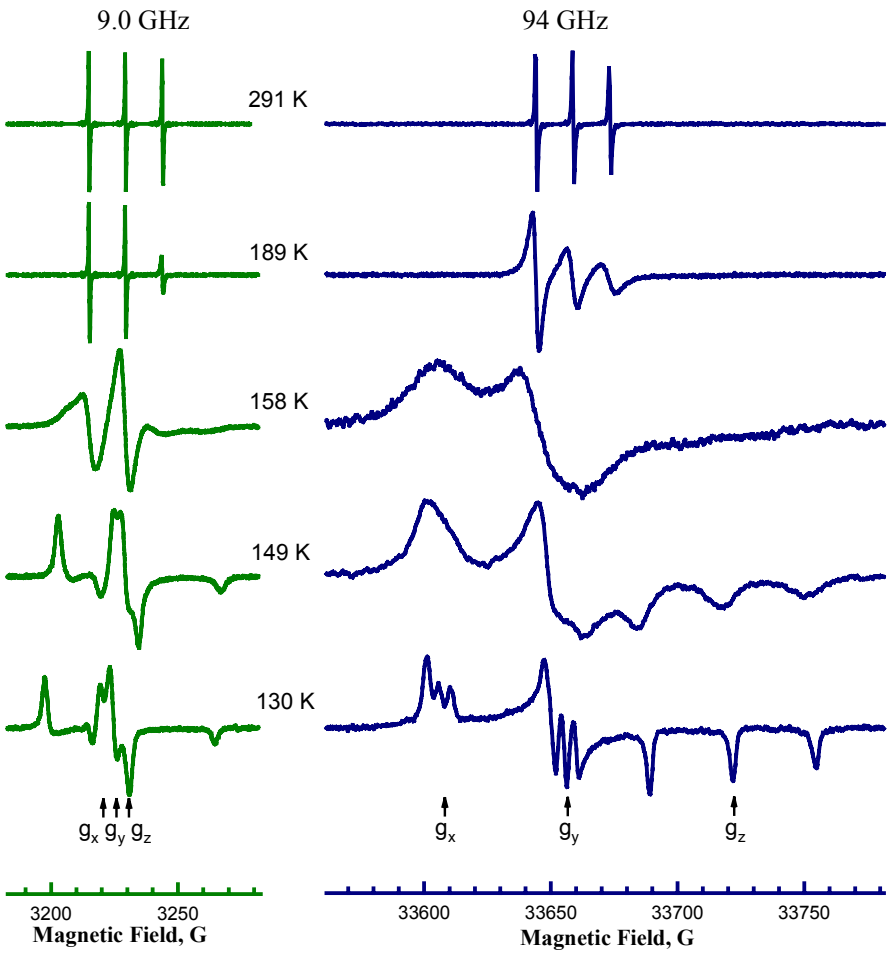

(Courtesy: Alex I. Smirnov, North Carolina State University)

b. Discuss the effect of frequency and temperature on the spectra. Take into account the change from the fast motional to the slow motional regimes.

c. Schematically draw the powder spectrum of the deuterated TEMPONE spin label at 94 GHz and assign all the peaks.

6

Metalloproteins

6-1 Introduction

There is a number of proteins that contains metal ions. The metals found in these so-called metalloproteins are ions of transition metals. For example, myoglobin is an iron-containing protein and the enzyme laccase contains copper. Transition metal ions often are paramagnetic by the presence of unpaired electrons in the d-orbitals, making them suitable for ESR research. The metal ions are associated with some or all of the functions of the metalloproteins. This means that changes occurring at the active sites of such proteins can be monitored specifically by ESR spectroscopy without the diamagnetic remainder of the protein confusing the spectrum. Thus ESR is capable of giving dynamic as well as structural information about the atomic level of the active sites of metalloproteins.

6-2 Spin-orbit coupling

In aromatic free radicals (for example naphthalene), the unpaired electron is generally delocalised over the whole molecule. In these molecules, the unpaired electron behaves almost as a free electron, so that the g-factor equals the free electron value., i.e. $g \approx g_e = 2.0023$. The g-values of nitroxide radicals are somewhat larger (g = 2.002 - 2.009), because the delocalisation of the unpaired electron is mostly confined to the π-orbital of the N-O group. In transition-metal ions the electrons are confined to the d-orbitals. This localisation gives rise to a large orbit angular moment that couples to the magnetic moment of the electron. By the effect of this strong spin-orbit coupling the g-values of transition-metal ions strongly deviate from the free electron value and the g-factor tensor **g** is very anisotropic. This anisotropy of the g-factor tensor is also strongly dependent on the environment of the metal ions, and this can be used as a monitor for the atomic structure around the metal ion in the active site of the protein.

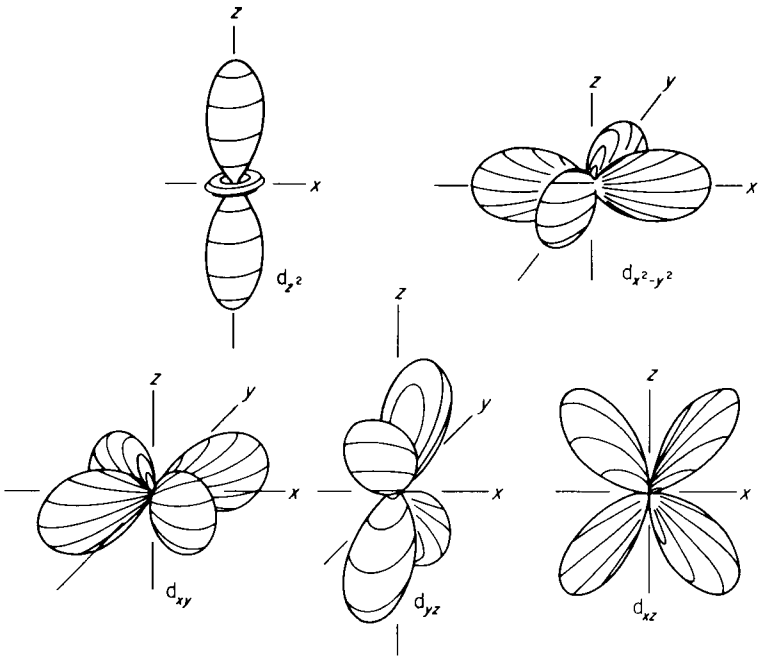

Figure 6-1.
The five d-orbitals of transition-metal ions. Each orbital can contain two electrons with opposite spins. The subscripts indicate the angular form of the orbital.

6-3 Ligand field splitting

In Fig. 6-1 the five d-orbitals of transition-metal ions are illustrated. Each orbital can contain two electrons with opposite spins. This gives a possibility of 10 electron configurations from d^1 (*e.g.* Mo^{5+}) to d^{10} (e.g. Cu^+). The electron configurations of the biologically important transition-metal ions are given in Table 6-1. With increasing number of d-electrons the orbitals are filled up with one electron each, all of the same spin (spin-up $\uparrow$). When all five orbitals contain one electron, the spins are then paired, by putting spin-down, $\downarrow$, electrons into each of the singly occupied orbitals in turn.

Table 6-1 lists the resultant net spins obtained in this way. Thus Mo^{5+} has one d-electron with spin-up and a total spin S = 1/2; Mn^{2+} has five d-electrons normally with spin-up and a total spin of S = 5/2; and Cu^{2+} has nine d-electrons, five with spin-up and four with spin-down and hence a net spin of S = 1/2. Cu^+ has ten d-electrons and a net spin of zero, hence no ESR signal is observable.

In a protein, but also in solution, transition-metal ions are surrounded by ligands. Ligands are negative or neutral molecules, or molecular groups (*e.g.* a histidine side chain) that contain all a characteristic pair of electrons. Typical examples are:

I^-, Cl^-, F^-, H_2O, CO_2, CO, CN^-, NH, C=O.

Table 6-1. Electron configurations for transition-metal ions of importance in biological ESR.

Mo^{5+}	d^1	↑					S = 1/2
Fe^{3+}, Mn^{2+}	d^5	↑	↑	↑	↑	↑	S = 5/2 (high spin)
		↑↓	↑↓	↑			S = 1/2 (low spin)
Fe^{2+}	d^6	↑↓	↑	↑	↑	↑	S = 2 (high spin)
		↑↓	↑↓	↑↓			S = 0 (low spin)
Co^{2+}	d^7	↑↓	↑↓	↑	↑	↑	S = 3/2 (high spin)
		↑↓	↑↓	↑↓	↑		S = 1/2 (low spin)
Cu^{2+}	d^9	↑↓	↑↓	↑↓	↑↓	↑	S = 1/2
Cu^{+}	d^{10}	↑↓	↑↓	↑↓	↑↓	↑↓	S = 0

By the presence of ligands, the energy degeneration of the d-orbitals is removed and a complication to the spin-pairing system arises, depending on the way in which the ligands cause energy-level splittings between the d-orbitals. If this so-called ligand field splitting is small then a high spin derivative is obtained as already outlined, but if the splitting is large the order of the spin pairing is altered, and a low-spin derivative is found, as indicated in Table 6-1. This shows the way the ligands can crucially determine the nature of the ESR spectrum. On the contrary, the ESR spectrum contains a considerably amount of information about the liganding and spin state of the transition-metal ion.

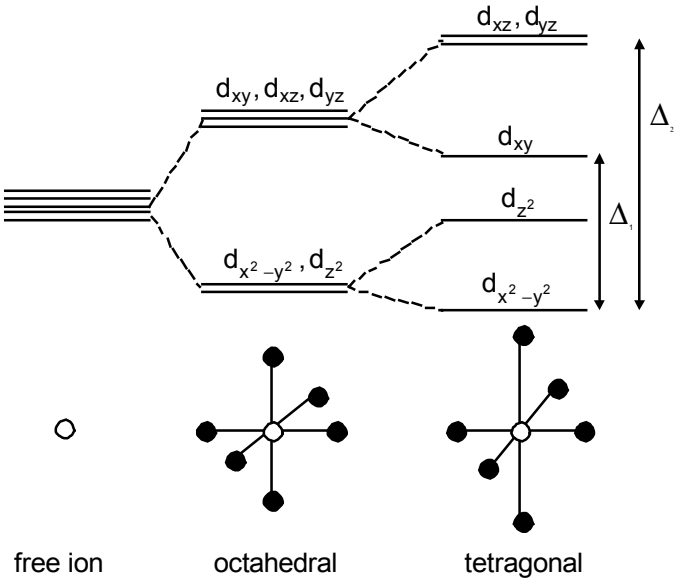

Figure 6-2.
The energy splitting of the d-orbitals, depending on the symmetry of the surroundings of the transition-metal ion.

The energy splittings, depending on the symmetry of the surroundings of the metal ion are shown in Fig. 6-2.

For an octahedral coordination the g factor tensor is isotropic, but for a tetragonal distortion of the octahedral symmetry, the g-factor tensor **g** is axially symmetric with the following elements:

$$g_{//} = g_e\left(1-\frac{4\alpha^2\lambda}{\Delta_1}\right) \qquad (6\text{-}1)$$

$$g_{\perp} = g_e\left(1-\frac{\alpha^2\lambda}{\Delta_2}\right)$$

where Δ_1 is the ligand splitting between the $d_{x^2-y^2}$ and d_{xy} orbitals, and Δ_2 is the splitting between $d_{x^2-y^2}$ and d_{xz}, d_{yz} (see Fig. 6-2). The parameter λ is the spin-orbit coupling constant, which is a measure of how strongly the spin and orbit angular moments are associated together in the absence of ligands, i.e. in the free ion. The parameter α is a measure of the degree of covalency, i.e. the extent to which the unpaired electron is moved off the metal ion (α is somewhat less than one). Thus the anisotropic g-values clearly give information about both the strength of the ligand interaction and the geometry of the metal-ligand complex. Similar perturbations are also found in the hyperfine splitting constants of the metal ion.

6-4 Myoglobin

Myoglobin is one of the subunits of hemoglobin. The protein does not show a cooperatively when binding oxygen, but its relative simplicity makes it very suitable for biophysical research using ESR. In myoglobin five coordination positions of the iron ion are occupied by nitrogen atoms of the porphyrin ring system and one by a histidine side chain of the protein. The sixth coordination position is taken by an oxygen or CO_2 molecule.

ESR research on myoglobin has been carried out on a Fe^{3+} derivative (metmyoglobin), containing H_2O at the sixth coordination position (see Fig. 6-3). In this molecule Fe^{3+} is present in the high-spin configuration with S = 5/2. Because the five d-electrons exhibit a very strong zero-field interaction, they behave as one S = 1/2 particle, giving simple ESR spectra. The anisotropy of the g-factor tensor is very large: $g_{//} = 2$ and $g_{\perp} = 6$.

By measuring the angular dependence of the g-factor of single crystals of metmyoglobin, the orientation of the porphyrin ring in the protein could be accurately determined. This angular dependence is given by:

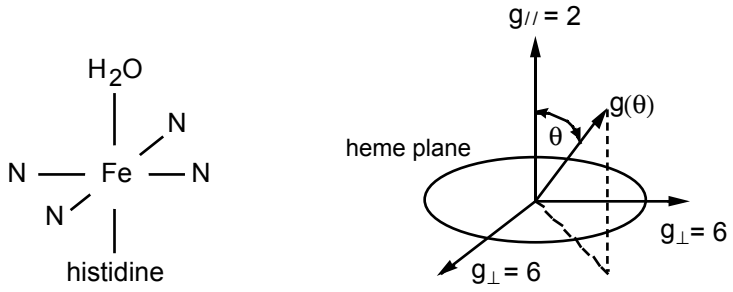

Figure 6-3.
Coordination and principal g-vales for metmyoglobin with respect to the heme plane of the porphyrin ring.

$$g(\theta)^2 = g_{//}{}^2 \cos^2\theta + g_{\perp}{}^2 \sin^2\theta = 4\left(1 + 8\sin^2\theta\right) \quad (6\text{-}2)$$

Similar research has been carried out on hemoglobin in single crystals, showing that the porphyrin rings were not parallel to each other as had previously been assumed.

6-5 Laccase

Laccase is a copper-containing protein. In solution Cu^{2+} shows ESR spectra with four sharp lines, because $I(Cu^{2+}) = 3/2$. In a solid, powder ESR spectra arise similar as for nitroxide radicals. For most copper complexes the g-factor tensor **g** and hyperfine tensor **A** are axially symmetric, given by:

$$g_{//} \approx 2.3, \qquad A_{//} \approx 16\,\text{mT}$$
$$g_{\perp} \approx 2.0, \qquad A_{\perp} \approx 1\ \text{mT}$$

The corresponding powder spectrum us schematically shown in Fig. 6-4. The splitting by $A_{\perp}$, which is small, is not observable in this spectrum.

The enzyme laccase catalyses the oxidation of hydroquinones. By chemical analysis it has been found that it contains four copper atoms and we may expect a far more complex powder spectrum as shown in Fig. 6-4. The ESR spectrum of a frozen solution of laccase run at 9 GHz is shown in Fig. 6-5. From an integration of the spectrum it turns out that two of the four copper ions contribute to the spectrum. This copper is present as Cu^{2+}. The two other copper ions are diamagnetic and can not be investigated by ESR.

By an analysis of the ESR spectrum in Fig. 6-5 it is found that there are two components (designated as type 1 and type 2) with different values of the **g** and **A** tensors:

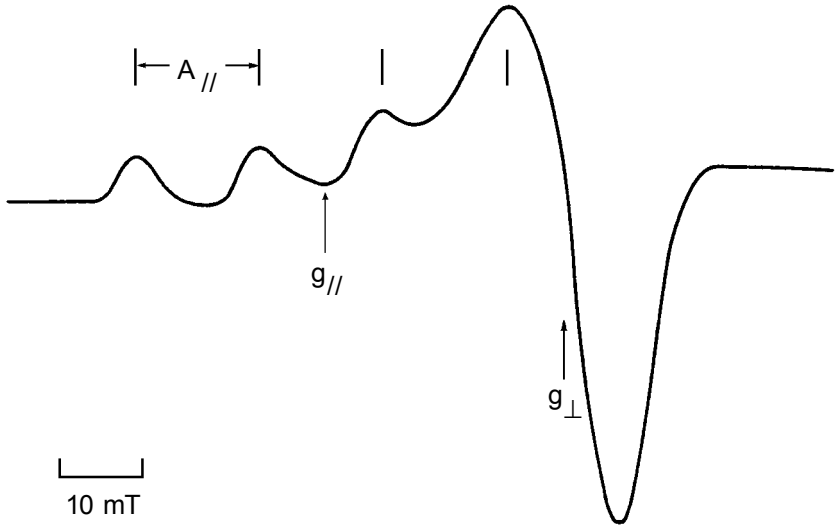

Figure 6-4.
Schematic illustration of the ESR powder spectrum of a Cu^{2+} complex.

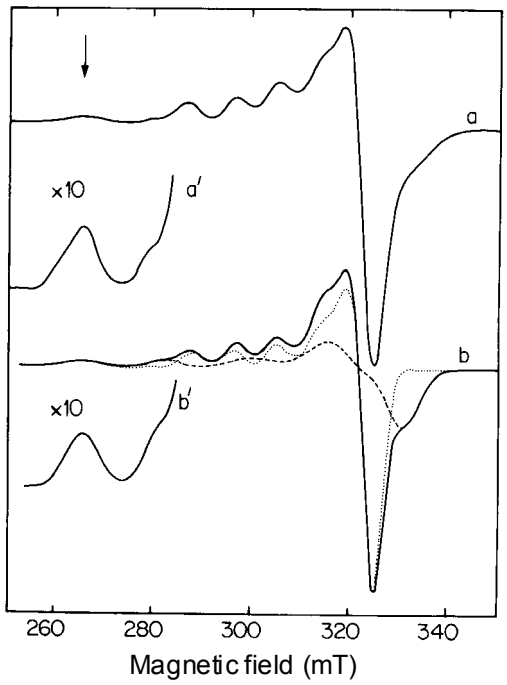

Figure 6-5.
Experimental (a) and simulated (b) 9 GHz ESR spectrum of laccase recorded at 77 K. Part of the spectrum (a' and b') is shown with 10 times higher gain. The dotted and dashed lines in (b) are the separated contributions from the two Cu^{2+} centres.

Type 1 copper is characterised by a narrow hyperfine splitting ($A_{//} \approx 9\,mT$). This value indicates a strong delocalisation of the electron density of the copper and suggests that this type 1 of copper has a redox function. Reduction of laccase with

the substrate hydroquinone leads to loss of the type 1 signal. This supports the redox role for type 1 copper centres.

Type 2 copper has a high value of the hyperfine splitting ($A_{//} \approx 17\,\mathrm{mT}$), which is close to that of simple copper complexes. This copper is not reduced by hydroquinone. This type 2 copper plays a role in the regulation of the enzyme activity, or alternatively is a site for stabilising the intermediates produced by the catalytic process.

7

Triplet ESR

7-1 Introduction

Aromatic molecules, such as naphthalene, can be brought into a triplet state by irradiating the sample with light. In the triplet state, the two unpaired electrons are oriented in a parallel way and the total spin S = ½ + ½ = 1. Triplet states are metastabile at liquid nitrogen temperature (77 K), but they live long enough to be measured by ESR spectroscopy.

7-2 The spin Hamiltonian

The spin Hamiltonian contains the following terms:

a. The Zeeman interaction of the two electrons with the external magnetic field.
b. The dipolar interaction between the electrons.
c. The hyperfine interaction of the electrons with the nuclei.

The interactions **a** and **b** are dominant. It can be assumed further that the anisotropic effects of the g-factor tensor can be neglected, so that the spin Hamiltonian of two electrons in the triplet state can be written as:

$$\hat{H} = g\mu_B \vec{\mathbf{B}} \bullet \left(\hat{\mathbf{S}}_1 + \hat{\mathbf{S}}_2\right) + \hat{\mathbf{S}}_1 \bullet \mathbf{D} \bullet \hat{\mathbf{S}}_2 \qquad (7\text{-}1)$$

We will chose an axes system {x, y, z} in which the dipolar tensor $\mathbf{D}$ is diagonal (this is the so-called principal axes system).

It is convenient to rewrite Eqn. 7-1 in terms of the total spin operator

$$\hat{\mathbf{S}} = \hat{\mathbf{S}}_1 + \hat{\mathbf{S}}_2$$

Furthermore, for spin-half particles, it can be shown that

$$\hat{\mathbf{S}}_1 \bullet \mathbf{D} \bullet \hat{\mathbf{S}}_2$$

can be written as

$$\tfrac{1}{2}\hat{\mathbf{S}} \bullet \mathbf{D} \bullet \hat{\mathbf{S}}$$

By these substitutions, Eqn. 7-1 transforms to

$$\hat{H} = g\mu_B \vec{\mathbf{B}} \bullet \hat{\mathbf{S}} + \tfrac{1}{2} \hat{\mathbf{S}} \bullet \mathbf{D} \bullet \hat{\mathbf{S}} \qquad (7\text{-}2)$$

Both unpaired electrons are in an electronic orbital of the molecule. Therefore we must average the principal values D_{xx}, D_{yy}, and D_{zz} of the tensor $\mathbf{D}$ over the electronic wave function ψ:

$$\langle D_{xx} \rangle = \int \psi^* D_{xx} \psi d\tau$$

It is common to denote the averaged principal values as -X, -Y, -Z, where

$$X = -\tfrac{1}{2} \langle D_{xx} \rangle, \text{ etc.}$$

Because the trace of the dipolar tensor remains zero, even after averaging over the electronic wave function, it is always true that

$$X + Y + Z = 0 \qquad (7\text{-}3)$$

It follows thus that Eqn. 7-2 can be rewritten as

$$\hat{H} = g\mu_B \left(B_x \hat{\mathbf{S}}_x + B_y \hat{\mathbf{S}}_y + B_z \hat{\mathbf{S}}_z \right) - X\hat{\mathbf{S}}_x^2 - Y\hat{\mathbf{S}}_y^2 - Z\hat{\mathbf{S}}_z^2 \qquad (7\text{-}4)$$

7-3 The dipolar spin Hamiltonian

Before solving the total Hamiltonian, it is interesting to examine first the dipolar part of the spin Hamiltonian. This corresponds to a situation in which there is no magnetic field, $\vec{\mathbf{B}}$ = 0. This is also referred to as the zero-field spin Hamiltonian. In the following, we shall see that the dipolar interaction will remove the degeneration of the triplet energy levels.

> ***Note***
> In the analysis of the spin Hamiltonian of an excited molecule, we may neglect the singlet state, for which the total spin quantum number is S = ½ - ½ = 0. This state is non magnetic, and will not display an ESR spectrum.

The dipolar interaction Hamiltonian is

$$\hat{H} = -X\hat{\mathbf{S}}_x^2 - Y\hat{\mathbf{S}}_y^2 - Z\hat{\mathbf{S}}_z^2 \qquad (7\text{-}5)$$

It is convenient to choose the zero-field spin functions T_x, T_y, and T_z as a basis set for solving the spin Hamiltonian. These spin functions, that have the property of being independent on direction, are given by (see Eqn. 2-67):

$$T_x = \tfrac{1}{2}\sqrt{2}(\beta\beta - \alpha\alpha)$$
$$T_y = \tfrac{1}{2}i\sqrt{2}(\beta\beta + \alpha\alpha)$$
$$T_z = \tfrac{1}{2}\sqrt{2}(\alpha\beta + \beta\alpha)$$

Because of this property, the zero-field spin functions are suitable as starting functions in the absence of a magnetic field. The zero-field spin functions have the following useful properties:

$$\hat{\mathbf{S}}_x T_x = 0 \qquad \hat{\mathbf{S}}_x^2 T_x = 0$$
$$\hat{\mathbf{S}}_x T_y = iT_z \qquad \hat{\mathbf{S}}_x^2 T_y = T_y \qquad (7\text{-}6)$$
$$\hat{\mathbf{S}}_x T_z = -iT_y \qquad \hat{\mathbf{S}}_x^2 T_z = T_z$$

The other relations follow by cyclic interchange of x, y, and z.

From these properties, it directly follows that the zero-field spin functions are eigenfunctions of the dipolar spin Hamiltonian:

$$\hat{H}T_x = -(Y + Z)T_x$$
$$\hat{H}T_y = -(X + Z)T_y$$
$$\hat{H}T_z = -(X + Y)T_z$$

By using Eqn. 7-3, it follows immediately that the energy levels are given by

$$U_1 = X, \qquad U_2 = Y, \qquad U_3 = Z \qquad (7\text{-}7)$$

This so-called zero-field splitting is illustrated in Fig. 7-1.

According to Eqn. 7-3, there are only two independent parameters that determine the zero-field splitting. These parameters are called the zero-field parameters D and E, given by

$$D = \tfrac{1}{2}(X + Y) - Z \qquad (7\text{-}8)$$
$$E = -\tfrac{1}{2}(X - Y)$$

Using these parameters, the dipolar Hamiltonian takes the following form:

$$\hat{H} = D\left(\hat{\mathbf{S}}_z^2 - \tfrac{1}{3}\hat{\mathbf{S}}^2\right) + E\left(\hat{\mathbf{S}}_x^2 - \hat{\mathbf{S}}_y^2\right) \qquad (7\text{-}9)$$

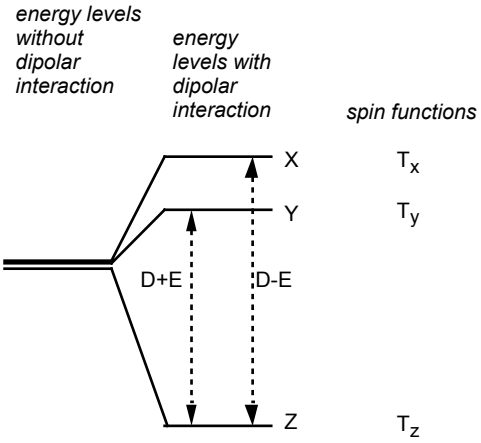

Figure 7-1.
Energy levels for a molecule in the triplet state.

Following Eqn. 7-8, it can be seen that in the case of axial symmetry (X = Y), parameter E = 0. This parameter is therefore sensitive for the **symmetry** and **shape** of the molecule forming the triplet state. The parameter D represents the distance between the two electrons in the molecule, and gives information about the **size** of the molecule.

7-4 Triplet state in magnetic field

In the presence of a magnetic field, the total spin Hamiltonian (Eqn. 7-4) must be solved. Taking the three zero-field spin functions T_x, T_y, and T_z as a basis set and using Eqn. 7-6, the Hamiltonian matrix becomes:

$$\hat{H}_{mm'} = \begin{pmatrix} X & -ig\mu_B B_z & ig\mu_B B_y \\ ig\mu_B B_z & Y & -ig\mu_B B_x \\ -ig\mu_B B_y & ig\mu_B B_x & Z \end{pmatrix} \tag{7-10}$$

It is possible the calculate a general solution of the problem, but it is useful to consider a simplified solution by assuming that the magnetic field $\vec{\mathbf{B}}$ //z. The Hamiltonian matrix, Eqn. 7-10 then simplifies to:

$$\hat{H}_{mm'} = \begin{pmatrix} X & -ig\mu_B B & 0 \\ ig\mu_B B & Y & 0 \\ 0 & 0 & Z \end{pmatrix} \tag{7-11}$$

where it is assumed that $B_x = B_y = 0$, and $B_z = B$.

Because this three-dimensional matrix blocks out in a two-dimensional matrix, the zero-field spin function T_z remains an eigenfunction with eigenvalue $U_3 = Z$, but T_x and T_y will be mixed.

Solving the two-dimensional matrix gives the two other eigenvalues:

$$U_{1,2} = \tfrac{1}{2}(X+Y) \pm \sqrt{\tfrac{1}{4}(X-Y)^2 + (g\mu_B B)^2} \qquad (7\text{-}12)$$

The energy levels as a function of the magnetic field value B are schematically shown in Fig. 7-2.

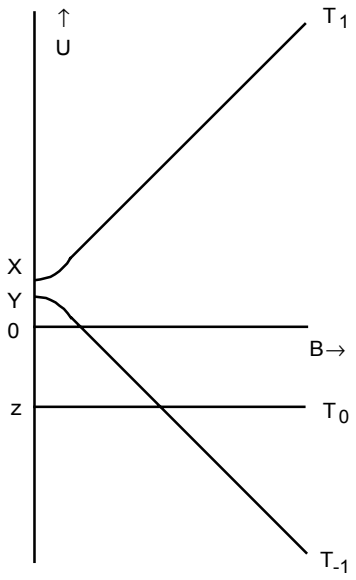

Figure 7-2.
Energy levels as a function of the magnetic field value B, for $\vec{\mathbf{B}}$ //z.

At increasing magnetic field values B, the dipolar interaction will lose from the Zeeman interaction, and gradually the zero-field spin functions T_x and T_y will transfer into the triplet functions T_1 and T_{-1}. In this magnetic field region, the dipolar interaction may be considered as a perturbation on the Zeeman interaction.

The powder triplet ESR spectra closely resemble the powder ESR spectra of nitroxide spin labels, as is shown in Fig. 7-3. It can be shown by applying Eqn. 7-12 that the zero-field parameters X, Y, and Z (or D and E) can be determined from the triplet ESR spectrum as indicated in Fig. 7-3.

The distances between the extreme in Fig. 7-3 are 3X, 3Y, and 3Z (expressed in Tesla). This can be verified from the energy levels in Fig. 7-2. At high magnetic field values, there are two transitions in Fig. 7-2: $T_{-1} \leftrightarrow T_0$ and $T_0 \leftrightarrow T_1$. The corresponding resonance values for $\vec{\mathbf{B}}$ //z can then be calculated from Eqn. 7-3 and 7-12:

$$B_{0\leftrightarrow 1} = \frac{h\nu}{g\mu_B} + \tfrac{3}{2}Z \qquad (7\text{-}13)$$

and

$$B_{-1\leftrightarrow 0} = \frac{h\nu}{g\mu_B} - \frac{3}{2}Z \tag{7-14}$$

where Z is now assumed to be expressed in Tesla.

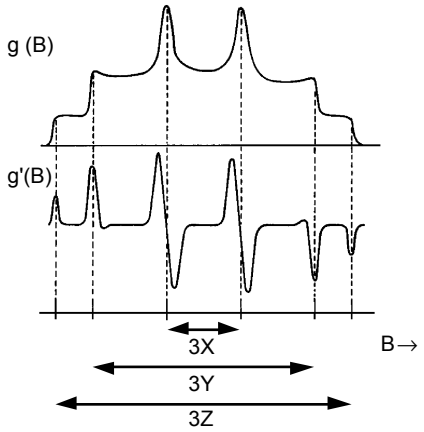

Figure 7-3.
Powder triplet ESR spectrum, showing the determination of the X, Y, and Z values (expressed in Tesla).

The distance between the two resonances is thus 3Z for $\vec{\mathbf{B}}$ //z. For $\vec{\mathbf{B}}$ //x or y, similar relations can be found. Note that the powder spectrum g(B) in Fig. 7-3 is a superposition of two powder spectra centred around

$$\frac{h\nu}{g\mu_B}$$

arising from the two transitions $T_{-1} \leftrightarrow T_0$ and $T_0 \leftrightarrow T_1$.

For example, assuming that Z is positive (hence X and Y are negative, see Eqn. 7-3) and |X| < |Y| (see Fig. 7-3), for the $T_0 \leftrightarrow T_1$ transition the three extreme occur at

$$\frac{h\nu}{g\mu_B} - \frac{3}{2}|Y| \;,\quad \frac{h\nu}{g\mu_B} - \frac{3}{2}|X| \;, \text{ and } \quad \frac{h\nu}{g\mu_B} - \frac{3}{2}|Z| \tag{7-15}$$

This gives a powder distribution g(B) with a maximum at

$$\frac{h\nu}{g\mu_B} - \frac{3}{2}|X|$$

Note

The powder spectrum in Fig. 7-3 consists of two ESR powder spectra, as shown in Fig. 5-4 that are mirrored and moved into each other.

Problems

Problem 7-1

Consider the spin Hamiltonian

$$\hat{H} = D\left(\hat{\mathbf{S}}_z^2 - \tfrac{1}{3}\hat{\mathbf{S}}^2\right) + E\left(\hat{\mathbf{S}}_x^2 - \hat{\mathbf{S}}_y^2\right)$$

Show that the zero-field spin functions T_x, T_y, and T_z are eigenfunctions of this Hamiltonian and calculate the energy levels.

Problem 7-2

Calculate the positions of the three extreme in a powder triplet ESR spectrum for the $T_{-1} \leftrightarrow T_0$ transition.

Problem 7-3

Schematically draw the powder triplet ESR spectrum in the case of axial symmetry for the dipolar interactions between the unpaired electrons (X = Y, or parameter E = 0). Compare this with the powder pattern arising from dipolar coupling effects in NMR (Course Book "Nuclear Magnetic Resonance Spectroscopy. A physicochemical view" by R.K. Harris, Fig. 6-1). What conclusions can you deduce?

Answers

Answer 7-2

For the case that $\vec{\mathbf{B}}$ //z we have the eigenvalues:

$$U_{1,2} = \tfrac{1}{2}(X+Y) \pm \sqrt{\tfrac{1}{4}(X-Y)^2 + (g\mu_B B)^2}$$

and

$$U_3 = Z$$

For a high magnetic field value B, we can neglect the term $\frac{1}{4}(X-Y)^2$ in the square root, giving

$$U_{1,2} = \tfrac{1}{2}(X+Y) \pm g\mu_B B$$

For the $T_{-1} \leftrightarrow T_0$ transition the energy difference is:

$$\Delta U = U_3 - U_2 = Z - \left\{\tfrac{1}{2}(X+Y) - g\mu_B B\right\}$$

Because

$$X + Y + Z = 0$$

we can write:

$$\Delta U = U_3 - U_2 = g\mu_B B + \tfrac{3}{2}Z$$

The resonance value for $\vec{\mathbf{B}}$ //z follows then from:

$$\Delta U = h\nu = g\mu_B B + \tfrac{3}{2}Z$$

giving

$$B_{-1\leftrightarrow 0} = \frac{h\nu}{g\mu_B} - \frac{3}{2}\frac{Z}{g\mu_B}$$

If we express Z in Tesla, we obtain Eqn. 7-14.

The calculations for $\vec{\mathbf{B}}$ //x or y are left to the reader.

Answer 7-3

Because we are dealing with axial symmetry, we can compare the situation for the powder triplet ESR spectrum with the line shape for a random distribution of simple radicals (S = ½) with an axially symmetric **g** tensor and no hyperfine interaction (see Fig. 5-3). This applies for each of the transitions: $T_{-1} \leftrightarrow T_0$ and $T_0 \leftrightarrow T_1$. To get the spectrum, schematically sketch the resonance positions for $\vec{\mathbf{B}}$ along and perpendicular to the symmetry axis. Then deduce the powder line shape function and finally draw the ESR powder spectrum dA(B)/dB.

Physically there is no difference between two electron spins having an axially symmetric dipolar interaction and two nuclei, which always have an axially symmetric dipolar interaction (based on the symmetry axis through the nuclei). Therefore the line shapes are identical.

Note that for the homonuclear case (which is identical to two electrons) we have to deal with an extra factor $\frac{3}{2}$ as compared to the heteronuclear case.

8

Basic NMR structure analysis

8-1 Introduction

One of the most attractive methods to study the three-dimensional structure of biological macromolecules is the application of two-dimensional high-resolution NMR spectroscopy. In this note the basic principles of various two-dimensional NMR methods will be presented in relation to the application to proteins, nucleic acids, and carbohydrates.

8-2 J modulation in a spin-echo experiment

First we will describe a spin-echo experiment for an AX-system with a coupling J between the A and X nuclei, which are assumed to be spin-½-particles. After applying a $90_{x'}°$ pulse, in the x'y' plane four vector components are present, indicated by $\mathbf{A}^+$, $\mathbf{A}^-$, $\mathbf{X}^+$, and $\mathbf{X}^-$, arising from the four resonances in the NMR spectrum. Initially these vectors coincide along the y' axis. If the rotation frame rotates with a frequency $\nu = ½(\nu_A + \nu_X)$, where ν_A and ν_X are the resonance frequencies of A and X nuclei, respectively, the precession frequencies of the four components is given by:

$\mathbf{A}^+$: ½ (δ + J) $\qquad$ $\mathbf{X}^+$: ½ (-δ + J) (8-1)

$\mathbf{A}^-$: ½ (δ - J) $\qquad$ $\mathbf{X}^-$: ½ (-δ - J) (8-2)

where $\delta = \nu_X - \nu_A$.

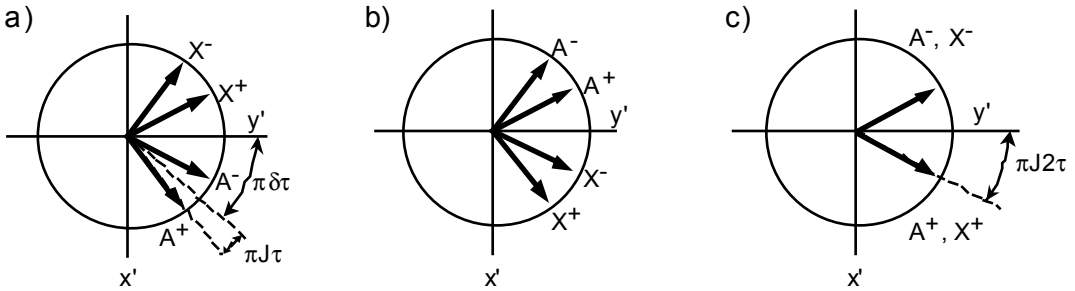

Figure 8-1.
Positions of the magnetisation vectors $\mathbf{A}^+$, $\mathbf{A}^-$, $\mathbf{X}^+$, and $\mathbf{X}^-$ during a spin echo experiment (see text).

The situation just prior to the $180_{y'}°$ pulse at time τ is shown in Fig. 8-1a. The $180_{y'}°$ pulse flips the magnetisation vectors by 180° around the y' axis, but also flips the nuclei itself. Therefore just after the $180_{y'}°$ pulse the vectors $\mathbf{A}^+$ and $\mathbf{A}^-$ but also $\mathbf{X}^+$ and $\mathbf{X}^-$ exchange position in the x'y' plane (see Fig. 8-1b). The situation at time 2τ is depicted in Fig. 8-1c. The vectors refocus only partly due to the coupling J. By this effect the height of the echo is reduced with a factor $\cos(\pi J 2\tau)$, as compared to the situation in which J = 0. The effect of τ on the echo height can most elegantly be studied using two-dimensional NMR.

8-3 Two-dimensional NMR

Two-dimensional NMR techniques can be subdivided into three main categories:

- J spectroscopy
  In two-dimensional J spectroscopy the parameters that determine the position of the resonance lines, *i.e.* δ and J, are separated.
- Shift correlation spectroscopy
  This class of experiments is an alternative for double-resonance experiments. In these experiments a correlation is made between coupling nuclei, exchanging nuclei or nuclei that have a cross-relaxation arising from dipolar couplings.
- Multiple quantum NMR
  This technique enables one to observe effects between nuclei that are not possible to measure in conventional 1D-NMR.

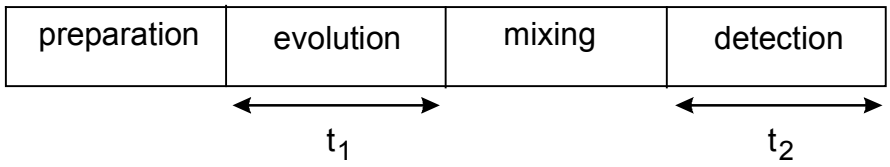

Figure 8-2.
Timing sequence for 2D-NMR spectroscopy.

In general a two-dimensional NMR experiment consists of four different time intervals, as is illustrated in Fig. 8-2. The first period is the preparation phase. After this phase there is an evolution period, determined by a time variable t_1. Then a mixing time is introduced (which can be left out in some experiments) and finally there is a detection period t_2. During mixing one can employ suitable pulse schemes for effecting coherence transfer, or monitor cross-relaxation or chemical exchange. In the fourth period, the acquisition of the final response of the observed system is recorded. The NMR signal is observed as a function of t_2 at various values for the evolution time t_1. This generates a two dimensional time-dependent NMR signal $S(t_1, t_2)$. This signal is Fourier transformed first along the t_2 dimension, and then along the t_1 dimension. Several digital manipulation techniques can be applied to the data sets to improve the signal-to-noise ratios and spectral line shapes.

8-4 Two-dimensional J spectroscopy

The principle of two-dimensional J spectroscopy is illustrated in the following example. Consider the $90_{x'}° - \tau - 180_{y'}°$ pulse sequence shown in Fig. 8-3 for an AX spin system.

The amplitude of the spin echo is modulated with a factor $\cos(\pi J t_1)$, and the time dependence (given by t_2) of the echo is determined by the resonance frequencies in the spectrum that are given in Eqn. 8-1 and 8-2. Putting things together this gives the results shown in Table 8-1. The resulting frequencies ν_1 and ν_2 in Table 8-1 corresponding to the two time variables t_1 and t_2 in Fig. 8-3, are shown in the contour plot in Fig. 8-4.

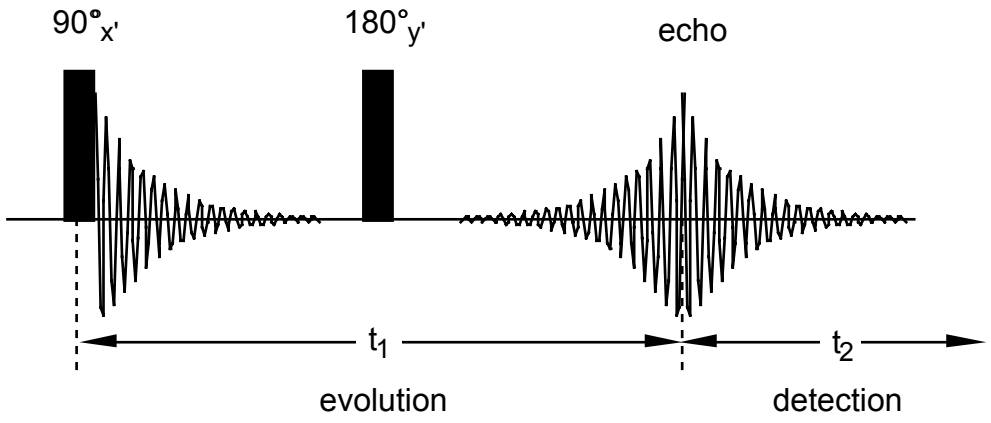

Figure 8-3.
Pulse sequence for two-dimensional J spectroscopy.

Table 8-1. Frequencies that are present in a two-dimensional NMR J spectroscopy experiment of a AX spin system.

Resonance	ν_1	ν_2
$\mathbf{A}^+$	$+\frac{1}{2}J$	$\frac{1}{2}(\delta + J)$
$\mathbf{A}^-$	$-\frac{1}{2}J$	$\frac{1}{2}(\delta - J)$
$\mathbf{X}^+$	$+\frac{1}{2}J$	$\frac{1}{2}(-\delta + J)$
$\mathbf{X}^-$	$-\frac{1}{2}J$	$\frac{1}{2}(-\delta - J)$

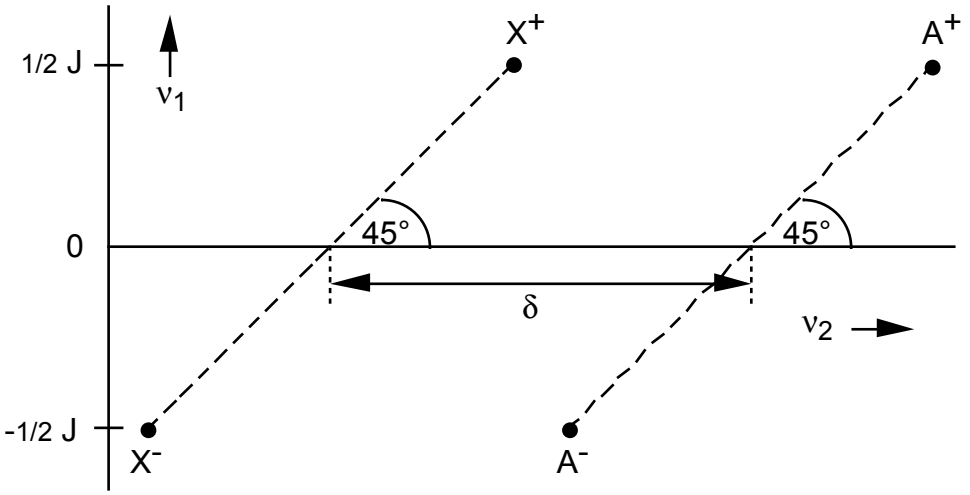

Figure 8-4.
Contour plot of the two-dimensional NMR J spectrum of an AX spin system.

In the two-dimensional NMR spectrum shown in Fig. 8-4, along the ν_2 axis the parameters δ and J are mixed. However, after a 45° projection it is possible to eliminate this effect, resulting in the spectrum of Fig. 8-5, where δ and J are separated.

In the case shown above the frequencies that determine the two-dimensional spectrum could be found immediately. However, in practice a two-dimensional Fourier transformation is needed to carry out the frequency analysis.

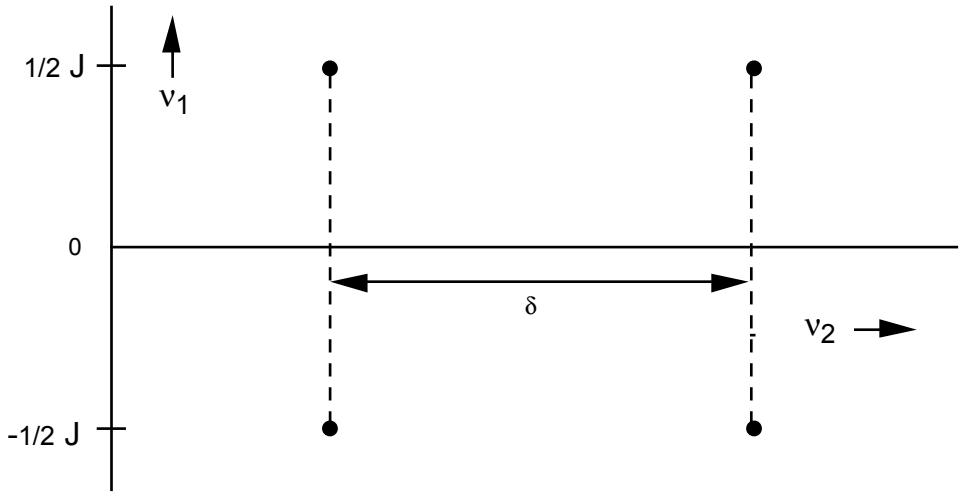

Figure 8-5.
45° projected contour plot of the two-dimensional NMR J spectrum of an AX spin system.

8-5 Shift correlation by homonuclear scalar coupling (COSY)

COSY is an example of shift correlation spectroscopy. The basis of a COSY experiment is the pulse sequence (the so-called Jeener sequence) shown in Fig. 8-6.

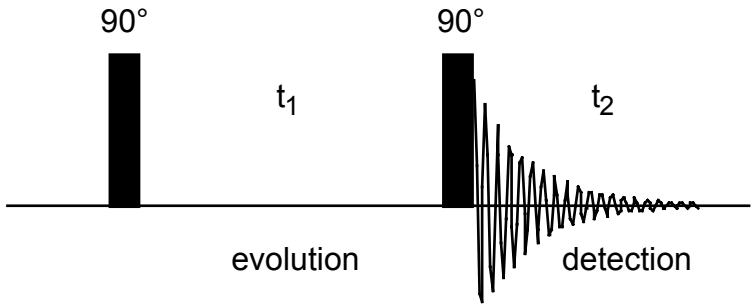

Figure 8-6.
Pulse sequence for 2D-COSY NMR

The principle is to create transverse magnetisation by the first 90° pulse and allow the phase coherence for all resonance lines in a spectrum to evolve during time t_1. The second pulse transfers the phase coherence via the J coupling to a related resonance. For example, for an AX spin system, it is possible by observing cross-peaks at frequencies($\nu_A \pm ½J$, $\nu_X \pm ½J$) to go through with proton-proton connectivities and hence proximities in molecules. The COSY spectrum of an AX spin system is shown in Fig. 8-7.

Ideally, one should be able to go from one end of a molecule to the other end by following up the cross-peak connectivities. As a result, valuable information about molecular conformation can be obtained. Two-dimensional COSY has therefore become an important analytical and structural tool in the area of biological systems, such as proteins, nucleic acids and polymers.

8-6 Two-dimensional cross-relaxation and chemical exchange (NOESY)

In contrast to the coherent effects discussed above, transfer of magnetisation can take place by incoherent processes such as the nuclear Overhauser effect (NOE) and via chemical exchange and conformational inter-conversions. One important distinguishing feature between coherent and incoherent magnetisation transfer processes is that, in the latter, there is no need for a through bond connectivity, such as a J coupling. It is enough that there is a process that can transfer information from one environment to the other via an exchange of locations or if the two nuclei involved have a finite through space dipolar coupling. It is possible to establish this through space proximity or exchange connectivity by double-resonance experiments, such as saturation transfer, selective population inversion, or studying the build-up of nuclear Overhauser enhancement in the one-dimensional sense. However, these experiments are too tedious and difficult to evaluate.

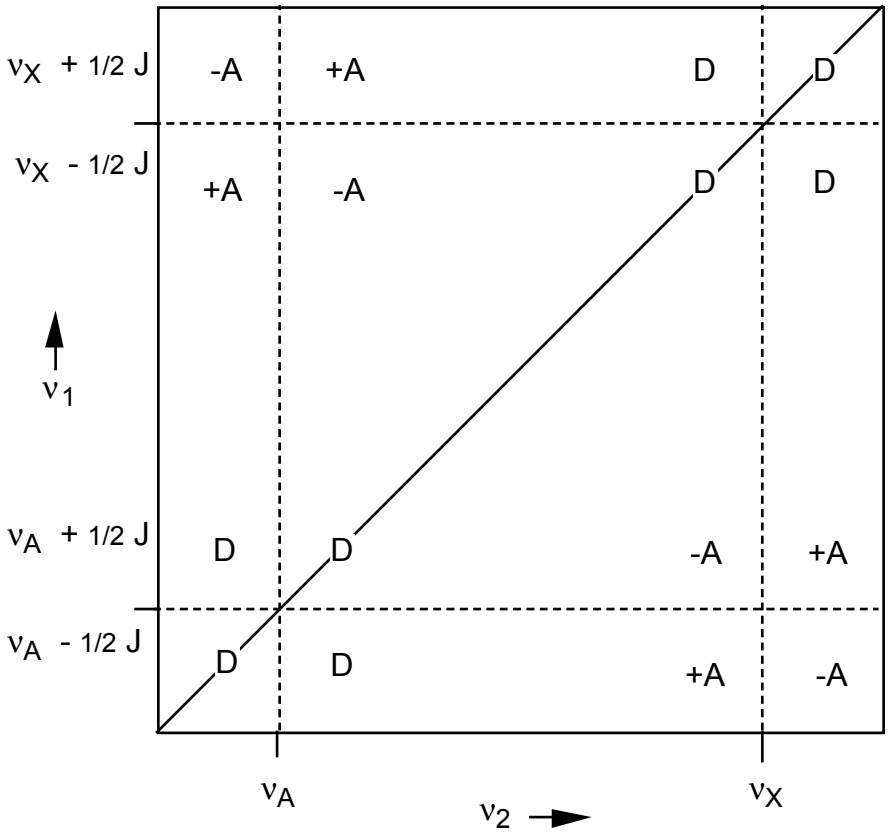

Figure 8-7.
Schematic representation of a two-dimensional COSY NMR spectrum of an AX spin system. The cross-peaks are in absorption phase (A). The diagonal peaks are in dispersion phase (D). The symbols + and - indicate the sign of the peaks.

Elegant 2D methods have been made available that can unravel complicated intra- and intermolecular pathways, correlate proximal nuclei in macromolecular folded backbones, and give insight into the three-dimensional structure of large macromolecules in solution, which are not accessible for study by X-ray methods.

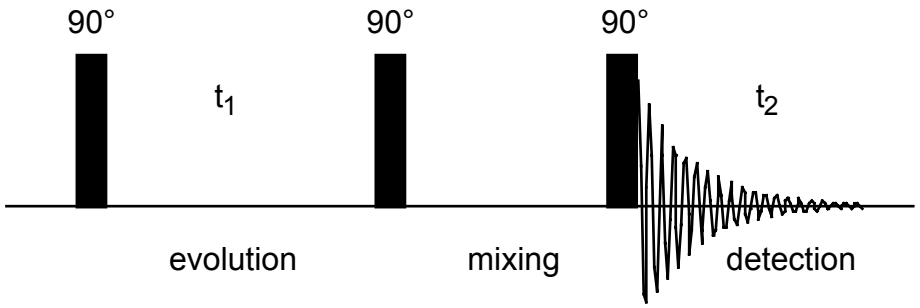

Figure 8-8.
Pulse scheme for a two-dimensional NOESY experiment.

The pulse scheme for a NOESY experiment is shown in Fig. 8-8. By the first 90° pulse, magnetisation is created in the z direction that depends on t_1, and for an AX system for example, on the resonance frequencies of A and X. Thus we label

populations in this case. These populations are not in equilibrium, so that during the mixing time Δ the spin systems will evolve to the equilibrium state. However, during this period, cross-relaxation takes place, by which magnetisation form nucleus A is transferred to X and vice versa.

This process is governed by the dipolar interactions between A and X and is called the NOE effect. Thus, the relaxation behaviour of the X nucleus depends on the populations of the energy levels of the A nucleus and vice versa. These populations have been modulated during t_1. After the observation pulse the z magnetisations of A and X are detected. In the case that A and X do not interact, the magnetisations are governed by the relaxation time T_1 of A and X. But if there exists a dipolar interaction between A and X, the signal amplitude of A is modulated by the resonance frequencies of A and X. The same is true for X. This means that cross-peaks are produced in the 2D-NMR spectrum. Also cross-peaks arise from the J coupling between A and X, unless COSY signals are suppressed. This can be carried out, for example, using a field gradient pulse during the mixing time, which destroys magnetisations in the xy plane.

8-7 Conformational analysis using proton NMR spectroscopy

In the process of conformational analysis using proton 2D-NMR spectroscopy the following steps can be considered:

- Assignment of NMR lines
  - Recognition of proton sub spectral patterns
  - Connectivity between spin systems
- Extraction of relevant NMR parameters (J, δ, NOE, chemical exchange)
- Model building (distance geometry)
- Structure refinement (molecular dynamics)

Problems

Problem 8-1

Analyse Fig. 8-9 showing a number of athletes competing for the first place. Why is there no winner?

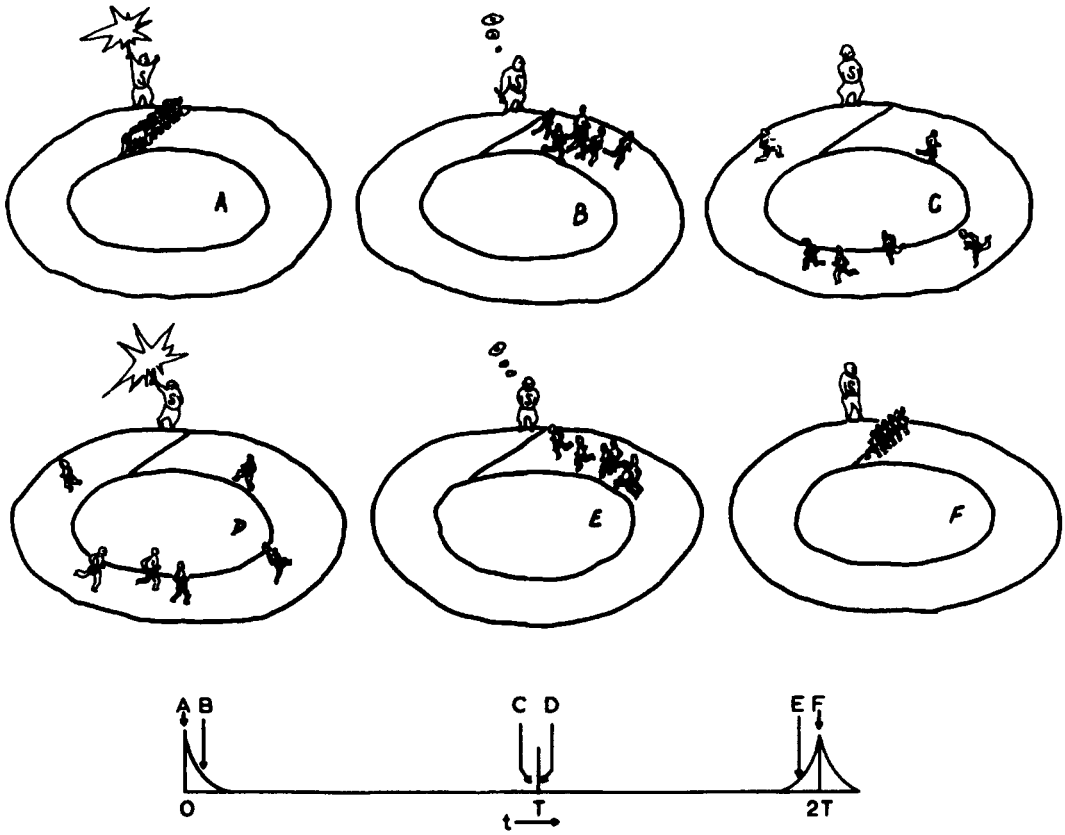

Figure 8-9.
Athletes competing for the first place.

Problem 8-2

The interpretation of 2D NMR spectra of proteins usually starts with the analysis of the cross peaks of individual amino acids. In particular, COSY spectra are important in this stage of the analysis, since the mechanism by which the cross peaks are generated in these spectra makes use of the *'through-bond'* J-couplings between the spins in the amino acids.

In Fig. 8-10, a peptide fragment is drawn, in which three amino acids are incorporated: alanine, valine, and isoleucine. The numbers between brackets indicate the resonance positions (on the ppm scale with respect to the standard DSS) of the different protons.

a. Assume that the J-splitting in cross-peak can be neglected, and that only cross-peaks appear between protons that are connected by a three bond (H-C-C-H) J-coupling or less. Construct the COSY spectrum of these different amino acids.

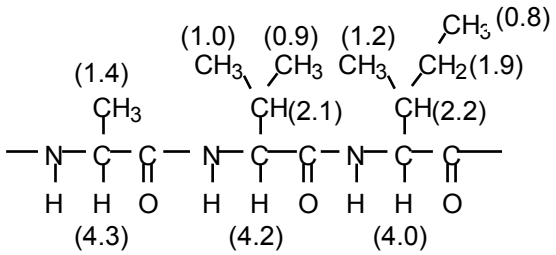

Figure 8-10.
Peptide fragment consisting of the amino acids alanine, valine, and isoleucine. The numbers between brackets indicate the chemical shift positions of the protons in ppm.

b. Total correlation spectroscopy (TOCSY) is a related pulse technique, in which all the cross peaks within a amino acid residue appear. Using this information, construct the TOCSY spectrum of these different amino acids.

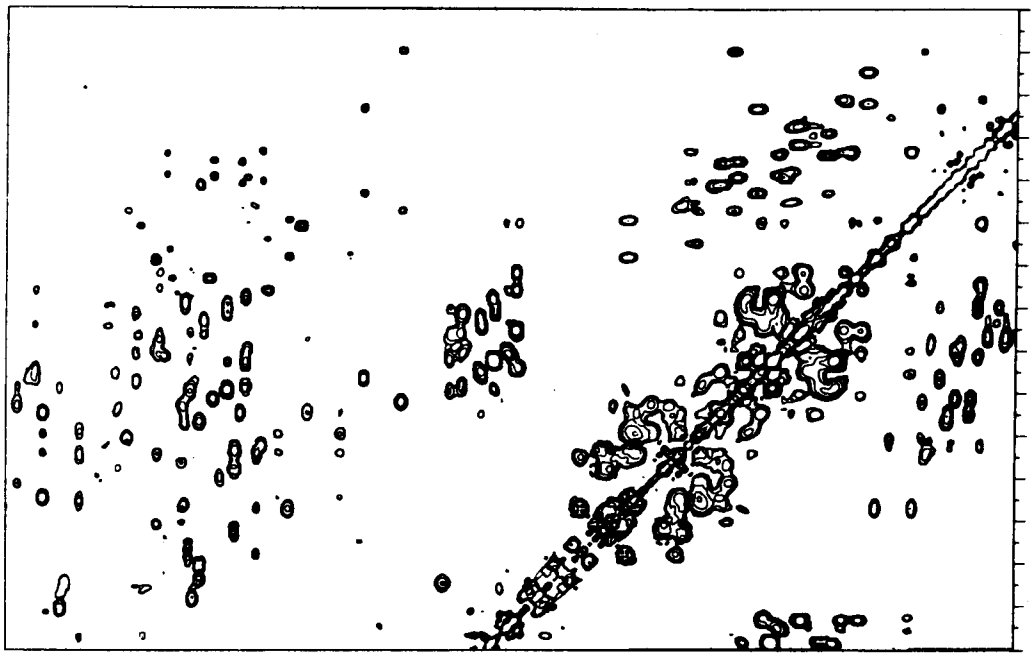

Figure 8-11.
Part of the TOCSY spectrum of the gene-5 protein encoded by the filamentous bacteriophage IKe.

c. Part of the TOCSY spectrum of the gene-5 protein encoded by the filamentous bacteriophage IKe is shown in Fig. 8-11. Indicate in this figure the cross peaks generated by the valine residues.

Problem 8-3

The interpretation of NMR spectra of proteins starts with the assignment of the cross peaks of the different amino acids, as described in problem 8-2. The next step is the so-called sequential analysis, in which amino acids are assigned to their position in the peptide chain. In this case, the cross peak patterns of the different amino acids are connected. This is possible via the cross peaks arising from proton-proton interactions that unequivocally relate two amino acids. For this relationship the connections with amide NH protons are essential. Since the NH protons do not display J couplings, NOESY spectra are needed to generate the corresponding cross peaks.

a. Indicate in the amino acid sequence in Fig. 8-12 which connectivities have to be generated to conduct a sequential analysis?

b. Some of these connectivities are indicators for the presence of standard secondary structure elements in a protein. Indicate these connectivities in Fig. 8-12.

c. Why is NOESY used to make sequential assignments?

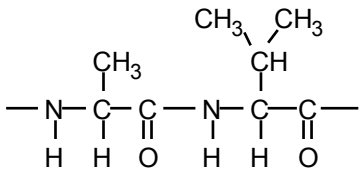

Figure 8-12.
Amino acid sequence to indicate sequential connectivities in a peptide chain.

Problem 8-4

After resolving the secondary structure, in terms of α-helix and β-structure, the last step in generating a protein structure by NMR is to determine the three-dimensional folding. This is carried by analysing the remaining cross peaks. What would be the most suitable technique to carry out this analysis: COSY, TOCSY, or NOESY? Motivate your answer!

Answers

Problem 8-1

There no winner because the athletes agreed to turn around by 180° after a second shot of the starter. The fastest athlete, who ran the largest distance will then finish equal with the slowest, who only ran a small distance. Note that because of the difference in speed, the athletes loose "phase coherence" in the course after the start.

Problem 8-2

a. See Fig. 8-13. Using the same principle you may construct the diagram for isoleucine.

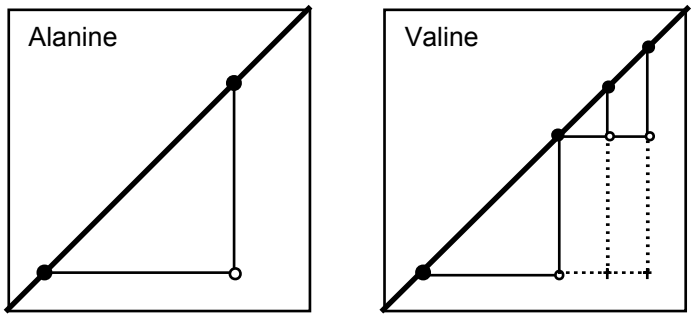

Figure 8-13.
The COSY (open circles) and TOCSY (crosses) diagrams for aniline and valine. Note that the actual COSY and TOCSY spectra are symmetric with respect to the diagonal and that the diagrams only show the lower half part of the spectrum.

b. See Fig. 8-13

c. See Fig. 8-13. Try to recognise this pattern in Fig. 8-11. There is only one valine. See Fig. 8-14.

Figure 8-14.
Valine pattern in 2D NMR spectrum of Fig. 8-11.

Problem 8-3

a. The connectivities are given in Fig. 8-15.

b. If one considers the structure of α-helices and β-sheets, it follows that in α-helices the d_{NN} distance is short as compared to the $d_{\alpha N}$ distance, whereas in β-sheets the situation is reversed: the $d_{\alpha N}$ distance is short, and the d_{NN} distance is long. (**Note**: you can easily check these distances in α-helices and β-sheets using a molecular modelling programme).

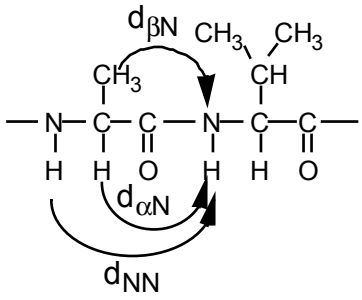

Figure 8-15.
Most important sequential connectivities in a peptide chain.

c. NOESY is based on dipolar interactions that act *'through-space* '. The J-couplings are too weak to detect by COSY or TOCSY. If one compares TOCSY and NOESY spectra, the NOESY spectra contain extra cross peaks between protons of different amino acid residues, because NOESY cross peaks are generated by a *'through-space* ' mechanism. An α-proton resonance may therefore exhibit a NOESY cross peak to its own and neighbouring amide proton.

Problem 8-4

COSY and TOCSY detect protons that are connected *'through-bond'*. It is impossible to determine a spatial folding by these techniques. NOESY is based on dipolar interactions that act *'through-space* '. This is the right method.

9

NMR imaging

9-1 Introduction

Spatial information about the distribution of magnetic nuclei can be obtained using NMR. This is due to the fact that the NMR resonance frequency depends on the magnetic field strength at the location of the nucleus. Therefore the object is immersed in an inhomogeneous magnetic field which is varying linearly over the object. The variation of the magnetic field is called a magnetic field gradient. **All NMR imaging methods utilize magnetic field gradients.** The presence of linear gradients has the effect of spreading out the resonance frequencies linearly over a range of frequencies. The larger the gradient strength the larger the frequency range.

9-2 Selective excitation

A short lasting pulse can cover a wide frequency ranges, whereas a long lasting pulse only covers a narrow frequency range. Utilizing this knowledge about the frequency range covered by the rf pulse in combination with the application of magnetic field gradients, one can limit the spatial region being excited. Such an rf pulse is called a selective pulse. The thickness of the slice Δx depends on both the rf pulse length τ and the strength of the magnetic field gradient G (see Fig. 9-1). This is given by the equation

$$\Delta x \cong \frac{4\pi}{\gamma G \tau} \qquad (9\text{-}1)$$

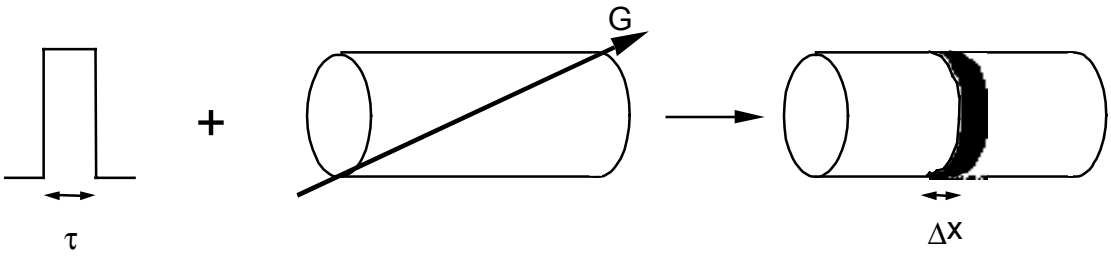

Figure 9-1.
The thickness of the excited slice Δx depends on the strength of the magnetic field gradient G and the pulse length τ.

For a pulse length of 3 ms and a gradient G of 1.2 mT/m (these are normal values for ^{1}H NMR) it follows from Eqn. 9-1 that $\Delta x \cong 1.3\ \text{cm}$.

A square pulse leads to a sin x/x shaped coverage in frequency range. This shape is reflected in the edge definition of the slice, which experiences a reduced rf intensity. To improve the slice definition, pulse tailoring is often employed. The pulse tailoring changes the pulse from being square wave formed to a form, which gives a sharper cut-off in the frequency range.

9-3 Projection reconstruction

When an NMR experiment is carried out in the presence of a magnetic field gradient the resonance frequency of the object is a direct measure of the spatial position. We can see this as follows. Consider a one-dimensional object with a proton density $\rho(x)$. This is placed in a linear field magnetic gradient G, so that the magnetic field B varies as follows

$$B = B_0 + Gx \tag{9-2}$$

From Eqn. 9-2 it follows that the Larmor precession frequency ω is position dependent:

$$\omega = \omega_0 + \gamma Gx \tag{9-3}$$

with

$$\omega_0 = \gamma B_0 \tag{9-3}$$

Taking a rotating axes system at frequency ω_0 and neglecting relaxation effects, the NMR free induction decay from the protons between x and x + dx is proportional to

$$\rho(x)\exp(i\gamma Gxt)\,dx \tag{9-4}$$

The complete NMR signal S(t) is then

$$S(t) = \int_{-\infty}^{+\infty} \rho(x)\exp(i\gamma Gxt)\,dx \tag{9-5}$$

A back Fourier transformation of the NMR signal in Eqn. 9-5 thus directly gives the proton density function.

In general, when an object is placed in a linear field gradient all nuclei in a plane perpendicular to the direction of the gradient will feel the same magnetic field value. Thus the resulting NMR signal is the projection of the density function $\rho(x,y,z)$ of the nuclei in that plane on the line given by the gradient. By making a number of projections in different directions, it is possible to reconstruct the image of the object. This principle is illustrated in Fig. 9-2.

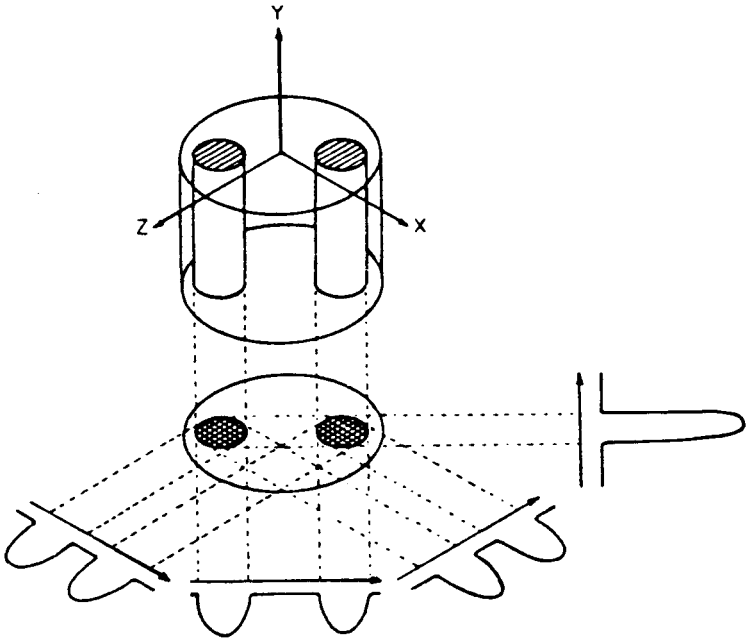

Figure 9-2.
Projection-reconstruction imaging.

9-4 2D NMR imaging

Another method of making an image reconstruction is based on the principle of two-dimensional Fourier transformation. This principle is illustrated in Fig. 9-3.

At the times P and Q a 90° pulse and 180° pulse are applied to the object, resulting in an echo centred at time O. Gradient G_z is used to select a slice of the object, in combination with the 90° and 180° pulses. A Gaussian profile of the pulses is chosen to avoid cut-off effects. After the 90° pulse different spins within the slice start to dephase due to the gradient G_z. This effect is compensated by the 180° pulse by choosing the timing of G_z such that

$$\int_P^Q G_z dt = \int_Q^R G_z dt \qquad (9\text{-}6)$$

In the period from R to S, the cross section $\rho(x,y)$ of the object is determined. The strength of the gradient G_y is varied between different experiments and allows for a evolution of the phase of the spins (phase encoding gradient), resulting in an amplitude modulation. When t_1 is the time that G_y is on, the amplitude modulation is $\gamma G_y y t_1$. Gradient G_x is effective during the detection of the echo and gives a frequency modulation of the echo signal given by $\gamma G_x x t_2$ (read or frequency encoding gradient). A two-dimensional Fourier transformation of the echo signal $S(t_1,t_2)$ gives the image $\rho(x,y)$ of the selected slice.

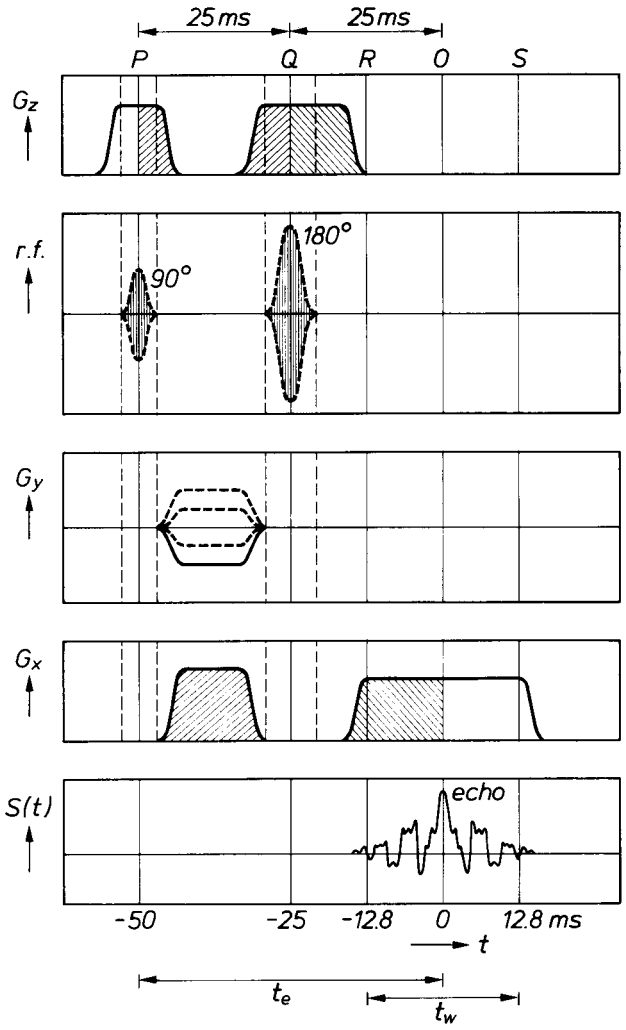

Figure 9-3.
Pulse and gradient sequence for two-dimensional NMR imaging. The 90° pulse in P and the 180° pulse in Q generate an echo centred at O. The period PR is the preparation period, and RS is the measuring period. Gradient G_z is used to select a slice of the object. The gradients G_x and G_y allow the determination of the density function $\rho(x,y)$. For the measurement of the slice the experiment is repeated with different values for G_y.

Problems

Problem 9-1

Selective excitation in NMR is a method to excite only a small part of an object. Consider a one-dimensional object in an imaging NMR system, having a magnetic field gradient G of 4.5 mT/m. The rf pulse length of the NMR system is τ_p.

a. Schematically draw the frequency spectrum of the NMR pulses and give a self-made definition of the excitation width (in frequency units). How is this excitation width related to τ_p?

b. Derive a relation between τ_p and the thickness of the slice that is excited. What would be the value of τ_p to excite a slice with a thickness of 0.2 cm?

Problem 9-2

Why do the rf pulses in Fig. 9-3 have a smooth bell shape?
(**Hint**: What is the frequency spectrum of a bell shape pulse as compared to a rectangular pulse?)

10

Miscellaneous problems

Introduction

The following problems are related to the topics of relaxation (Bloch equations, T_1, and T_2, relaxation theory) and pulse NMR (see Course Book "Nuclear Magnetic Resonance Spectroscopy. A physicochemical view" by R.K. Harris, chapters 3 and 4).

Problem 10-1

Consider a water sample in a high-resolution FT-NMR spectrometer. The spectrometer is exactly in-resonance. The T_2 value of the water protons is very short (T_2 = 1 ms). The T_1 value is 2 s.

We apply a 90°_x pulse to the sample and the free induction decay (FID) is detected in the normal way. The pulse width may be neglected.

a. Sketch the change of the magnetisation vector in the rotating frame after the 90°_x pulse as a function of time.

The pulse experiment is extended by giving two 90°_x pulses separated by a time τ.

b. Sketch the change of the magnetisation vector after the second pulse as a function of time for different values of time τ.

Finally, a pulse sequence is applied of 90°_x pulses separated by a repetition time τ. This is the actual pulse sequence for obtaining a FT-NMR spectrum.

c. Show that the signal intensity I of the water sample is given by

$$I(\tau) = I(\infty)\left[1 - \exp(-\tau / T_1)\right]$$

where $I(\infty)$ is the signal intensity for $\tau = \infty$.

Under the condition that T_2 is short, this is an alternative method to determine the T_1 value in a normal FT-NMR experiment. This method is called "progressive saturation".

d. Which value of the repetition time τ should be taken to avoid saturation of the sample?

Problem 10-2

Consider a water sample of which the relaxation times T_1 and T_2 are much longer than the time scale of the NMR experiment.
With a pulsed NMR spectrometer the following pulse sequence is applied to the sample:

$$90^\circ_x - \tau - \left[180^\circ_x - \tau - \right]_n$$

where n = 5.

The time τ is 1 ms. The NMR signal is detected out-of-phase along the x axis of the rotating frame.

The magnet of the NMR spectrometer is very homogeneous. The frequency is set, such that the sample is +125 Hz out-of-resonance.

a. What is the angle over which the sample magnetisation rotates in the xy plane of the rotating frame between the pulses?

b. Sketch the behaviour of the magnetisation during the pulse sequence.

c. Sketch the NMR signal as a function of time for n = 5.

d. What is the NMR signal in case the sample is in-resonance?

Problem 10-3

Spin echo NMR is a useful technique to determine flow. This is applied to flow in plant stems and blood vessels. The most simple method is based on the following spin echo pulse sequence:

$$90^\circ_x - \tau - \left[180^\circ_y - 2\tau - \right]_n$$

Consider a capillary filled with water through a NMR coil with a length l (see Fig. 10-1). The water in the capillary is stationary.

a. Show that the echo height h(t) during the pulse sequence is given by

$$h(t) = h(0)\exp(-t/T_2)$$

where t is the time, T_2 is the spin-spin relaxation time and h(0) the echo height for t = 0.

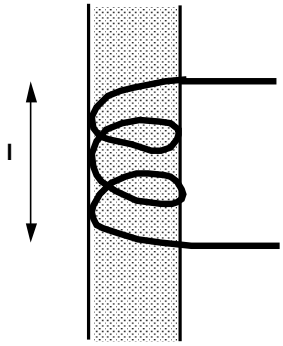

Fig. 10-1.
Schematic illustration of a capillary filled with water through a NMR coil with a length l

b. What would be the result of a series of 180°_y pulses only:

$$\left[180^\circ_y - 2\tau -\right]_n \ ?$$

Assume that the water in the capillary flows with one flow rate v (this is called plug flow).

c. Calculate the fraction of water in the NMR coil after time t that has received a 90° pulse. What has happened if t > l/v?

d. Show that for plug flow the echo height is given by the equations

$$h(t) = h(0)\left(1 - \frac{v}{l}t\right)\exp(-t/T_2) \text{ if } t < l/v,$$

and

$$h(t) = 0 \text{ if } t < l/v.$$

Problem 10-4

Consider the Bloch equations of a sample with volume V (in m^3) in which water molecules flow in and out. The water flow rate is constant with a velocity Q (in m^3/s).

a. Show that the change of magnetisation by the inflow is given by

$$d\mathbf{M}/dt = \mathbf{k}(Q/V)M_0$$

in which M_0 is the equilibrium magnetisation and **k** the unity vector in the z direction.

b. Show that the effect of outflow of water is given by:

$$d\mathbf{M}/dt = -(Q/V)\mathbf{M}$$

c. Add these terms to the Bloch equations and discuss the effect of in and outflow on the relaxation times T_1 and T_2.

Problem 10-5

Consider a water sample in a high-resolution NMR spectrometer. We apply a pulse sequence consisting of the following three pulses:

$$90°_x - \tau - 180°_y - 2\tau - 180°_x$$

where x and y indicate the phase of the pulses. The time τ is 5 ms.

a. The relaxation times of the water sample are $T_1 = T_2 = 2.5$ s. Explain why in the pulse experiment relaxation effects may be neglected.

b. Make a clear sketch of the behaviour of the magnetisation in the rotating axes system during the pulse experiment, assuming that the NMR spectrometer is exactly in resonance.

c. Now the NMR spectrometer is 10 Hz out resonance. Sketch again the path of the magnetisation during the pulse experiment.

Problem 10-6

Consider a water sample in a high-resolution NMR spectrometer with a very homogeneous magnet. We apply a pulse sequence consisting of the following three pulses:

$$90°_x - \tau - 180°_x - \tau - 180°_x$$

where x indicates the phase of the pulses. The time τ is 25 ms. The NMR spectrometer is 15 Hz out resonance. Relaxation effects may be neglected.

a. Calculate the rotation angle of the magnetisation about the z axis between the 180° pulses.
b. Make a clear sketch of the path of the magnetisation in the rotating axes system during the pulse experiment.
c. Is the final result after applying the series of pulses dependent on the time τ? Motivate your answer.

Problem 10-7

Using an NMR spectrometer, we determine the two-dimensional spectrum of an AX_3 spin system. For this reason, we apply the following pulse sequence:

$$90°_x - \tau - 180°_y$$

where x and y indicate the phase of the pulses.

a. What are the phase angles of the various components of the magnetisation of nucleus A in the xy plane of the rotating axes system at time $t = 2\tau$. Motivate your answer.

b. Sketch the normal and 45° projected two-dimensional NMR spectrum. Clearly indicate along the axes which parameters are plotted.

Problem 10-8

The T_1 relaxation time (in s) of the proton resonance of some molecule groups of a small peptide Pep25 (consisting of 25 amino acid residues) in the absence and presence of phosphates of different length is determined at 10 and 25°C (see table below).

The total phosphate concentration is constant in all experiments, but the phosphate is present as monofosfaat (P), tetraphosphate (4P), or 18-phosphate (18P). Pep25 has three lysines and six arginines. De NMR experiments are carried out at 600 MHz.

Table 10-1. T_1 relaxation data of peptide Pep25 in the absence and presence of phosphates of different length is determined at 10 and 25°C.

Phosphate length	Temperature (°C)	T_1 (s) $(\gamma CH_3)_2$ Val3	T_1 (s) δCH_2 Arg	T_1 (s) εCH_2 Lys
no salt	10	0.44	0.40	0.51
P	10	0.43	0.40	0.46
4P	10	0.44	0.38	0.36
18P	10	0.43	0.28	0.33
no salt	25	0.50	0.43	0.63
P	25	0.49	0.43	0.57
4P	25	0.49	0.41	0.41
18P	25	0.49	0.38	0.43

a. Explain on the basis of dipolar relaxation theory, why in all cases T_1 increase on increasing temperature.

b. Calculate the rotational correlation time of the rotational motions of the amino acid side chains from Table 10-1, in the absence of salt.
c. The T_1 values of the δCH_2 resonances of the arginine side chains and the εCH_2 resonances van de lysine-zijketens decrease if the length of the polyphosphate

increases. However, the T_1 values of the $(\gamma CH_3)_2$ protons of valine at position 3 are unaffected. On basis of this finding, what can you conclude about the interaction of polyphosphate with Pep25? Make a clear drawing to support your answer.

Given:
At the conditions used, the side chains of Arg and Lys are charged.

Side chain lysine: $HC\text{-}CH_2\text{-}CH_2\text{-}CH_2\text{-}CH_2\text{-}NH_2$
$\alpha \qquad\qquad\qquad\qquad \varepsilon$

Side chain arginine: $HC\text{-}CH_2\text{-}CH_2\text{-}CH_2\text{-}NH\text{-}C\text{-}(NH_2)(NH)$
$\alpha \qquad\qquad\quad \delta$

Side chain valine: $HC\text{-}CH_2\text{-}(CH_3)_2$
$\alpha \qquad\quad \gamma$

Problem 10-9

The following equation is often used in ^{1}H NMR on biomolecules to estimate the line width Δ of a resonance on basis of the molecular weight M:

$\Delta = M/1000$ (Δ in Hz; M in Dalton)

a. Derive this equation from the dipolar relaxation theory and clearly indicate the assumptions that you need to make.

Cowpea chlorotic mottle virus (CCMV) is a spherical plant virus with a molecular weight M of 5×10^6 Da.

b. Calculate the theoretical line width of a proton resonance of CCMV. Which conclusions can you draw, considering the fact that the chemical shifts of ^{1}H NMR spectra cover a range of about 10 ppm?

The experimental ^{1}H NMR spectrum of CCMV at 400 MHz consists of a couple of relatively sharp resonances with a line width varying between 10 and 40 Hz. The total integral of this spectrum indicates that about 15% of the protons contributes to this spectrum.

c. Which conclusions can you draw from this NMR spectrum? Take into account your findings from item **b**.

Problem 10-10

The ^{1}H NMR spectrum of AMP in aqueous solution in the presence of various concentrations of Mn^{2+} is given in Fig. 10-2.

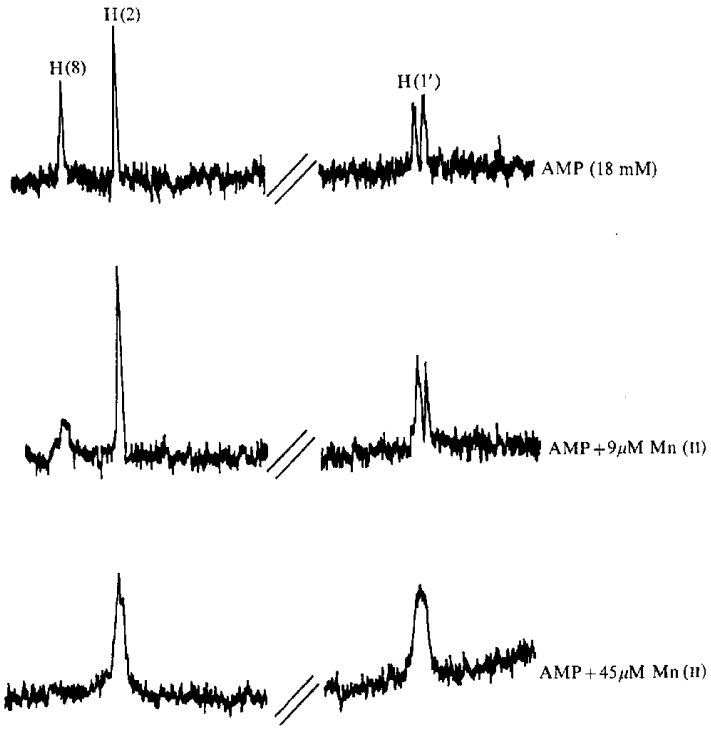

Fig. 10-2.
The ^{1}H NMR spectrum of AMP in aqueous solution in the presence of various concentrations of Mn^{2+}.

a. Explain the line broadening effects that can be observed in the NMR spectrum. Which relaxation mechanisms are responsible for the line broadening effect?

b. Based on the NMR spectra, determine the binding place of the Mn^{2+} ion to the AMP molecule (see Fig. 10-3). Motivate your result.

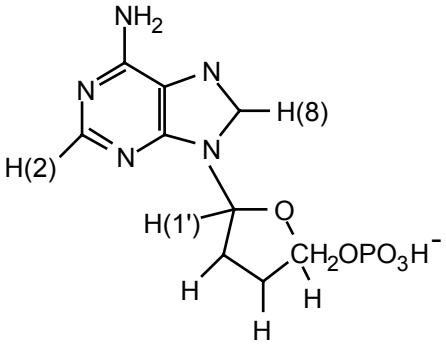

Fig. 10-3.
Chemical structure of AMP.